CHARACTERIZATION OF CYTLEK1 AS A NOVEL REGULATOR OF THE LIS1 PATHWAY

By

Victor Soukoulis

Dissertation

Submitted to the Faculty of the

Graduate School of Vanderbilt University

in partial fulfillment of the requirements

for the degree of

DOCTOR OF PHILOSOPHY

in

Cell and Developmental Biology

May, 2005

Nashville, Tennessee

Approved:

Professor David M. Bader

Professor Raymond N. DuBois

Professor Vivien A. Casagrande

Professor John S. Penn

Professor Guoqiang Gu

ACKNOWLEDGEMENTS

There are a number of people who deserve acknowledgement for their invaluable support that has made this dissertation work possible. First, I would like to thank my mentor, David Bader, for providing me the opportunity to work in his laboratory on this stimulating project. His excitement for science and creation of a fun, energizing work environment were instrumental in motivating and guiding me through this scientific endeavor. I would also like to recognize the other members of my committee for their continued input and support: Raymond DuBois, Vivien Casagrande, John Penn, and Guoqiang Gu. The Cell Biology and MSTP administrations have been instrumental in the completion of this thesis, and I would like to especially thank Terry Dermody, David Robertson, Jena Fletcher, Ellen Carter, and Elaine Caine. This work would not have been possible without the financial support of the National Institutes of Health.

All members of the Bader laboratory, past and present, have been critical in their help and in making each day of work an enjoyable and exciting experience. Thus, I would like to recognize Mabelle Ashe, Ryan Pooley, Sam Reddy, Kristin Price, Megan Osler, Travis Smith, Aya Wada, Anna Ripley, Bettina Wilm, Michiya Kawaguchi, Hillary Hager, Ellen Dees, Brian Robertson, and Cheryl Seneff. I have enjoyed working with each of you and have developed friendships that will last a lifetime. I would specifically like to thank Mabelle for guiding me in the LEK1 project, showing me the sights of Nashville, and becoming a truly cherished friend. Kristin and Ryan have made working on LEK1 always interesting, and I have thoroughly enjoyed their company both in and out of lab. I would also like to recognize a fellow MSTP classmate, Dan Boyer, who has been a friend and colleague throughout my medical and graduate school years.

Finally, and most importantly, I wish to thank my parents for their continuous unlimited love and support. They have provided me from the earliest age with the abilities and confidence to achieve my goals. Without their hard work and sacrifices, none of this work would have been even remotely possible.

TABLE OF CONTENTS

LIST OF FIGURES

CHAPTER I

INTRODUCTION

Regulation of Proliferation and Differentiation

During embryonic development, proliferation must be carefully balanced with differentiation in order to produce a mature, functional organ. Inappropriate initiation or termination of either of these processes can have dire consequences on the organism, resulting in congenital malformations and tumorigenesis. Since every tissue has unique functions and needs, each controls proliferation and differentiation differently. The developmental mechanisms that determine the balance of these two processes are not well characterized but of utmost importance in understanding embryogenesis and tumorigenesis.

The diversity of regulatory systems can be witnessed by examining three systems: the small intestine, skeletal muscle, and cardiac muscle. The small intestine is subjected to harsh and varied environmental conditions due to the enzymes required to digest a plethora of nutritional components. For this reason, the enterocyte population retains and utilizes its proliferative ability throughout the life of an organism (Ross et al., 1995). Continuously, epithelial cells from a stem cell population at the base of intestinal crypts undergo cell division and migrate towards the tips of the villi to replace older enterocytes that have been shed. Even though proliferation of enterocytes never ceases, it still is regulated for the health of the organism. Dysregulation leads to uncontrolled growth and tumor formation (Cotran et al., 1999). The situation in skeletal muscle is different in important respects (Naya and Olson, 1999; Buckingham, 2001). During development, mesodermal precursor cells in the somites are actively proliferating while transcription factors, such as Pax3, MyoD, and Myf5, combinatorially regulate myoblast commitment. These myoblasts continue dividing as they travel to the regions of the body where skeletal muscle will eventually form. After reaching an appropriate population size, the transcription factor myogenin is somehow activated and signals initiation of differentiation. However, for differentiation to occur in skeletal myoblasts, they must first undergo cell cycle arrest by a mechanism that is not well understood but is postulated to involve retinoblastoma (Rb) protein (Yee et al., 1998). After this arrest, myocytes fuse to form myotubes and eventually mature skeletal muscle. Similar to the intestine, however, skeletal muscle retains a stem cell

population, called satellite cells, that can be recruited to proliferate in order to replace damaged muscle.

In cardiac muscle, on the other hand, there is no proliferation in the terminally differentiated tissue. As in skeletal muscle, there is a pathway of transcription factors (Nkx2.5, MEF2C, and others) that regulates the activation of genes involved in differentiation (Sucov, 1998; Pasumarthi and Field, 2002). However, cardiomyocytes, unlike their skeletal counterparts, are unique in that they continue to proliferate in the embryonic heart at the same time as they begin to undergo differentiation. The reasons for the ability of these cardiomyocytes to proliferate and differentiate simultaneously are not well understood, although Rb once again may be involved (McGill and Brooks, 1995). During the first postnatal week of development in mouse, these cardiomyocytes receive a signal to permanently exit the cell cycle and undergo terminal differentiation (Soonpaa et al., 1996; Soonpaa and Field, 1998). The exact triggers of this cell cycle arrest and terminal differentiation remain unclear. Nonetheless, the result is that cardiomyocytes are incapable of proliferation after this process is complete, although this has become a source of great controversy recently (Mathur and Martin, 2004), and there does not seem to be a clear stem cell population, as in skeletal muscle (Soonpaa and Field, 1998). For this reason, myocardial infarctions are a leading cause of death in humans (Center for Disease Control and Prevention, Atlanta, GA). Understanding the mechanisms of control of terminal differentiation in the heart and other tissues is thus of great scientific and clinical value.

The LEK Family of Proteins

Studies in our laboratory identified LEK1, a murine member of the LEK family of proteins (Goodwin et al., 1999). The name of the family comes from the approximately 40% leucine, glutamic acid, and lysine (LEK) amino acid composition of the proteins. The known proteins comprising this family are LEK1 (mouse), CMF1 (chicken), and Mitosin/CENP-F (human). These LEK family members are large proteins (approximately 300 kDa in size) that have conserved sequences (Figure 1) with Mitosin/CENP-F being 75% homologous at the amino acid level to LEK1. In addition, they share a similar domain structure (Liao et al., 1995; Zhu et al., 1995a; Zhu et al., 1995b; Goodwin et al., 1999). The N-terminus is comprised of a cluster of leucine zippers. The central region is predicted to fold into a coiled coil arrangement and contains a spectrin repeat along with additional leucine zippers. The identified domains in the C-

terminus include a nuclear localization signal (NLS), a helix-loop-helix (HLH) dimerization domain, an atypical Retinoblastoma (Rb) binding site, and numerous leucine zippers. Despite this homology, individual members of the LEK family display, as discussed below, unique expression patterns and activities.

Mitosin/CENP-F was initially identified in a screen for proteins that interact with Rb (Liao et al., 1995; Zhu et al., 1995b). Two separate laboratories used a different name for essentially the same protein, and it is referred to here by both: Mitosin/CENP-F. It exhibits a cell cycle-specific expression pattern without any known tissue specificity (Liao et al., 1995; Zhu et al., 1995b). The protein first begins to be expressed throughout the entire nucleus during late S phase of the cell cycle. Its distribution then changes, presumably due to alterations in phosphorylation status, during M phase when it becomes localized to the outer plate of the chromosomal kinetochore. The regions required for kinetochore binding have been identified (Zhu, 1999), and they are present to some degree, albeit incompletely, in all LEK family members. As mitosis proceeds, Mitosin/CENP-F is also detected on the spindle apparatus and, later, at the cellular midbody (Liao et al., 1995; Zhu et al., 1995b). The protein is also found transiently at the nuclear envelope in late G_2 phase. Following completion of mitosis, the protein is rapidly degraded. In terms of function, Mitosin/CENP-F, predominantly through its kinetochore interaction, is believed to play a role in mitotic checkpoint control, as dominant negative N-terminal truncations of the protein result in inhibition of proliferation due to a G_2/M arrest (Zhu et al., 1995b). Not surprisingly, increased expression of Mitosin/CENP-F has been detected in various human cancers (de la Guardia et al., 2001; Esguerra et al., 2004).

More recently, it has been suggested that farnesylation of Mitosin/CENP-F at a C-terminal CAAX motif may be required for several of its functions (Hussein and Taylor, 2002). Protein farnesylation is a post-translational modification that consists of the addition of a 15-carbon isoprenoid lipid molecule to the sulfur atom in a C-terminal cysteine (Sinensky, 2000). This reaction is catalyzed by the enzyme farnesyltransferase. Interestingly, presence of the CAAX motif is required for a dominant negative Mitosin/CENP-F protein to delay G_2/M progression (Hussein and Taylor, 2002). Additionally, mutation of this farnesylation motif significantly decreases the ability of Mitosin/CENP-F to localize to the nuclear envelope and kinetochore during mitosis. Degradation of the protein after mitosis also is dependent on the CAAX motif. Notably, this farnesylation motif is conserved among the known LEK family

Structure of the LEK Family of Proteins

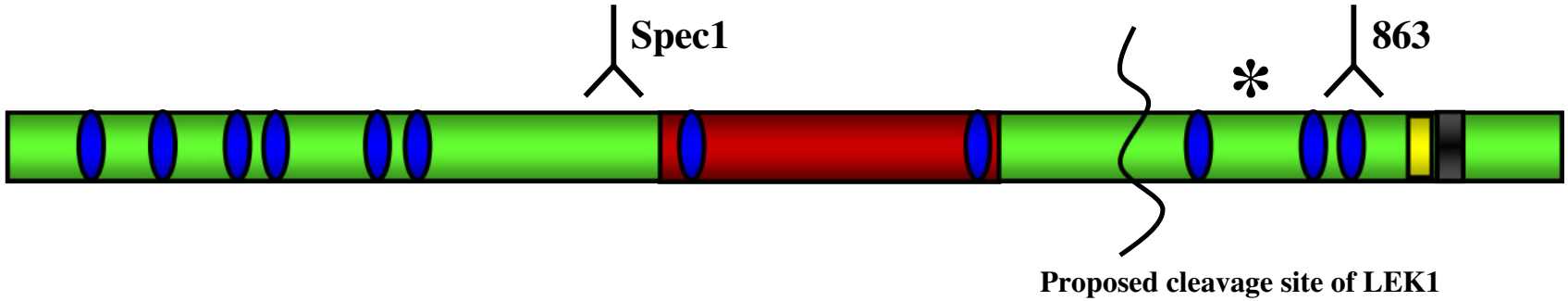

N-terminus

- No known function
- Numerous leucine zippers
- Predicted coiled-coil structure
- Spectrin repeat

C-terminus

- Functional NLS
- Atypical Rb binding site
- Numerous leucine zippers
- HLH dimerization domain

Figure 1. **Structure of LEK family proteins.** Members of the family include LEK1 (mouse), Mitosin/CENP-F (human), and CMF1 (chicken). The proteins share a similar domain structure.

members but has only been studied with respect to Mitosin/CENP-F. Since farnesylation is emerging as an important post-translational modification of several proteins involved in regulation of proliferation, such as the proto-oncogene Ras and Mitosin/CENP-F, farnesyltransferase inhibitors are being looked at as a new potential drug class in the treatment of cancer (Russo et al., 2004).

As is common for the LEK family, the chicken member, CMF1, differs substantially from Mitosin/CENP-F in terms of its expression and function. CMF1 was first identified in a chicken expression library screen searching for proteins reactive to an antiserum against the basic helix-loop-helix (bHLH) domain of MyoD, an important muscle transcription factor (Wei et al., 1996). Surprisingly, the CMF1 protein itself does not display strong homology to any known member of the bHLH family of myogenic factors. As with all LEK family members, CMF1 has an atypical Rb binding site, and the protein has been shown to bind Rb both *in vitro* and *in vivo* (Redkar et al., 2002). The expression of CMF1 is regulated during embryonic development, and the protein is specifically expressed in skeletal and cardiac myocytes (Wei et al., 1996; Dees et al., 2000). Expression is highest during early embryonic stages and significantly decreases after embryonic day 7 (Pabon-Pena et al., 2000). It cannot be detected in adult animals, suggestive of a role during development. Even though CMF1 contains a NLS that has been determined to be functional when attached to a reporter protein, CMF1 itself is observed predominantly in the cytoplasm of myocytes *in vitro* and *in vivo* (Dees et al., 2000; Pabon-Pena et al., 2000). However, very early myoblasts in primary culture do have transient expression of a nuclear form of CMF1 (Dees et al., 2000), and one group has reported detecting nuclear CMF1 in the embryo (Redkar et al., 2002). Since expression of CMF1 precedes expression of muscle-specific proteins such as sarcomeric myosin heavy chain (sMHC), it was postulated that CMF1 might play a role in muscle differentiation. Indeed, inhibition of CMF1 expression in cultured myoblasts and mesodermal cells using antisense technology results in a substantial decrease in sMHC expression, suggesting that CMF1 is important for myocyte differentiation (Wei et al., 1996; Dees et al., 2000). Notably, every cell expressing sMHC also expressed CMF1. Thus, CMF1 is currently believed to play a critical role in the differentiation of skeletal and cardiac myocytes during embryogenesis.

LEK1, the murine member of the LEK family, differs from both Mitosin/CENP-F and CMF1 and is the primary focus of the experiments presented in this document. The LEK1 cDNA

was partially cloned via reverse transcriptase polymerase chain reaction (RT-PCR) from embryonic heart RNA using degenerate primers based on the sequence of other LEK family members (Goodwin et al., 1999). These clones were then used as probes to screen a whole embryo cDNA library. A Southern blot analysis of mouse genomic DNA using a LEK1 probe reveals a single band, suggesting the presence of only one LEK family member in mouse. Interestingly, a Northern blot displays two closely-spaced bands of 10 kb each. Thus, the *LEK1* mRNA may be alternatively spliced. Previous studies in our laboratory demonstrate that the LEK1 protein undergoes a post-translational cleavage event (Figure 2), at an unknown site, to produce two peptide products: N-terminal cytLEK1 and C-terminal nucLEK1 (Pabon-Pena et al. unpublished data). Most work has focused on the smaller nucLEK1, which is predominantly found in the nuclei of cells.

During embryogenesis, LEK1 is expressed at highest levels during early development (E8.5) in all tissues, not just myocytes as for CMF1, and its expression diminishes as development proceeds (Goodwin et al., 1999). The protein and mRNA cannot be readily detected in adult mice with the exception of the oocyte in females. Interestingly, expression in the heart and liver differs from other tissues, as the *LEK1* mRNA level progressively increases in these organs during the course of embryonic development. In the heart specifically, *LEK1* mRNA is detected until neonatal day 4 (N4), after which point it abruptly disappears. NucLEK1 protein expression follows with a similar decrease after neonatal day 5. Very interestingly, this reduction in LEK1 expression coincides with the period when cardiomyocytes are undergoing permanent cessation of mitosis and terminal differentiation (Soonpaa et al., 1996; Soonpaa and Field, 1998). It was thus postulated that LEK1 may a play a role in this process during cardiac development.

A function for LEK1 in terminal differentiation of cardiomyocytes was supported by the discovery that nucLEK1 binds to all three known Rb family members (Rb, p107, p130) both *in vitro* and *in vivo* (Ashe et al., 2004). This interaction occurs within the critical pocket region of these proteins. In addition to their important effects on cell cycle regulation, Rb family members have been implicated more recently in the control of apoptosis and differentiation during development (Tam et al., 1995). It is currently postulated that nucLEK1 may serve as an inhibitor of Rb family member function by binding and sequestering these proteins, thus maintaining cells in a proliferative, non-differentiative state during development. With

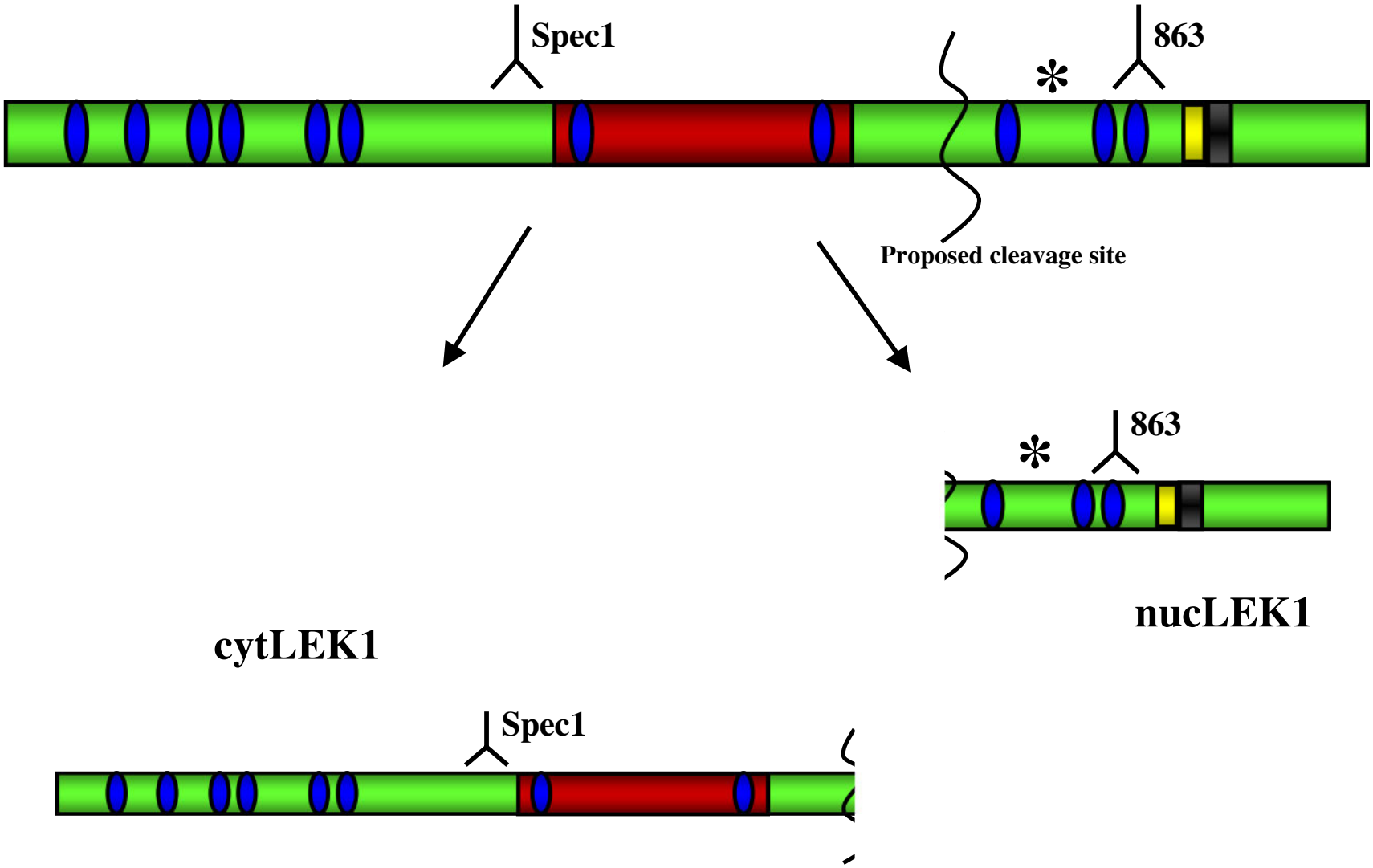

Figure 2. **Cleavage of LEK1 into two peptide products.** LEK1 is post-translationally cleaved into N-terminal cytLEK1 (containing Spec1 antibody epitope) and C-terminal nucLEK1 (863 epitope).

downregulation of LEK1, the anti-proliferative function of Rb family members is then restored and differentiation can proceed.

Indeed, experiments disrupting LEK1 expression support this hypothesis. Cell culture studies in 3T3 fibroblasts reveal that LEK1 depletion using morpholino antisense oligomers results in a G_1/S cell cycle arrest consistent with activation of Rb family member function (Ashe et al., 2004). Additionally, cells are also delayed in G_2/M phase entry. However, cells are eventually able to overcome the cell cycle arrest but cannot maintain this recovery and instead begin to undergo apoptosis. Thus, proper LEK1 expression is required for 3T3 fibroblast proliferation and survival. Additional evidence of a role for LEK1 in cell proliferation and differentiation comes from studies with C2C12 skeletal myoblasts (Ashe et al. unpublished data). It has been observed that these cells express LEK1 in their myoblast state but expression of the protein is downregulated as they undergo differentiation upon serum deprivation. Depletion of LEK1 using morpholino oligomers in C2C12 cells results in premature differentiation as measured by sMHC expression and myotube formation. In summary, these experiments on LEK1 suggest that the protein plays an important role in the regulation of proliferative and differentiative processes during embryonic development.

The Spectrin Repeat

Prior to examination of the specific role of the cytoplasmic cytLEK1 protein, we initially hypothesized that it may have a cytoskeletal function. Our hypothesis of a cytoskeletal role was supported by the presence in cytLEK1 of a single spectrin repeat, which is a domain composed of three antiparallel α-helices in a coiled-coil assembly that is found in a wide array of proteins (Djinovic-Carugo et al., 2002). Typically, a heptad periodicity is evident at the level of the primary sequence, and several aromatic residues within the hydrophobic core of the domain are conserved. The repeats are best known for their presence in multiple copies (4-20) in the spectrin superfamily (α- and β-spectrin, α-actinin, dystrophin, and utrophin) whose members are primarily involved in actin cross-linking. However, they are found in other diverse proteins as well. Various proteins, including the Dbl family, contain single or multiple spectrin repeats that are postulated to act in conjunction with a neighboring Rho-GEF domain but are not always directly involved in cytoskeletal function (Alam et al., 1997; Estrach et al., 2002). As is evident, the roles of spectrin repeats, as well as their exact sequences, are quite varied (Djinovic-Carugo

et al., 2002). Long chains of repeats often separate functional parts of the protein where length can be critical for actin cross-linking. At the same time, repeats of any length can serve as docking regions for proteins involved in cytoskeletal and signal transduction functions. Repeats can also play a role in the formation of protein dimers. In addition, the spectrin repeat is structurally elastic, so it often found in structures such as the sarcomere that are subject to intense amounts of mechanical stress. There are many examples in the literature of known interactions occurring via spectrin repeats: □-spectrin binds ankyrin (Kennedy et al., 1991); □-actinin binds integrins, titin, a LIM protein, and a rho kinase (Otey et al., 1990; Mukai et al., 1997; Xia et al., 1997; Young et al., 1998); and dystrophin binds actin (Rybakova et al., 1996). Thus, it is clear that the spectrin repeat, which is also found in cytLEK1, may serve as a binding site for various proteins, most of which have a cytoskeletal role.

The Role of LIS1

The microtubule network of cells is a key cytoskeletal element and plays a critical role in a range of functions (Lodish, 2004). One of its main partners of action is dynein, a large minus end-directed motor protein. Dynein is important for basic cellular functions in all organisms and has been the subject of extensive research (Gibbons, 1996; Hirokawa, 1998; Banks and Heald, 2001). The process of mitosis is especially reliant on dynein, which plays critical roles in chromosome alignment, spindle orientation, and chromosome movement toward poles. Additionally, dynein function is important for both nuclear and cellular migration. Many vesicles and organelles, such as the Golgi, utilize dynein motor function for proper positioning and trafficking within the cell. However, the precise regulation and mechanism of function of microtubules and dynein remain poorly understood, despite knowledge of their involvement in specific molecular pathways and their interaction with several important partner proteins.

One such partner is LIS1, a 45 kDa microtubule-associated protein with seven WD (tryptophan-aspartic acid) repeats. LIS1 initially generated interest due to the discovery that mutations in the protein are associated with type I lissencephaly in humans (Reiner et al., 1993; Chong et al., 1997; Lo Nigro et al., 1997; Pilz et al., 1998). This disorder is characterized by developmental neuronal defects that result in agyria (smooth brain surfaces) and disordered cortical layering. These abnormalities cause mental retardation, seizures, and other neurological conditions. Interestingly, LIS1 was first studied in the fungus *Aspergillus nidulans*, where the

NudF protein is the homolog to LIS1 and shares 62% identity. Mutation of NudF in fungi causes defects in nuclear migration, a process that is especially critical in this organism, and results in decreased colony size (Xiang et al., 1995). Notably, this phenotype is identical to that which results from mutations of dynein and dynactin in fungi (Beckwith et al., 1998). In fact, a dynein (NudA) mutant is able to suppress the NudF mutation (Willins et al., 1997). Thus, dynein and LIS1 appear to operate in the same genetic pathway. Of interest with respect to our work, NudE mutants exhibit the same nuclear migration phenotype and suppression ability, and NudE has been shown to directly bind NudF (Efimov and Morris, 2000). In support of the phenotype observed in these experiments in fungi, mutations in the yeast homolog of LIS1, Pac1, were examined and discovered to result in an inability to properly orient the nucleus during cell division (Geiser et al., 1997; Lee et al., 2003). These mutant yeast also exhibit defects in mitotic spindle function.

Defects in nuclear positioning and migration are intriguing because of the observed neuronal defects associated with LIS1 mutations in humans. Nuclear migration in fungi bares a significant similarity to the movement of nuclei within migrating neurons during mammalian development. Such neurons first extend leading processes and then require their nuclei to relocate to a final position in the formed nervous system (Wynshaw-Boris and Gambello, 2001). Aberrations in this process lead to improper cellular migration and thus developmental defects. In order to examine the function of LIS1 during mammalian development, a homozygous null mouse for *LIS1* was developed (Hirotsune et al., 1998). *LIS1* is ubiquitously expressed during development and adulthood, but highest levels of the protein are found in neurons. In fact, neurons contain 15 to 30 times as much of the protein as most other cell types. Complete absence of the LIS1 protein results in post-implantation lethality. Thus, LIS1 is absolutely required for embryonic development, especially before E9.5. Animals heterozygous for *LIS1* mutations are viable but exhibit defects in brain structure similar to those observed in humans with lissencephaly (Hirotsune et al., 1998). Compound heterozygous mice have a more severe phenotype and generally die within a few days of birth. The severe brain defects observed consist of enlarged ventricles and disorganization of layers of the cortex and hippocampus. The mutant neurons migrate more slowly *in vitro* and *in vivo*, suggesting that defects in migration are at least partially responsible for the neuronal defects. This is a cell autonomous effect, as migration abilities are not rescued by co-culturing the neurons with wild-type neurons. A different targeted

deletion of *LIS1* in mice has also been created that leads to the generation of a shorter LIS1 protein (Cahana et al., 2001). While the homozygous mice are again lethal, the heterozygous mice are viable and confirm the previous results by displaying abnormalities in brain structure. Mutant neurons from these animals also display decreased migration speeds and, additionally, have aberrant morphology. Finally, LIS1 is also essential in *Drosophila melanogaster*, as mutant flies exhibit defects in nuclear positioning and early embryonic lethality (Liu et al., 1999; Swan et al., 1999; Lei and Warrior, 2000; Liu et al., 2000). Notably, these flies have severe deficiencies in the proliferation of several types of cells, including neuroblasts. In summary, these genetic experiments have shown that mutations of LIS1 likely result in lissencephaly due to defective migration and proliferation of neuronal precursors.

The binding partners of LIS1 provide clues as to how the protein functions in processes such as movement and cell division. While LIS1 is also known as Pafah1b1 for being a non-catalytic subunit of platelet-activating acetylhydrolase isoform Ib (Hattori et al., 1994), its non-enzymatic interactions appear to be of more importance. As was initially suspected in fungi and later confirmed in mammalian cells, LIS1 directly binds to dynein to form a complex that also contains the $p150^{glued}$ subunit of dynactin (Willins et al., 1997; Faulkner et al., 2000; Sasaki et al., 2000; Smith et al., 2000; Tai et al., 2002). Specifically, dynamitin, which is a component of the dynactin complex, and the intermediate and heavy chains of dynein have been shown in these studies to directly interact with the WD repeats of LIS1. Not surprisingly given the relationship between microtubules and dynein, LIS1 is associated, albeit not exclusively, with the microtubule fraction of cell supernatants (Sapir et al., 1997; Smith et al., 2000). Additionally, LIS1 has been shown to bind to the C-terminus of CLIP-170 (Coquelle et al., 2002), a protein involved in dynactin regulation at growing microtubule ends and the kinetochore. LIS1 can also potentially homodimerize, although any importance of such an association is not yet clear. Finally, LIS1 interacts with the two murine isoforms of NudE: NudE and Nudel (Feng et al., 2000; Niethammer et al., 2000; Sasaki et al., 2000). This important set of interactions will be discussed in more detail shortly.

The subcellular distribution of LIS1 fits well with the known characteristics of its binding partners. In neurons of the developing mouse, LIS1 initially has a punctate distribution pattern with a portion of the protein being centrosomal (Sasaki et al., 2000; Tanaka et al., 2004). By neonatal stages, the protein shifts to the axon, where it is predominantly found in adult neurons

in vivo. In neuronal cell cultures, LIS1 is also cytoplasmic with highest concentrations located at cell bodies and growth cones (Smith et al., 2000). The most detailed analyses of the subcellular distribution of LIS1, however, come from studies of non-neuronal cells, especially fibroblasts. In such cells, LIS1 exhibits a predominantly perinuclear punctate localization (Niethammer et al., 2000; Smith et al., 2000). It is found at regions of high microtubule density, including the centrosome, and the protein can also be detected on microtubule tracks (Smith et al., 2000). However, the colocalization between LIS1 and microtubules is not conclusive (Faulkner et al., 2000). In support of co-immunoprecipitation data, both dynein and dynactin colocalize with LIS1 near the nucleus (Smith et al., 2000). However, this colocalization is not complete, especially toward the cell periphery, suggesting that LIS1 does not associate with all dynein and dynactin complexes in a cell. Additionally, LIS1 is present, along with dynein and related proteins, at the leading edge of the cell cortex in migrating fibroblasts, as expected considering its putative role in cell movement (Faulkner et al., 2000; Dujardin et al., 2003). Finally, LIS1 is found, through an interaction with dynein, at the kinetochores of early mitotic cells (Faulkner et al., 2000), which is consistent with a role in dynein-mediated spindle functions during cell division.

The most enlightening data on the function of LIS1 come from experiments looking at its role in various cell culture environments. Emphasizing the critical importance of LIS1 for cellular functions in a wide variety of cell types, these data have been obtained using cells ranging from fibroblasts to neurons to epithelial cells. Overexpression and knockdown studies of LIS1 have revealed a large array of alterations in the localization of LIS1 partner proteins. For example, dynein, dynactin, and Nudel are mislocalized in such experiments (Faulkner et al., 2000; Sasaki et al., 2000; Smith et al., 2000), thus revealing the importance of LIS1 function for the proper cellular distribution of key proteins of the dynein pathway. However, the responses to LIS1 alteration are not consistent among various publications. For example, fibroblasts from *LIS1* heteryzogous mice have been shown to have a more perinuclear accumulation of dynein as a result of this decreased level of LIS1 protein (Sasaki et al., 2000). Paradoxically, overexpression of LIS1 in cultured fibroblasts also results in an inward redistribution of dynein towards the nucleus (Smith et al., 2000). Such seemingly conflicting results, which are very common in the LIS1 field, may perhaps be explained by differences in expression levels or cell

types. However, clearly more work is necessary to determine the exact role of LIS1 in the localization of its binding partners.

As would be expected from a protein interacting with dynein and the microtubule network, LIS1 functional studies have revealed its critical importance with regards to the cytoskeleton. Overexpression of LIS1 has been shown to result in microtubule disarray in interphase cells (Faulkner et al., 2000; Smith et al., 2000). The uniform distribution of microtubules from centrosomes is lost, and the usual radiating arrays from this organizing center are now absent. Importantly, □-tubulin, a key component of the centrosome, remains intact in these cells (Smith et al., 2000), suggesting that the centrosomes are presumably formed and localized properly. Thus, LIS1 is critical for interaction of the centrosome with microtubules but not for the stability of the centrosome itself. The importance of LIS1 in microtubule organization and formation is reinforced by experiments examining microtubule network repolymerization after addition of nocodazole, a microtubule depolymerizing agent. In LIS1-overexpressing cells, microtubule networks are able to reform after nocodazole challenge but in an aberrant fashion (Smith et al., 2000). Fewer of the microtubules are attached to the centrosomes, and, instead, there is an increase in unattached fragments at the cell periphery. Thus, LIS1 may play a role in stabilizing microtubules at the organizing center and also transporting microtubule segments to the periphery.

Since LIS1 is important for microtubule formation and transport, it may also be expected to be involved in the positioning of organelles, usually membranous ones, dependent on dynein and microtubule function. One such organelle is the Golgi apparatus, whose perinuclear localization near the centrosome relies on movement by dynein motors on microtubule tracks (Allan and Vale, 1991; Corthesy-Theulaz et al., 1992). Indeed, alteration of LIS1 function disrupts the normal positioning of the Golgi as observed by using markers specific for this organelle. In fibroblasts heterozygous for *LIS1*, the Golgi is less tightly perinuclear and instead more dispersed throughout the cell (Sasaki et al., 2000; Smith et al., 2000). This defect can be corrected by overexpressing LIS1 in these cells and thus positioning the Golgi closer to the nucleus (Smith et al., 2000). These results suggest that LIS1 plays an important role in the dynein-mediated process of organelle positioning. Once again, however, conflicting results are present, as other studies have revealed no effect on Golgi localization when overexpressing full-length or truncated LIS1 in cells (Faulkner et al., 2000; Tai et al., 2002).

Another key aspect of LIS1 function, based on early *in vitro* and *in vivo* experiments, involves regulation of cell migration (Hirotsune et al., 1998; Cahana et al., 2001). Cell culture experiments have confirmed the importance of LIS1 in cell movement and shed light on the mechanisms involved. Overexpression of LIS1 results in increased migration of neurons (Tanaka et al., 2004), in agreement with the presumed role of LIS1 in enhancing cell movement. Indeed, expression of a dominant negative LIS1 protein in fibroblasts interferes with cell migration (Dujardin et al., 2003). Similar phenotypes are observed in this set of experiments when inhibiting the function of dynactin and dynein, thus suggesting a common role for all these proteins in regulating cell movement. Indeed, all three proteins localize to the leading cell cortex during healing of wounded fibroblast monolayers (Dujardin et al., 2003). Other experiments have suggested that the localization of dynactin to microtubule tips, including at the leading edge, may be dependent on LIS1 (Faulkner et al., 2000). However, recent studies have proposed that other proteins, such as CLIP-170, may be more critical for this process (Lansbergen et al., 2004). Further insight into the mechanism of LIS action on neuronal migration specifically has come from experiments revealing defective coupling of the nucleus and centrosome in migrating neurons from *LIS1* heterozygous mice (Tanaka et al., 2004). These results coincide with the well-known role of LIS1 in nuclear movement in various organisms (Xiang et al., 1995; Geiser et al., 1997; Lei and Warrior, 2000; Lee et al., 2003) and support the model that positioning of the nucleus is important for neuronal motility. Recent data have provided further confirmation of this nucleus-centrosome uncoupling in neurons through the examination of embryos electroporated with LIS1 RNAi (Shu et al., 2004). Notably, doublecortin (DCX) has been revealed to have a similar function to LIS1 with regard to this coupling process in neurons and can even rescue *LIS1* mutants (Tanaka et al., 2004).

The final important role of LIS1 in cellular processes involves another critical dynein-regulated microtubule process: mitosis. Overexpression of both full-length and dominant negative LIS1 proteins in cells has severe effects on spindle organization and mitotic progression (Faulkner et al., 2000; Tai et al., 2002). The phenotypes observed are very similar to those resulting from overexpression of the dynamitin subunit of dynactin, a key regulator of spindle function (Echeverri et al., 1996). An overall increase in mitotic index is observed, and the cells have disrupted spindle organization with abundant multipolar spindles evident (Tai et al., 2002). Additionally, unaligned chromosomes are prominent, suggesting that LIS1 plays a role both in

spindle formation and in spindle attachment to the kinetochores of chromosomes. Further experiments utilizing injection of anti-LIS1 antibodies reveal similar mitotic defects, such as an increased duration of prometaphase and misalignment of chromosomes (Faulkner et al., 2000). Notably, removal of endogenous LIS1 from the kinetochore does not alter the attachment of other critical components within that structure (Tai et al., 2002), thus suggesting that LIS1 plays a separate role in kinetochore function from affecting kinetochore formation. Indeed, LIS1 may bind to the kinetochore through direct interactions with motor proteins, especially the dynein-dynactin complex (Tai et al., 2002).

In summary, a crude model for LIS1 function can be proposed at this point from the current body of literature. Throughout the cell, the primary effects of LIS1 appear to result from its interactions with dynein-mediated processes. In the cytoplasm, LIS1 promotes the outward movement of microtubule segments, which is critical for migration, through its interaction with non-translocating dynein motors. Conversely, non-tethered motors act with LIS1 to bring dynein, dynactin, and membranous organelles, such as the Golgi, towards the centrosome. Similar processes may be at work in retrograde axonal transport within neurons. Additionally, LIS1 plays a role at the centrosome in both the organization of the microtubule network and the coupling of the centrosome to the nucleus as part of a critical process for neuronal migration. The exact function of LIS1 at microtubule ends near the cell cortex remains unclear at the moment. In mitotic cells, LIS1 is involved in spindle formation and maintenance, kinetochore attachment to the spindle, and chromosome organization. Whether LIS1 is required for the dynein-mediated process of chromosomal kinetochore-to-pole movement is still unknown, because the severe effects of LIS1 dysfunction at early mitotic stages have precluded examination of later mitotic events. Importantly, each of these functions of LIS1 listed above is still not well-understood and significant gaps remain as to the exact nature of interactions that are involved in each process. However, considerable progress has been made in recent years in better understanding the exact mechanism of LIS1 action, and the LIS1-interacting proteins NudE and Nudel have emerged as important players in several of these cellular events.

NudE(L) Function in the LIS1 Pathway

NudE and Nudel are protein isoforms that are mammalian homologs of the *nudE* gene product of *A. nidulans*. As has been previously mentioned, *nudE* is a genetic suppressor of

mutations in the LIS1-dynein pathway in this organism (Efimov and Morris, 2000), and thus is considered to be an important member of this pathway. NudE and Nudel are highly conserved among all mammals, although their murine isoforms will be the primary focus of this discussion, and share 55% sequence identity. As will be explained in further detail, these proteins have slightly different expression patterns and distinct but overlapping functions. It is still unclear exactly what their separate roles are, and thus they are sometimes grouped together here and referred to as NudE(L). *Nudel* mRNA is present throughout the mouse but is found at highest levels in the brain, kidney, ovary, and heart (Sasaki et al., 2000). *Nude* mRNA exhibits a similar pattern with overall lower levels of expression, except in the brain and ovary (Feng et al., 2000; Sasaki et al., 2000). NudE and Nudel proteins have a similar distribution to each other with highest levels found in the brain, heart, skeletal muscle, and testis (Niethammer et al., 2000; Sasaki et al., 2000; Yan et al., 2003). Although there is not complete agreement on this point, Nudel may be slightly more abundant overall in the mouse than NudE (Feng and Walsh, 2004). Notably, there is a difference in the timing of expression of these two isoforms during development. Nudel is first detected at embryonic day 13.5, and it begins to accumulate until neonatal day 5 (Niethammer et al., 2000; Sasaki et al., 2000). After that point, it is expressed in a fairly stable fashion throughout adulthood. On the other hand, *NudE* appears at embryonic day 11 and peaks five days later (Feng et al., 2000). It then begins to slowly decrease to a low level maintained through adulthood. This difference in expression timing alone suggests that NudE may be more important during early to mid embryonic development, whereas Nudel may play a larger role in late embryonic development continuing into adulthood. However, such delineation in the roles of these two proteins during development has not yet been achieved.

The binding partners of NudE and Nudel shed light onto their expected subcellular distributions and functions. Both proteins were discovered in yeast two-hybrid screens for LIS1 interactors (Feng et al., 2000; Niethammer et al., 2000; Sasaki et al., 2000). Interestingly, the two proteins were also detected in two-hybrid assays as interactors of Mitosin/CENP-F, the human member of the LEK family (Feng et al., 2000; Yan et al., 2003). However, this interaction was not pursued any further by the relevant laboratories. Additional yeast two-hybrid and co-immunoprecipitation studies have confirmed the interaction of NudE(L) with LIS1 and revealed an additional interaction with dynein (Feng et al., 2000; Niethammer et al., 2000; Sasaki et al., 2000). While each experiment notes a different dynein chain (heavy, intermediate, and light), the

importance of this observation is not especially significant, as the interaction of NudE(L) with the larger dynein complex is the critical finding. Studies utilizing truncated Nudel proteins have narrowed the LIS1-binding domain to the N-terminal coiled coil of Nudel, which is a highly conserved region (85% identity) with NudE (Sasaki et al., 2000). In fact, the interaction of LIS1 with NudE also requires the coiled coil domain of NudE (Feng et al., 2000). Interestingly, the dynein-binding domain in Nudel is C-terminal and interacts with two separate domains within the dynein heavy chain (Sasaki et al., 2000). Only one of these domains in dynein is involved in LIS1-dynein binding, suggesting that Nudel may possibly play a complex role in regulating interactions of other proteins with dynein. Sciatic nerve ligation studies suggest that LIS1 and Nudel do indeed associate with dynein motors during retrograde transport (Sasaki et al., 2000). In addition to the interaction with dynein and LIS1, there are other less studied interactions worth noting. It has been shown that both NudE and Nudel can homodimerize, likely through an N-terminal region, which does not overlap any other known functional domains (Sasaki et al., 2000; Feng and Walsh, 2004). The importance of this observation is just now being unraveled. Finally, NudE specifically can be co-immunoprecipitated with □-tubulin, a key component of the centrosome (Feng et al., 2000). However, it is unclear whether this interaction is direct or whether both proteins are simply part of the same larger complex.

The known protein interactions of NudE and Nudel are in agreement with results from further biochemical experiments. For example, Nudel is primarily isolated in the insoluble fraction of cell lysates (Niethammer et al., 2000), consistent with a protein that is part of membranous or cytoskeletal structures. Additionally, the importance of the NudE-LIS1 interaction is reinforced by the fact that missense mutations in LIS1 related to lissencephaly abolish the binding between these two proteins (Feng et al., 2000). This result suggests that interference with NudE function may be partially responsible for the defects observed in that disease.

As would be expected from their homology and similar binding partners, NudE and Nudel also exhibit fairly similar subcellular distributions in a wide variety of cell types. In embryonic neurons, Nudel is first detected in a perinuclear region around the centrosome, but it slowly migrates to the axon in postnatal stages and remains there throughout adulthood (Sasaki et al., 2000). In general, in most cell types examined, NudE and Nudel have a perinuclear distribution with concentration of the protein around the centrosome (Feng et al., 2000;

Niethammer et al., 2000; Yan et al., 2003). However, it is worth reiterating that the proteins have both a centrosomal and non-centrosomal distribution and do not exhibit an exclusive preference for either. The exact nature of the distribution seems to be related to the cell cycle, as will be discussed shortly, and to the cell type, as COS-7 cells have more NudE at centrosomes (Yuanyi Feng, personal communication) while mouse embryonic fibroblasts have little evident centrosomal localization of Nudel (Niethammer et al., 2000). Consistent with the binding data, Nudel has been shown to colocalize throughout the cell, including the periphery, with dynein (Niethammer et al., 2000). Interestingly, this colocalization with dynein away from the nucleus is specific to Nudel, as it is not evident with LIS1 (Smith et al., 2000). Clearly, however, the localization and function of LIS1 are important for the distribution of Nudel, as overexpressing LIS1 leads to increased accumulation of Nudel near the nucleus (Niethammer et al., 2000). Conversely, fibroblasts from *LIS1* heterozygous mice have more dispersed Nudel within the cell, although this result has not been consistently observed (Sasaki et al., 2000).

Since the LIS1 pathway is important for cell division, the subcellular distribution of NudE and Nudel has also been examined in mitotic cells. Very interestingly, both proteins have been observed on mitotic spindles and colocalize on these structures with dynein (Yan et al., 2003; Feng and Walsh, 2004). While one laboratory has observed NudE on chromosomal kinetochores (Feng and Walsh, 2004), as has been noted for other LIS1 family members, another group did not detect Nudel on kinetochores (Yan et al., 2003). It remains unclear whether this is due to actual differences between NudE and Nudel or due to variations in techniques and reagents used. NudE has further been observed at the cleavage furrow of dividing cells (Feng and Walsh, 2004). Both NudE and Nudel have been detected at the spindle poles of mitotic cells, but the localization of the latter there is not as prominent (Yan et al., 2003; Feng and Walsh, 2004).

Interestingly, localization of NudE(L) to sites such as the spindle poles may be dependent upon phosphorylation status. It was initially observed that Nudel exists as a doublet on Western blots from brain lysate (Niethammer et al., 2000; Sasaki et al., 2000), suggesting the presence of a post-translational modification. Indeed, Nudel is a phosphorylation substrate of cyclin-dependent kinase 5 (cdk5), a serine/threonine kinase involved in neuronal migration (Niethammer et al., 2000; Sasaki et al., 2000). Interestingly, it has been shown that inhibition of this phosphorylation event in neurons results in a more focused distribution of Nudel within the cell (Niethammer et al., 2000; Sasaki et al., 2000). More recent data suggest that 14-3-3 proteins

may also play a role in regulating Nudel phosphorylation by cdk5 (Toyo-oka et al., 2003). Further experiments have revealed that Nudel may be a phosphoprotein in various cell types during mitosis, specifically, due to cell cycle-dependent phosphorylation by cdc2 and/or Erk2 (Yan et al., 2003). Notably, cdc2 kinase is involved in control of the G2/M transition (Smits and Medema, 2001). Studies using mutant Nudel proteins suggest that this phosphorylation event may be responsible for translocating Nudel from the centrosome/spindle poles to the spindle itself upon the onset of mitosis (Yan et al., 2003). Additionally, phosphorylated Nudel has increased affinity for LIS1 (Yan et al., 2003), so this modification may function to regulate interactions between various LIS1 family members. It is unclear, however, whether phosphorylation of NudE has any role endogenously. While transfected NudE protein can be phosphorylated by cdc2, there are no data utilizing a NudE-specific antibody against endogenous protein (Yan et al., 2003). Additionally, endogenous NudE, unlike Nudel, is detected as a single band on Western blot (Feng et al., 2000). Thus it would appear that, unlike for Nudel, there is little direct evidence to suggest that phosphorylation of NudE normally occurs and is important for NudE function.

Recently, *NudE* and *Nudel* knockout mice have been generated. The *Nudel* -/- mice are early embryonic lethal and have not yet been thoroughly examined (Hirotsune et al. unpublished data). The absolute necessity of Nudel is not surprising, as depletion of Nudel in cell culture using RNAi results in massive cell death (Liang et al., 2004). Interestingly, NudE is able to partially rescue the defect in this system, even though its presence in *Nudel* knockout mice is not sufficient to eliminate or severely delay embryonic lethality. *NudE* knockout mice, on the other hand, are viable into adulthood (Feng and Walsh, 2004). The primary phenotype examined so far relates to development of the brain, even though the mice also have defects in other tissues (Yuanyi Feng, personal communication). The *NudE* -/- mice have significantly smaller brains than wild-type or *NudE* +/- littermates, as a result of a thinner and smaller cortex (Feng and Walsh, 2004). Notably, this is not due to an increase in apoptosis. Instead, the microcephaly is a result of defective neuronal migration and neurogenesis, which are processes also disrupted in *LIS1* mutant organisms (Hirotsune et al., 1998; Liu et al., 2000). More specifically, there is a decrease in the number of cortical progenitor cells in the brains of *NudE* -/- mice due to mitotic defects (Feng and Walsh, 2004). These abnormalities consist of altered cleavage planes, mislocalized chromosomes, and abnormal spindle assembly and structure. Once again, many of

these defects have been observed when disrupting LIS1 function (Faulkner et al., 2000; Tai et al., 2002). Supporting data on NudE function come from *Xenopus laevis* experiments. Injecting truncated *NudE* mRNA coding for only the LIS1-binding domain into embryos results in severe defects in formation of the brain and eyes (Feng et al., 2000). Although the authors did not observe any abnormalities in other tissues, they attribute this to a possible dosage effect, suggesting that NudE may be most critical for development of head structures.

Cell culture studies provide further evidence as to the cellular roles of NudE and Nudel. Overexpression of Nudel, but not LIS1 in the same set of experiments, has been shown to shift dynein localization more to the periphery (Niethammer et al., 2000). These data suggest that Nudel may play a role in directing the motor protein to its proper subcellular position. However, other experiments have shown the exact opposite result where there is no effect on dynein placement from full-length Nudel, while LIS1 does have an effect (Sasaki et al., 2000; Smith et al., 2000). Instead, expression of a dominant negative form of Nudel causes a change in dynein localization (Sasaki et al., 2000). Under these conditions, dynein becomes more concentrated around the nucleus, consistent with *LIS1* +/- cell data from the same laboratory but not other independent experiments on LIS1 (Sasaki et al., 2000; Smith et al., 2000). With regard to NudE, overexpression of the protein in cells results in disordered microtubule arrays that radiate from the areas of highest NudE expression, rather than the centrosomes (Feng et al., 2000). Additionally, the normal distribution of □-tubulin is disrupted and this centrosomal protein diffuses throughout the cytoplasm. These data are consistent with a protein that is part of the LIS1 pathway of microtubule regulation and that also has been shown to be a component of the centrosome. The authors suggest that NudE may thus regulate formation of the centrosome. Notably, other studies on Nudel mutants do not reveal, albeit in data not shown, any disorganization of microtubules (Liang et al., 2004). Once again, it is unclear if this represents a fundamental difference between NudE and Nudel functions or differences in underlying experimental techniques.

Building upon the data concerning localization changes of LIS1 pathway proteins, research has begun to examine the broader role of NudE and Nudel in cellular functions of this pathway. As has been previously mentioned, dynein is essential for the positioning of many membranous organelles near the nucleus in a microtubule-dependent fashion. To examine the role of Nudel on such processes, a dominant negative approach was used (Liang et al., 2004).

Nudel mutants lacking either the dynein-binding or LIS1-binding domain exhibited notable phenotypes, whereas full-length Nudel and, interestingly, double mutant Nudel (both dynein- and LIS1-binding domains absent) showed less severe effects. Thus, the function of Nudel in LIS1 pathway processes appears to require both binding domains, suggesting that the interplay of dynein, LIS1, and Nudel is critical for dynein activity. Studies utilizing Nudel RNAi support this model by revealing that Nudel knockdown results in decreased association of LIS1 with dynein (Shu et al., 2004). The phenotypes observed from expression of the dominant negative Nudel binding domain mutants consist of fragmentation and dispersion of lysosomes, endosomes, and the Golgi (Liang et al., 2004). There is also a reduction in protein secretion. Interestingly, these effects are specific to the function of minus end-directed motors, such as dynein, as vesicles relying on kinesin motors for movement remain unaffected. Additionally, lysosome trafficking was observed in living cells and found to be inhibited, but only with respect to inward dynein-dependent motion. These results are supported by Nudel RNAi experiments that reveal Golgi fragmentation due to Nudel knockdown (Liang et al., 2004).

Further experiments utilizing Nudel RNAi have revealed additional effects on LIS1 pathway functions. Nudel knockdown results in an accumulation of microtubules near the nucleus after a combination nocodazole/vinblastine treatment (Shu et al., 2004). Thus, Nudel is important for microtubule transport to the periphery, as has been noted for LIS1 in similar experiments (Smith et al., 2000). Nudel is also required for neurofilament assembly and transport, and thus neuronal integrity (Nguyen et al., 2004). Administration of Nudel RNAi to a neuroblastoma cell line results in changes similar to those observed in neurodegenerative processes. Another important phenotype arising from Nudel knockdown relates to processes critical for neuronal migration. Depletion of Nudel using RNAi results in an inhibition of nuclear translocation, as measured by nuclear migration distance, and causes nuclei to oscillate randomly (Shu et al., 2004). As a reminder, movement of neurons requires leading process extension, nuclear translocation, and trailing process retraction (Wynshaw-Boris and Gambello, 2001). The microtubule network forms a connection from the cell cortex to the centrosome to the nucleus that is critical for this migration process. Careful examination of the Nudel-depleted cells reveals that there is a loss of this critical microtubule structure normally surrounding the nucleus and connected to the centrosome (Shu et al., 2004). As a result, the distance between centrosome and nucleus is significantly increased in these cells, as has been previously observed in *LIS1* +/-

neurons (Tanaka et al., 2004). Somewhat surprisingly, there are no changes in microtubules at the leading edge, despite the presence of several LIS1 pathway members there.

To further study these processes in an *in vivo* environment, Nudel RNAi was administered *in utero* and formation of the brain examined (Shu et al., 2004). As expected, the authors observe severe defects in positioning of neurons due to abnormalities in neuronal migration. However, there are no changes in proliferation, which is surprising given other NudE and LIS1 studies (Faulkner et al., 2000; Tai et al., 2002; Feng and Walsh, 2004), or in leading process movement. Instead, an increase in the nucleus-centrosome distance is again observed, suggesting an uncoupling of these two structures (Shu et al., 2004). This Nudel-knockdown phenotype can be partially rescued by overexpressing LIS1. Conversely, however, Nudel is unable to abrogate effects caused by LIS1 depletion. A model is proposed where Nudel and LIS1 activate dynein, and, in turn, dynein sustains microtubule bundles between the nucleus and the centrosome. Dynein then moves along this microtubule network towards the centrosome, thus also pulling the nucleus along and allowing neuronal migration to proceed. The role of doublecortin, which has been shown to also regulate nucleus-centrosome distance (Tanaka et al., 2004), in relation to Nudel is currently unclear.

Finally, the role of NudE in mitotic processes has been more carefully examined in cell culture to better understand the cell division defects observed in *NudE* knockout mice (Feng and Walsh, 2004). A novel approach was taken that emphasized examining the function of the homodimerization domain in NudE. The authors used dominant negative constructs that were deficient for self-association but contained all other known binding domains within NudE. The effects of such mutants would then presumably be primarily the result of inhibiting self-association of NudE. The authors do note, however, that due to the high homology (90%) of the truncated region to Nudel, some effects may also be caused by Nudel dysfunction. Also, any currently unknown interactions involving this domain would be disrupted. Interestingly, expression of these dominant negative mutants, and full-length NudE to a lesser extent, results in severe mitotic arrest of cells in culture (Feng and Walsh, 2004). Mono- and multi-polar spindles are observed, as well as mispositioned spindles. Since expression of the NudE mutants very quickly results in abnormal centriole numbers, defective centrosome duplication may be occurring and at fault for many of the defects. Notably, there is no increase in microtubule depolymerization, suggesting that the effects noted may indeed be specific to the role of the self-

association domain of NudE. The authors also do not observe any mitotic defects with LIS1 overexpression in their experimental system, despite reports to the contrary (Faulkner et al., 2000), and suggest that NudE may perhaps be more required for mitotic progression than LIS1. In combination with the *NudE* knockout mouse data (Feng and Walsh, 2004), the above results suggest that NudE plays a critical role in spindle formation and function, and disruption of this pathway is especially detrimental to progenitor cells and their subsequent migration and differentiation.

In summary, an early model for NudE(L) function is emerging from these published data (Figure 3). While the exact nature of the difference between NudE and Nudel is not yet well-understood, the two isoforms share significant similarities and are grouped together for our purposes here. The characterized interactions for NudE(L) are with dynein and LIS1. The three-way interplay of these proteins is crucial for proper LIS1 pathway function, although any role of phosphorylation in regulating these interactions remains unclear. The localization of NudE(L), and thus presumably its site of action, in non-dividing cells is predominantly around the nucleus with a fraction of the protein located at the centrosome. Its presence on the spindle apparatus during mitosis underlies its importance in directing proper cellular division. While it plays an important role during brain development, NudE(L) function extends to other tissues, signifying its importance in many aspects of embryonic development. In a wide range of cell types, NudE(L) has been shown to be involved in activities of the LIS1 pathway, such as microtubule organization and organelle positioning. Its critical developmental functions primarily encompass the processes of migration and proliferation. More specifically, its role in nucleus-centrosome coupling is essential for proper nuclear translocation during cell movement. Additionally, it regulates spindle assembly and function, potentially through homodimerization. Despite recent progress in this research field, the precise role of NudE(L) within the still-evolving family of LIS1 pathway members remains unclear. Importantly, while several functions of NudE(L) have been derived experimentally, the mechanisms behind these effects are almost completely unknown. Discovery of additional binding partners may be required in order to generate a true model for NudE(L) action.

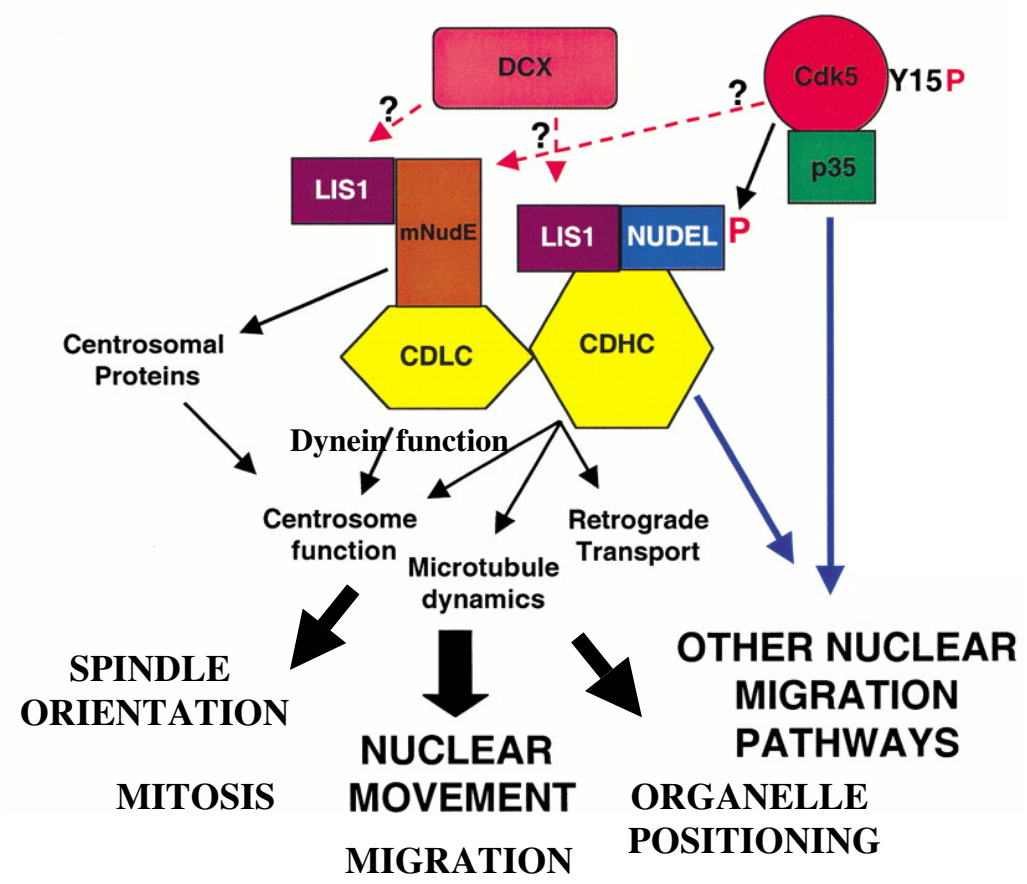

Figure 3. **Model of LIS1 pathway**. See text for details. Adapted from Wynshaw-Boris et al., 2001.

Summary of this Thesis

In the studies presented here, we reveal that cytLEK1 binds NudE and is a novel member of the LIS1 pathway. Thus, examination of cytLEK1 may be a key factor to better understanding the functions of this pathway, which is extremely important for a diverse set of developmental processes. LIS1 pathway members play a critical role in fundamental cellular processes, such as differentiation, proliferation, and migration. Therefore, determining the precise nature of their actions will lead to significant insight into the complex process of embryogenesis. However, the functions of LIS1 pathway members, despite their importance, remain poorly understood at the present time. Our studies here provide additional insight into the proteins involved in the regulation of the LIS1 pathway. In chapter II, we present data on the expression and localization of cytLEK1 in various cells and tissues. In addition to revealing, for the first time, the exact nature of cytLEK1 distribution, experiments in this chapter provide further evidence suggestive of the action of cytLEK1 as a regulator of the LIS1 pathway. In chapter III, we show that cytLEK1 and NudE interact through distinct domains in each protein. We confirm the validity of this interaction through detailed colocalization studies. Finally, in chapter IV, we reveal the functional importance of this cytLEK1-NudE interaction on the LIS1 pathway, especially with regard to morphology and microtubule regulation. Finally, we discuss the implications of our research within a model for cytLEK1 action and elaborate on future experiments needed to further examine the role of cytLEK1. Taken together, our studies reveal that cytLEK1 is essential for cellular functions regulated by the LIS1 pathway and thus may play a critical role in fundamental processes during development.

CHAPTER II

CHARACTERIZATION OF LEK1 EXPRESSION AND DISTRIBUTION

Introduction

The LEK family of proteins consists of molecules with diverse expression patterns and functions (see Introduction). Mitosin/CENP-F has a cell cycle-specific expression pattern and localizes predominantly to the chromosomal kinetochore during mitosis (Liao et al., 1995; Zhu et al., 1995b). CMF1 expression, on the other hand, is regulated during embryonic development with a tissue specificity for striated myocytes (Wei et al., 1996; Dees et al., 2000; Pabon-Pena et al., 2000). It has a dynamic localization that changes from the nucleus to the cytoplasm as the chick embryo matures. In addition to its own unique expression pattern, LEK1 exhibits an added level of complexity, as it is post-translationally cleaved to produce two peptide products: cytLEK1 and nucLEK1. Initial studies have focused almost exclusively on examination of nucLEK1 (Goodwin et al., 1999; Ashe et al., 2004). This protein localizes to the nucleus of cells in most developing tissues. Its expression diminishes as development proceeds until it is essentially absent in adult mice (Goodwin et al., 1999). In the heart, the nucLEK1 protein rapidly disappears after neonatal day 5, which coincides with the period when cardiomyocytes are undergoing permanent cessation of mitosis and terminal differentiation (Soonpaa et al., 1996; Soonpaa and Field, 1998). Unlike nucLEK1, the expression pattern and localization of cytLEK1 in the developing mouse and in cultured cells has never been previously examined in detail. Thus, we wished to characterize the distribution of cytLEK1 in order to compare it to other LEK family members, including nucLEK1, and to gain insight into its function. Importantly, the discovery of its interaction with NudE, a LIS1 pathway member, directed us to more carefully examine the presence of cytLEK1 on certain subcellular structures related to this pathway.

In this chapter, we present data investigating the expression and distribution of cytLEK1 in several cell lines and tissues during murine development. Similar to nucLEK, cytLEK1 exhibits a dramatic decline in protein level in the heart at postnatal stages. Importantly, this decrease coincides with a distinct change in the localization of cytLEK1 in this tissue. Examination of cytLEK1 and nucLEK1 expression in additional developing tissues provides insight into the wide distribution of these proteins and helps direct further functional studies.

Observations from cultured cells confirm and build upon previous data concerning the general subcellular distribution pattern of cytLEK1 and nucLEK1. The results from 3T3 fibroblasts and C2C12 myoblasts additionally provide novel and important insights into the localization of these proteins on the spindle apparatus during mitosis. Pre-extraction studies support the role of cytLEK1 in the cytoskeletal functions that are discussed in later chapters. Additionally, transfected cytLEK1 protein exhibits a colocalization with the microtubule network, suggestive of an important link to the cytoskeleton. In order to create further reagents for these types of experiments, five new polyclonal antibodies to cytLEK1 and nucLEK1 were developed and characterized. In summary, the experiments in this chapter, for the first time, study cytLEK1 expression and localization. These data reveal that cytLEK1 exhibits a developmentally-regulated distribution with some tissue-specific differences and that it appears to interact with key cytoskeletal components. Both cytLEK1 and nucLEK1 also have the potential to function in mitotic processes based on their presence on the spindle apparatus. These results are consistent with data presented in this document on cytLEK1 regulation of the LIS1 pathway and help guide future functional experiments.

Materials and Methods

Tissue preparation for immunohistochemical analysis

Mouse embryonic tissues were isolated and washed in PBS prior to placement in O.C.T compound (Sakura). This mixture was then frozen in a methanol/dry ice bath and stored at –20˚C until sectioning. Frozen tissues were cryosectioned with a thickness of 7 μm on a Jung CM 3000 cryostat (Leica). Successive sections were collected on gelatin coated slides and stored at –20˚C until immunohistochemical analysis.

Tissue preparation for western blot analysis

Mouse embryonic tissues were isolated and washed in PBS. Samples were mixed with 5X sample buffer (0.312 M Tris-HCl pH 6.8, 10% sodium dodecyl sulfate, 25% 2-mercaptoethanol, 0.05% bromophenol blue) prior to three rapid pulses on a sonicator (Virtis) on ice. Samples were then placed at 95˚C for 5 min and stored at –80˚C until Western blot analysis.

Affinity purification of rabbit polyclonal antibodies

Five polyclonal antibodies to LEK1 peptides were generated in rabbits (Biosynthesis). Three of these antibodies were against cytLEK1 peptides and were named based on the letter "C" followed by the approximate amino acid location of the injected peptide in the LEK1 sequence. Their names and peptide sequences were as follows: C264 (DCSSLPGEPHSAQLLHQA), C1127 (NTNKHSMSATD), and C1403 (LSSKEVRVHFAELQEKF). Two of the antibodies were against nucLEK1 peptides and were named based on the letter "N" followed by the approximate amino acid location of the injected peptide in the LEK1 sequence. They were as follows: N2088 (ECEKQTISKALEVALK), and N2690 (SCRQLEGEKEMLQKEL).

The antisera were affinity purified using the injected peptide and a SulfoLink kit (Pierce). The manufacturer's protocol was modified to accommodate standard published methods (Backstrom and Sanders-Bush, 1997). Briefly, the SulfoLink Coupling Gel was equilibrated with Coupling Buffer. The peptide (Biosynthesis) was coupled to the column by mixing with the Coupling Gel for a 2 h incubation followed by three washes with Coupling Buffer. To block nonspecific binding sites, the coupled column was incubated with 0.05 M cysteine in Coupling Buffer for 30 min with mixing. The coupled column was then washed four times with Wash Buffer, three times with high salt (500 mM NaCl) Tris pH 7.6, and three times with Elution Buffer. The coupled column was then equilibrated by washing three times with TBS. Each antiserum was diluted with an equal volume of TBS prior to filtration (0.25 □m pore size). The filtered antiserum was then added to the coupled column and allowed to flow through. This was followed by three washes of the coupled column with Sample Preparation Buffer and three with high salt TBS. The protein was eluted by applying glycine buffer (50 mM pH 2.7). Eluate was collected in 1 mL fractions. Protein concentration of each fraction was estimated by determining the OD_{280} (Shimadzu). Fractions of interest were pooled and neutralized by the addition of 1 M Tris pH 9.5.

To confirm specificity, all antibodies were subject to peptide competition for both immunofluorescence and Western blot applications. To ensure complete competition, a one hundred molar excess of peptide was added, as calculated by determining antibody concentration and total number of epitope binding sites. Antibody was mixed with peptide in 1% BSA in PBS

(immunofluorescence) or TBST (Western blot) for 1 h during sample incubation. Testing was conducted against endogenous LEK1 and transfected protein.

Cloning of cytLEK1

Since the full cytLEK1 cDNA had never been cloned, a reverse transcription polymerase chain reaction (RT-PCR)-based approach was utilized to complete this project. Attempted cloning from bacteriophage cDNA libraries was not fruitful due to the large size of the cytLEK1 transcript (approximately 6.5 kb). Additionally, the length and A/T-richness of the transcript required the use of special RT-PCR systems adapted for such conditions. As the yield of full-length cytLEK1 from RT-PCR was insufficient for further cloning, a two-step approach was used to amplify two overlapping fragments of cytLEK1. Thus, one RT-PCR reaction utilized a FLAG-and-MluI-containing forward primer complementary to the start site of LEK1 and a reverse primer complementary to a unique SphI site at 3185 bp of LEK1. The second reaction consisted of a forward primer complementary to this same SphI site and a reverse primer containing a complementary stop codon and SalI site. Together, these two fragments covered the 1-6630 bp region of LEK1 and thus slightly more than the predicted size of full length cytLEK1. Each fragment was amplified on an iCycler gradient PCR machine (Bio-Rad) from 200 ng E10.5 mouse heart RNA (provided by Dr. Mabelle Ashe) using the Superscript One-Step RT-PCR system (Invitrogen). Each RT-PCR product was gel purified using a QiaQuick kit (Qiagen) and cloned into the pCR-XL-TOPO vector for large inserts (Invitrogen). Clones were then fully sequenced and compared to each other and the at-the-time incomplete LEK1 sequence from NCBI and Celera. The two clones with the most accurate sequences were selected for further experiments. This analysis revealed four total point mutations, which were not silent, likely caused by the high fidelity Taq polymerase utilized in the Superscript kit. Each of these point mutations was corrected through a PCR-based site-directed mutagenesis approach. A triple ligation (MluI/SphI/SalI) was then performed to join the two cytLEK1 fragments in pCI-neo (Promega). Sequencing confirmed the success of the ligation in forming pCI-neo-cytLEK1 containing the 1-6630 bp region of LEK1 with a 5' FLAG tag. The final sequence of full-length LEK1 had now been obtained for the first time and was submitted to NCBI.

Cell culture

COS-7 and NIH 3T3 cells (ATCC) were maintained in Dulbecco's Modified Eagle's Medium (DMEM; Cellgro) supplemented with 10% fetal bovine serum, 100 μg/mL penicillin/streptomycin, and L-glutamine. C2C12 cells (ATCC) were grown in Dulbecco's Modified Eagle's Medium (DMEM) supplemented with 20% fetal bovine serum, 100 μg/mL penicillin/streptomycin, and L-glutamine. All cell lines were maintained in a 95% air-5% CO_2 humidified atmosphere at 37˚C.

Transfections

3T3, COS-7, and C2C12 cells were grown to 40-60% confluency and transfected using FuGENE6 (Roche) per manufacturer's instructions. Briefly, FuGENE was added to a tube containing OptiMEM medium (Cellgro) and gently mixed. DNA was then added and gently mixed. After a 15 min incubation, the FuGENE-DNA mixture was pipetted into wells containing cells and fresh medium. For each well of a 4-well slide, 0.25 μg of total DNA was utilized for transfection. For each 10 cm plate, 3 μg of total DNA was utilized for transfection. Cells were generally grown for 24-48 h prior to collection for further examination.

Western blotting

Lysates were incubated with 5X sample buffer (0.312 M Tris-HCl pH 6.8, 10% sodium dodecyl sulfate, 25% 2-mercaptoethanol, 0.05% bromophenol blue) for 5 min at 95˚C. After boiling, samples were separated by sodium dodecyl sulfate-polyacrylamide gel electrophoresis (SDS-PAGE). Proteins on the gel were transferred overnight on ice to 0.45 μm pore size Immobilon-P PVDF transfer membrane (Millipore). Membranes were blocked with 2% BSA in TBST for 1-2 h at room temperature. Primary antibody was then applied for 1-2 h with shaking. After three washes with TBST, the membrane was incubated with alkaline phosphatase-conjugated secondary antibody for 1 h with shaking. This was followed with three TBST washes and one alkaline phosphatase buffer wash. Membranes were developed using NBT-BCIP (Roche) in alkaline phosphatase buffer and scanned into digital format (Hewlett-Packard).

Immunochistochemistry and microscopy

Cells grown on glass chamber slides (Nalge Nunc) or frozen tissues on gelatin coated slides were gently washed with PBS and fixed with 70% ethanol for 20 min. Samples were then washed briefly in PBS, permeabilized with 0.25% Triton X-100 in PBS for 10 min, and blocked in 2% BSA in PBS for a minimum of 1 h. Primary antibodies in 1% BSA in PBS were applied overnight at 4˚C. After three PBS washes, secondary antibodies were applied for 1 h at room temperature. The slides were washed three times with PBS and twice with water before cover slips were attached with Aqua Poly/Mount (PolySciences). Cells were visualized by fluorescence microscopy on an AX70 (Olympus) or, for confocal analysis, an LSM510 (Zeiss) microscope. Digital images were captured and processed using Magnafire (Optronics), Metamorph (Universal Imaging), and Photoshop (Adobe) software.

Antibodies

A polyclonal anti-FLAG antibody was acquired from Sigma. The monoclonal antibody against □-tubulin was also manufactured by Sigma. The polyclonal antibodies against dynein and CENP-A were purchased from Santa Cruz. Polyclonal antibody Spec1 to a cytLEK1 peptide (aa 1826-45) was generated in rabbits (Biosynthesis) and affinity purified using the injected peptide (Backstrom and Sanders-Bush, 1997). Polyclonal antibody 863 to a nucLEK1 peptide (aa 2872-88 aa) was similarly prepared. Alexa 488 and Alexa 568 conjugated secondary antibodies were obtained from Molecular Probes. Anti-mouse alkaline phosphatase conjugated secondary antibodies for Western blot were purchased from Sigma. DAPI was used to visualize nuclei (Boehringer Mannheim).

Results

Characterization of LEK1 antibodies

For reference, an initial series of characterization studies of the previously established cytLEK1 (Spec1) and nucLEK1 (863) antibodies was conducted and is presented here. Both of these antibodies have been extensively and successfully examined in the past for specificity to LEK1, including through expression library screens and *in vitro* translational studies (Goodwin et al., 1999; Pabon-Pena et al. unpublished data). Creation of a full-length cytLEK1 construct

(see Materials and Methods) allows testing of antibodies, for the first time, with transfected cytLEK1 protein. The cytLEK1 antibody detects on Western blot the product of a FLAG-tagged cytLEK1 construct transfected into COS-7 cells (Figure 4 A). No band is observed in non-transfected COS-7 cells, confirming specificity for cytLEK1. Additionally, the cytLEK1 and nucLEK1 antibodies recognize endogenous cytLEK1 and nucLEK1 in lysates from 3T3 fibroblasts and C2C12 myoblasts on Western blot (Figure 4 B). The larger cytLEK1 and smaller nucLEK1 bands are also visible in embryonic day 12.5 murine hearts (Figure 4 C). To confirm immunoreactivity in immunofluorescence assays, FLAG-tagged cytLEK1 or nucLEK1 constructs were transfected into COS-7 cells. The cytLEK1 antibody correctly detects the transfected cytLEK1 protein in the cytoplasm (Figure 5 A). Additionally, the nucLEK1 antibody identifies the transfected nucLEK1 protein, which contains an NLS, within the nucleus. These distribution patterns match the localization of endogenous proteins in C2C12 myoblasts (Figure 5 B). CytLEK1 is present in the cytoplasm with a higher concentration near the nucleus, whereas nucLEK1 localizes to the nucleus of these cells.

Examination of LEK1 expression in the murine heart during development

While expression of nucLEK1 in the developing heart has previously been examined (Goodwin et al., 1999), the expression pattern of cytLEK1 is unknown. Thus, experiments were undertaken to study the cytLEK1 protein at key stages during heart development. Tissue sections were examined from mice at the following stages of development: embryonic day 16.5 (E16.5), neonatal day 2 (N2), neonatal day 4 (N4), neonatal day 7 (N7), neonatal day 10 (N10), and adult (Figure 6). Distribution of nucLEK1 is confirmed to be predominantly nuclear at all stages, as has been previously published (Goodwin et al., 1999). The only change observed is a decrease in the percentage of nuclei staining positive for nucLEK1 during progression of postnatal development. In adult hearts, nucLEK1 cannot be readily detected, although occasionally a few cells with low levels of expression are present. Similar to nucLEK1, cytLEK1 is mostly absent in adult hearts. However, an unexpected distribution pattern is observed for cytLEK1. In agreement with data from cell culture experiments, cytLEK1 is distributed primarily in the cytoplasm at all embryonic stages of the heart examined. However, surprisingly, much of the protein seemingly localizes to the nucleus beginning at neonatal day 2, where it remains throughout postnatal development. Upon higher-power examination of these postnatal cardiomyocytes, a difference in

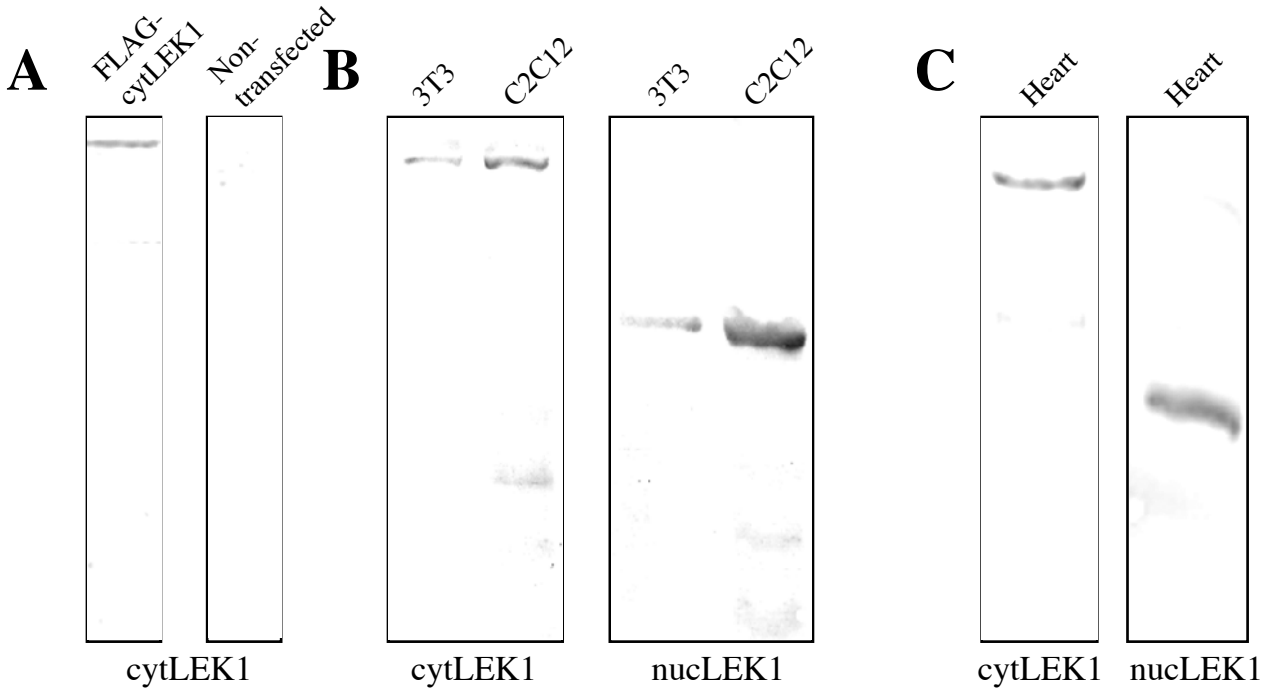

Figure 4. **Western blot characterization of LEK1 antibodies.** A) COS-7 cells were transfected with a FLAG-tagged cytLEK1 construct. Lysates were collected and blots were probed with the antibody to cytLEK1 (Spec1). The antibody detects only the FLAG-cytLEK1 band from these cells and no band is seen in non-transfected COS-7 cells, confirming its specificity for cytLEK1. B) 3T3 fibroblast and C2C12 myoblast cell lysates were collected for detection of endogenous cytLEK1 and nucLEK1 on Western blot. The larger cytLEK1 and smaller nucLEK1 (863) bands are visualized by the appropriate antibody and no other bands are seen. C) Heart tissue was collected for detection of endogenous cytLEK1 and nucLEK1. Once again, the cytLEK1 and nucLEK1 bands are visualized by the antibodies.

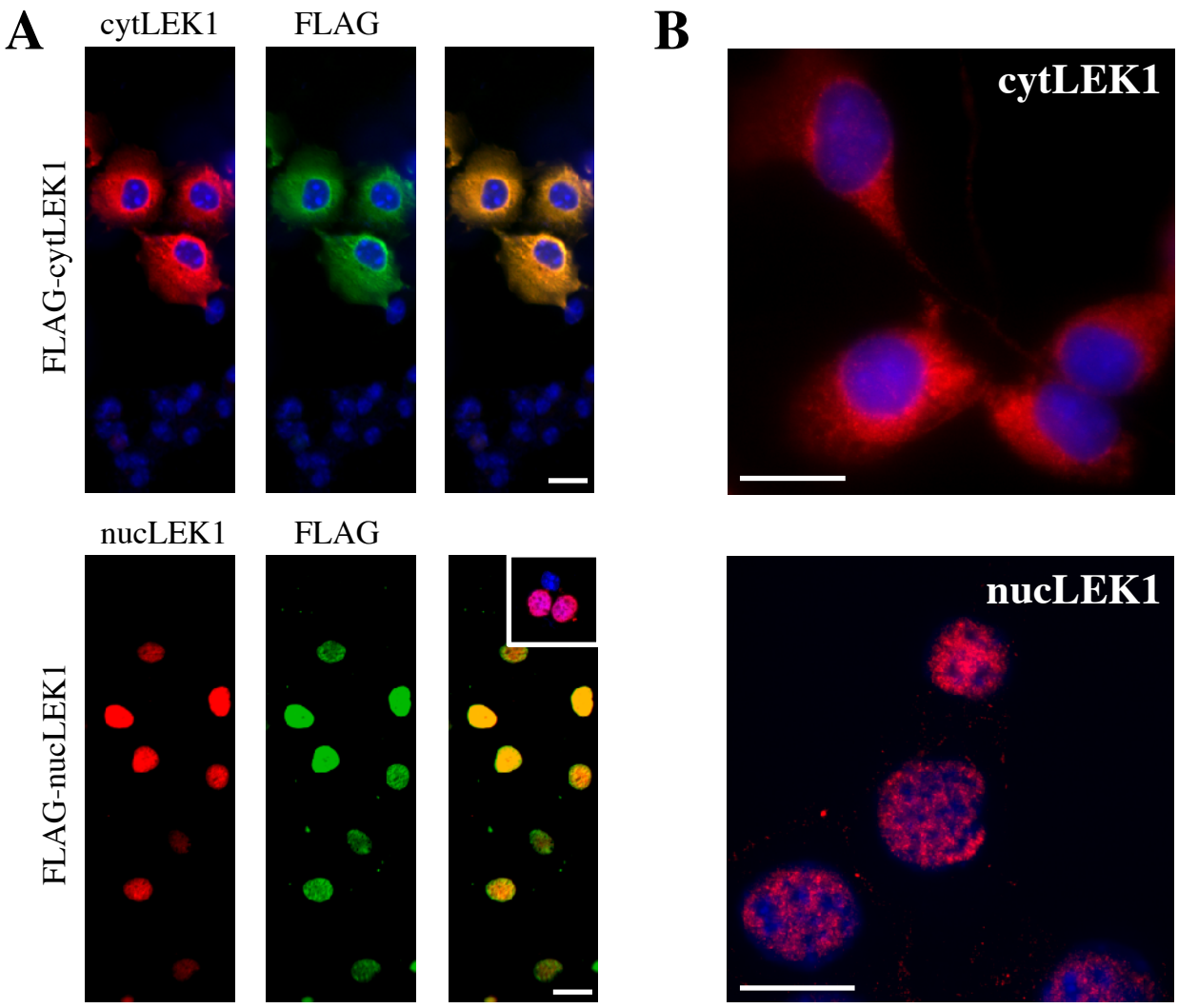

Figure 5. **Immunofluorescence characterization of LEK1 antibodies.** A) FLAG-cytLEK1 or FLAG-nucLEK1 was transfected into COS-7 cells. Each transfected protein was detected with the appropriate antibody against LEK1 (red) in addition to a FLAG antibody (green). As expected, cytLEK1 (Spec1) is cytoplasmic while nucLEK1 (863), which contains a NLS, is found in the nucleus. The specific colocalization shows proper detection of LEK1 protein by the LEK1 antibodies without nonspecific fluorescence. E) C2C12 myoblasts were examined for endogenous localization of cytLEK1 and nucLEK1. Whereas cytLEK1 is distributed in the cytoplasm of cells, nucLEK1 exhibits a primarily nuclear localization. DAPI (blue) was used to visualize nuclei. Bars, 10 μm.

the nuclear localization of the two LEK1 protein products is observed. Whereas nucLEK1 is found throughout most of the nucleus, similar to experiments with C2C12 myoblasts, cytLEK1 has a significantly more punctate nuclear staining pattern (Figure 7). Therefore, despite both proteins being localized to the nucleus during these postnatal stages, their distribution patterns are not identical. This discrepancy suggests that these results are not a consequence of an increase in uncleaved LEK1 detected by both antibodies, although direct experiments testing this theory would require the existence of both monoclonal and polyclonal LEK1 antibodies. Future confocal analysis may be of assistance and help distinguish between true nuclear labeling and tight perinuclear staining. In summary, the surprising change in localization at neonatal day 2 for cytLEK1 is intriguing, since it correlates with the period when cardiomyocytes are undergoing permanent cessation of mitosis and terminal differentiation (Soonpaa et al., 1996; Soonpaa and Field, 1998).

To complement the immunofluorescence data, analysis of expression levels of nucLEK1 and cytLEK1 was conducted by Western blot. Although *LEK1* mRNA in the heart has been shown to be dramatically downregulated after neonatal day 4 (Goodwin et al., 1999), there have been no studies examining whole-organ protein expression level. Our results here reveal that the highest levels of expression of both cytLEK1 and nucLEK1 proteins occur at late embryonic stages (Figure 8). This is then followed with a subsequent decrease in expression levels, most dramatic for cytLEK1, throughout postnatal development until adulthood, when neither protein can be detected on Western blot. Thus, the presence and, presumably, function of LEK1 in the adult heart is significantly reduced compared to its developmental role. Importantly, full-length LEK1 is not detected at any stage by Western blot, suggesting that cleavage of the protein is complete.

Examination of LEK1 expression in the murine intestine during development

Studies were undertaken to examine the distribution of cytLEK1 and nucLEK1 in the developing mouse intestine. Such experiments have not been previously conducted for any LEK family member and are interesting due to the important nature of proliferative processes in intestinal function. In this organ, enterocytes undergo cell division throughout the entire life of the organism (Ross et al., 1995). This scenario provides a useful contrast with the heart where proliferation ceases relatively abruptly at postnatal stages (Soonpaa et al., 1996; Soonpaa and

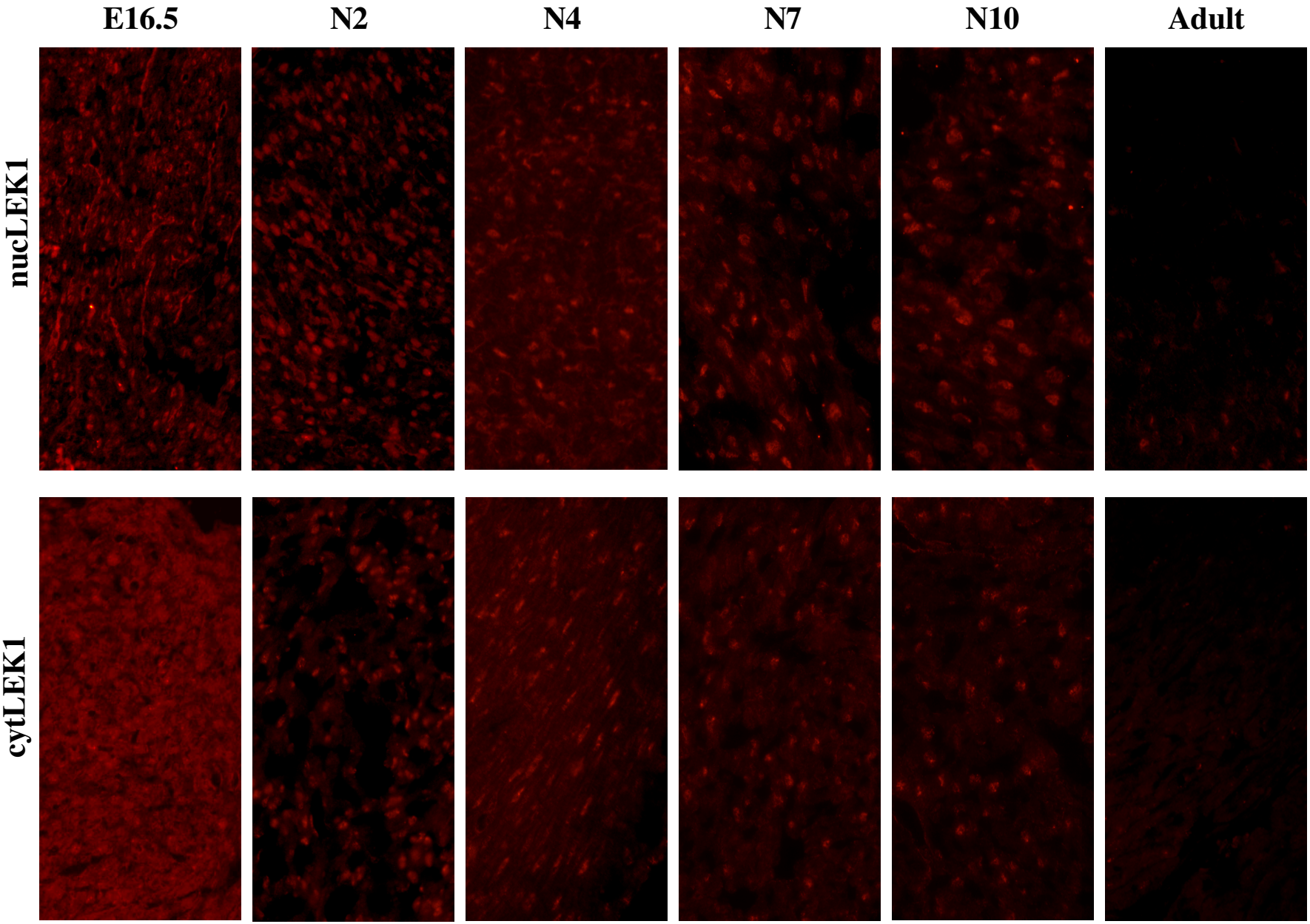

Figure 6. **Immunohistochemical analysis of LEK1 expression in embryonic day 16.5 to adult murine hearts.** NucLEK1 expression (red) is always nuclear throughout development and is not clearly detected in adult hearts. CytLEK1 expression (red) is predominantly cytoplasmic at embryonic stages. However, beginning at N2, the expression becomes nuclear until adulthood when cytLEK1 is not detected.

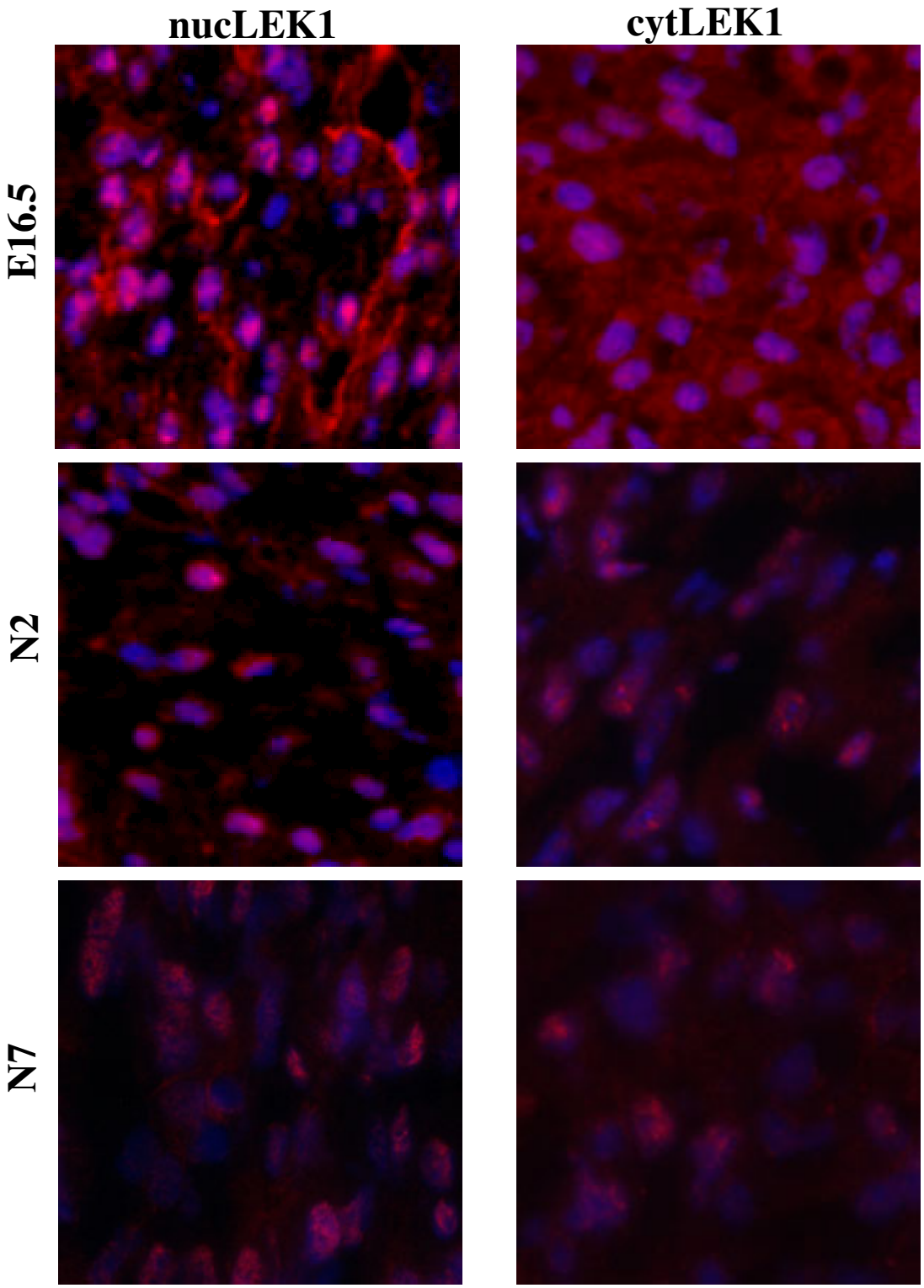

Figure 7. **Immunohistochemical analysis of LEK1 expression in embryonic day 16.5 to neonatal day 7 murine hearts.** NucLEK1 expression (red) throughout development is always nuclear. CytLEK1 expression (red) is predominantly cytoplasmic at E16.5. However, beginning at N2, the expression becomes nuclear although it is less widespread in the nucleus than nucLEK1. DAPI (blue) was used to visualize nuclei.

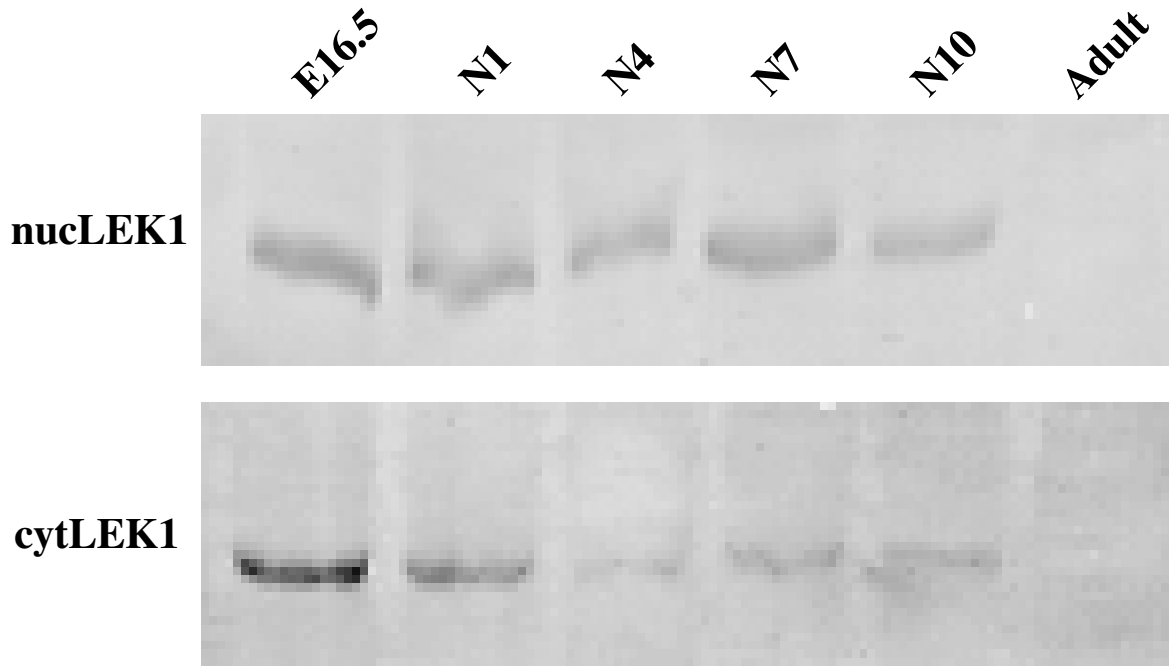

Figure 8. **Western blot analysis of LEK1 expression in embryonic day 16.5 to adult murine hearts.** The highest levels of expression for cytLEK1 and nucLEK1 occur at embryonic stages. This is followed by a subsequent decrease in expression levels, most dramatic for cytLEK1, throughout postnatal development. Neither protein can be detected in adult hearts.

Field, 1998). Thus, any role of LEK1 in these two distinct settings of cell division processes can be better understood. Small intestine tissue sections were analyzed from various postnatal mice with the appropriate LEK1 antibodies. Notably, nucLEK1 seems to be expressed at a higher level than cytLEK1 in this tissue based on immunofluorescence data. CytLEK1 is detected at a fairly low level within most cells in a diffuse cytoplasmic distribution at neonatal day 2 and then quickly disappears at later timepoints (Figure 9 A). Conversely, nucLEK1 has strong expression in the nucleus at neonatal days 2 and 4 throughout the villi of the small intestine (Figure 9 B). While there may be increased nucLEK1 immunofluorescence in some intestinal crypts, there is no clear pattern throughout multiple sections. Interestingly, the level of nucLEK1 expression dramatically declines by neonatal day 7, despite the fact that enterocytes remain proliferative through adulthood. These data thus appear to reinforce the hypothesis that LEK1, or at least nucLEK1 in this setting, plays a critical role in proliferation during embryonic development but not in later adult stages (Goodwin et al., 1999; Ashe et al., 2004).

Examination of LEK1 expression throughout the developing embryo

In order to examine the expression of cytLEK1 in a wide variety of tissues throughout murine development, an expansive Western blot approach was undertaken. There were no previous studies that had carefully examined the protein levels of either LEK1 cleavage product in a diverse set of tissues. Liver, heart, skeletal muscle, and brain tissues were collected from mice at the following stages of development: embryonic day 12.5 (E12.5), embryonic day 18.5 (E18.5), neonatal day 1 (N1), neonatal day 4 (N4), neonatal day 10 (N10), and adult (Figure 10). Notably, cytLEK1 is detected at E12.5 in the heart and in skeletal muscle but not in any other tissues. By E18.5, robust expression is also seen in the brain. Interestingly, there are multiple evenly-spaced bands in all positive samples from the brain, suggesting the potential for oligomerization of cytLEK1 in this tissue. By N1, cytLEK1 protein is also detected in the liver. Expression of cytLEK1 in all four tissues continues through N4. By this time point, liver expression is robust but there has been a slight decrease in the heart and skeletal muscle. CytLEK1 can only be readily detected in the liver and brain at N10, albeit at a lower level than previous postnatal stages. Notably, there is a very faint band in the heart lysate lane. In the adult mouse, cytLEK1 is not detected in any of the four tissues examined, consistent with previous work showing that the highest levels of LEK1 expression occur in the developing mouse

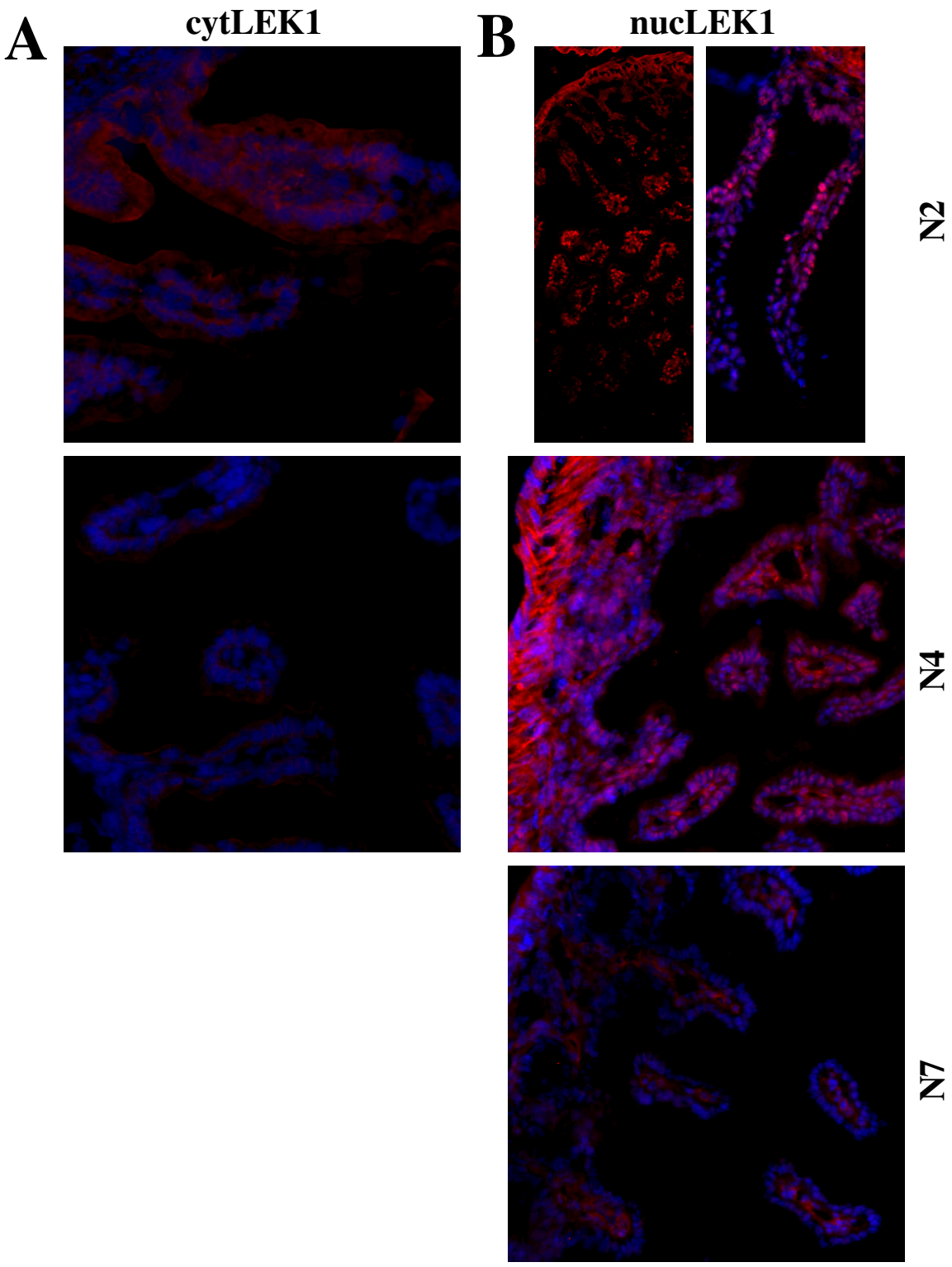

Figure 9. **Immunohistochemical analysis of LEK1 expression in neonatal day 2 to day 7 murine intestine.** A) CytLEK1 expression (red) is detected at a low level at N2 and then quickly disappears by N4. B) NucLEK1 expression (red) is strong at N2 to N4 throughout the nucleus of most cells in the intestinal villi. The expression level dramatically declines by N7. DAPI (blue) was used to visualize nuclei.

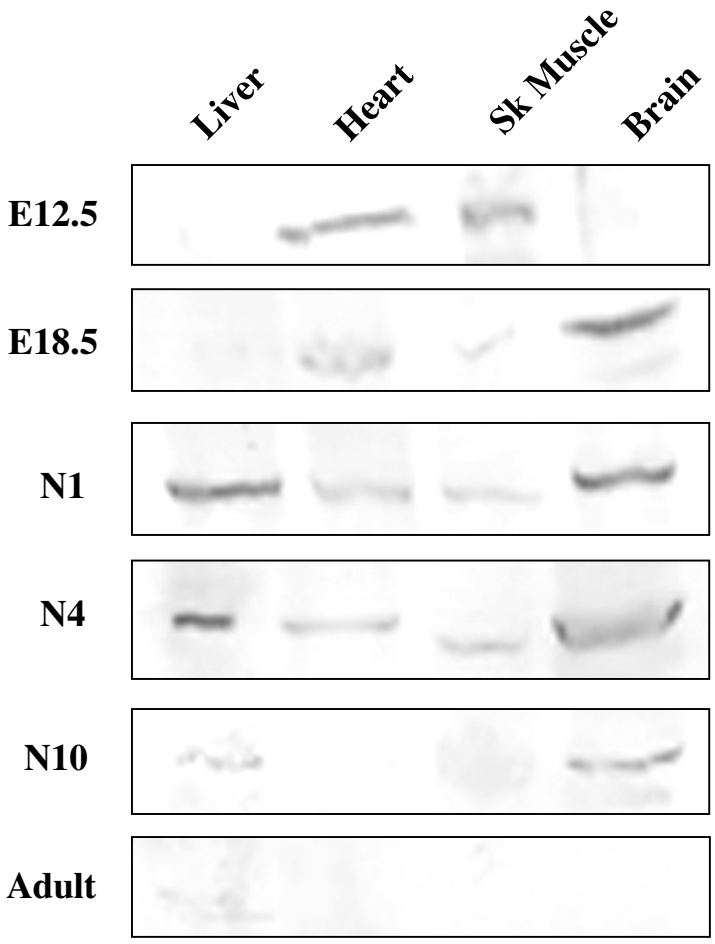

Figure 10. **Western blot analysis of cytLEK1 expression in multiple tissues during murine development.** CytLEK1 expression is initially detected only in the heart and skeletal muscle. The protein is later also observed in the liver and brain. After neonatal day 4, a low level of expression remains only in the liver and brain. CytLEK1 cannot be detected in any adult tissues examined.

(Goodwin et al., 1999). Additionally, immunofluorescence data support this Western blot analysis and reveal, for example, that cytLEK1 is highly expressed in the cytoplasm of liver cells at neonatal days 1 through 10. Conversely, nucLEK1 is not well detected in such cells at these timepoints.

Localization of cytLEK1 in murine cells

In order to better characterize cytLEK1 distribution in cells, immunofluorescence studies were conducted in various murine cell lines. Analysis of both 3T3 fibroblasts (Figure 11 A) and C2C12 myoblasts (Figure 11 B) reveals a predominantly cytoplasmic distribution pattern for the protein. Additionally, cytLEK1 localizes more intensely to a perinuclear location within cells. During mitosis, cytLEK1, like nucLEK1 is mostly excluded from regions containing DNA (Figure 11 B inset). The exact distribution of cytLEK1 in dividing cells will be discussed shortly. These results here confirm that cytLEK1 is a cytoplasmic protein with an increased concentration near the nucleus.

Change in cytLEK1 subcellular distribution upon pre-extraction

Since cytLEK1 is shown in later chapters to be a member of the LIS1 pathway, experiments were undertaken to determine if the endogenous protein is associated with the cytoskeleton. A detergent extraction approach was utilized for these experiments (Sapir et al., 1997; Toomre et al., 1999; Giodini et al., 2002). A specific region of cytLEK1 (C domain) confers detergent resistance (chapter IV), thus at least a subset of endogenous cytLEK1 would be expected to persist after detergent pre-extraction. Indeed, in both 3T3 fibroblasts and C2C12 myoblasts, partial resistance is observed (Figure 12). Very interestingly, cytLEK1 around the nucleus remains after detergent pre-extraction, while the majority of protein towards the periphery is washed out. This result is in agreement with our data showing that cytLEK1 colocalizes strongly with LIS1 family members near the nucleus but significantly less towards the periphery (chapter III). Additionally, in cells undergoing cytokinesis, it appears that insoluble cytLEK1 localizes to the midbody region, similar to tubulin (Figure 12 C). Our control experiments reveal that this selective resistance based on subcellular localization is specific to cytLEK1, as dynein exhibits little change after pre-extraction. Thus, it appears that perinuclear

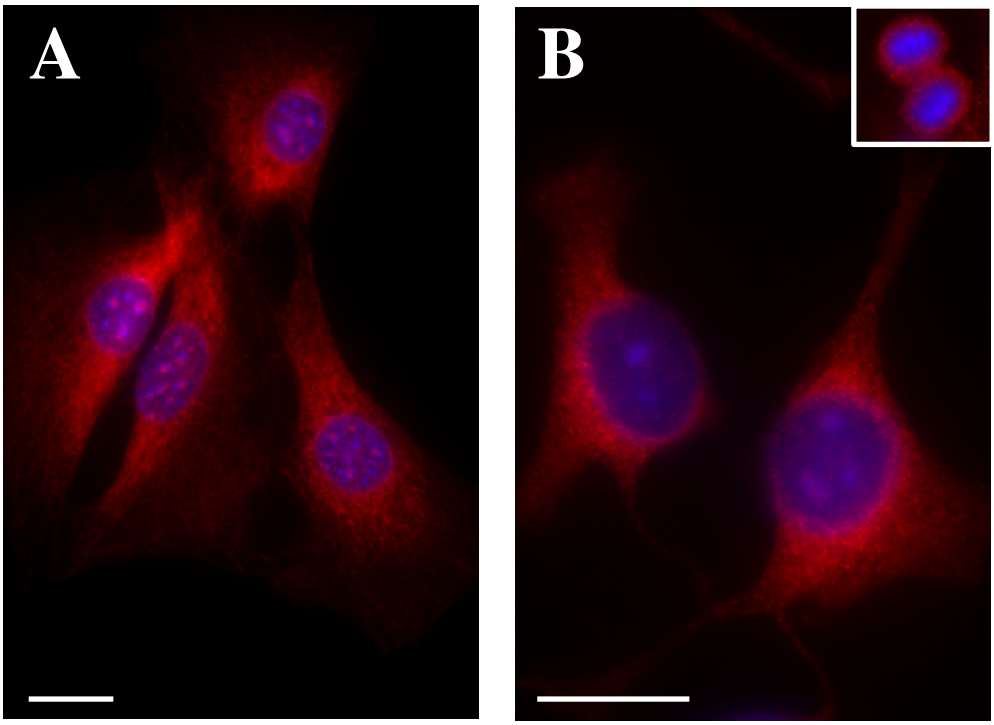

Figure 11. **Distribution of cytLEK1 in murine cell lines.** CytLEK1 is distributed widely in the cytoplasm of both 3T3 fibroblasts (A) and C2C12 myoblasts (B). The protein is concentrated more highly around the nucleus. In mitotic cells, cytLEK1 is excluded from regions containing DNA (inset of B). DAPI (blue) was used to visualize nuclei. Intense nuclear puncta are a secondary antibody artifact. Bars, 10 μm.

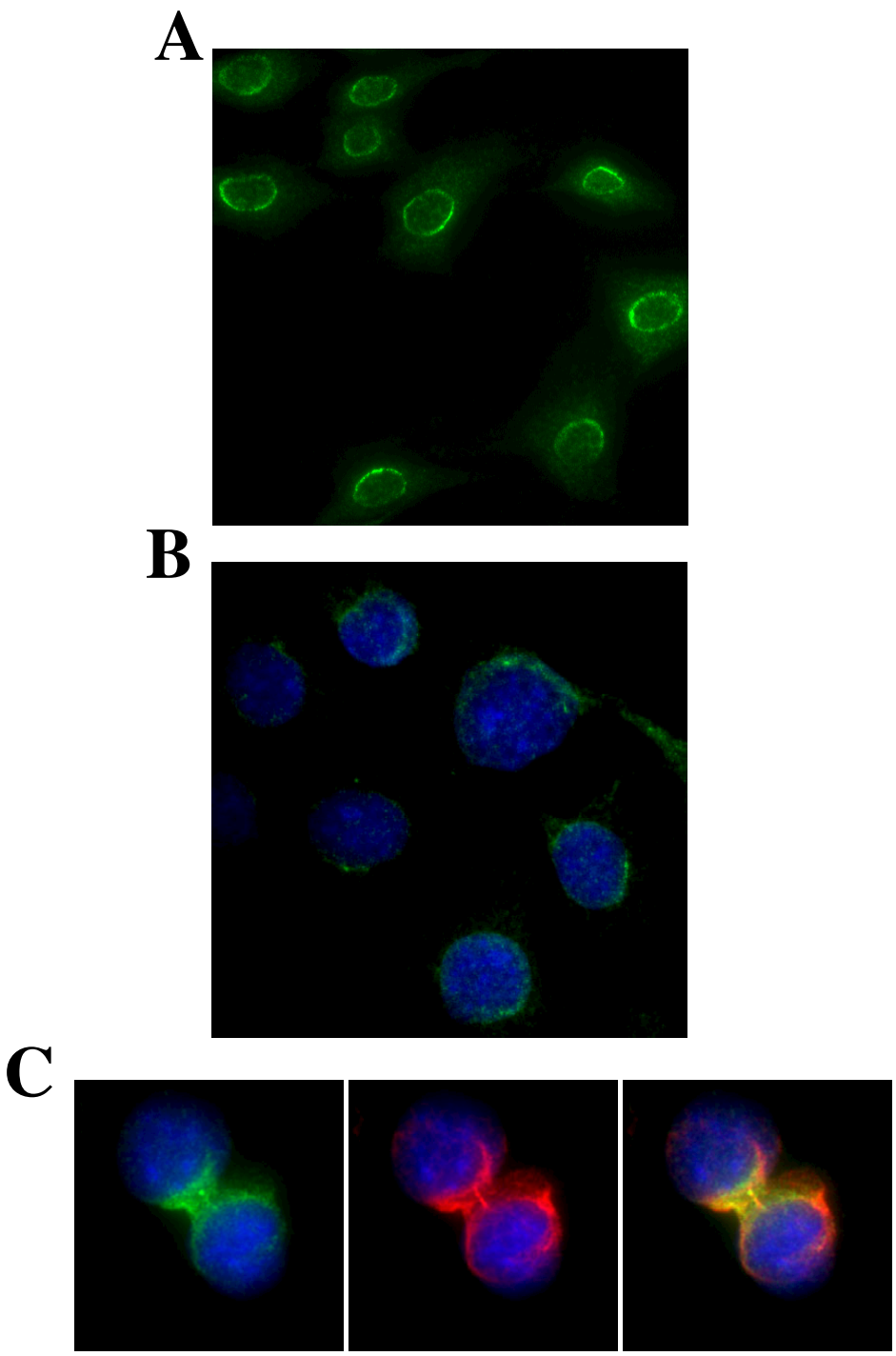

Figure 12. **Endogenous cytLEK1 is partially resistant to detergent pre-extraction.** CytLEK1 is in green. A) In 3T3 fibroblasts, the detergent resistant pool of cytLEK1 is located tightly around the nucleus. B) In C2C12 myoblasts, a similar pattern is detected with a less tightly perinuclear distribution. C) In dividing C2C12 cells, the insoluble cytLEK1 is observed at the midbody region, similar to tubulin (red). DAPI (blue) was used to visualize nuclei.

cytLEK1 likely has a stronger cytoskeletal association than peripheral cytLEK1, which may have different, currently unknown, binding partners.

Localization of cytLEK1 and nucLEK1 in dividing cells

Initial studies on nucLEK1 suggested that the protein does not colocalize with the DNA material in mitotic cells (Goodwin et al., 1999). Further low-power experiments generally confirm this result for cytLEK1, in addition to nucLEK1, in various murine cells (Figure 11 B inset). However, while the majority of each protein does not colocalize with the DNA material, detailed studies have never been conducted to examine the precise localization of the two proteins in cells undergoing mitosis. Since LIS1 family members have been shown to be present on the spindle apparatus of mitotic cells (Faulkner et al., 2000; Yan et al., 2003; Feng and Walsh, 2004), experiments were undertaken to more carefully analyze the distribution of cytLEK1 and nucLEK1 in dividing 3T3 fibroblasts.

These experiments reveal that, although the majority of cyLEK1 and nucLEK1 protein is indeed not found on the mitotic apparatus, a subset of each protein population is localized to the spindles and spindle poles. For cytLEK1, the most prominent localization of the protein is at the spindle poles (Figure 13), as can be observed through various stages of mitosis. Based upon these data, however, cytLEK1 appears to be most abundant at the spindle pole during early mitotic stages and then decreases as cell division proceeds. Although more difficult to visualize, cytLEK1 is also distributed on the spindle itself in a punctate distribution (Figure 14). Notably, no cytLEK1 can be clearly detected on kinetochore structures, as most of the relevant protein appears to be on the spindle itself. Colocalization studies with antibodies to a centromeric protein (CENP-A) were uninformative due to poor labeling by these antibodies. However, conclusively proving the absence of cytLEK1 from kinetochores will likely require the increased resolution available from deconvolution microscopy. It is not surprising though that this labeling of the spindle apparatus described here was missed in initial studies due to the high amount of cytLEK1 protein located outside the area of the mitotic apparatus.

NucLEK1 can also be found on the mitotic spindle, although it is significantly less prominent than cytLEK1 on the same structures. It can be detected faintly on the spindle itself and also at the spindle poles (Figure 15 A). Interestingly, in at least one case, nucLEK1 labels two very distinct dots within the spindle pole, suggestive of the two centrioles (Figure 15 B).

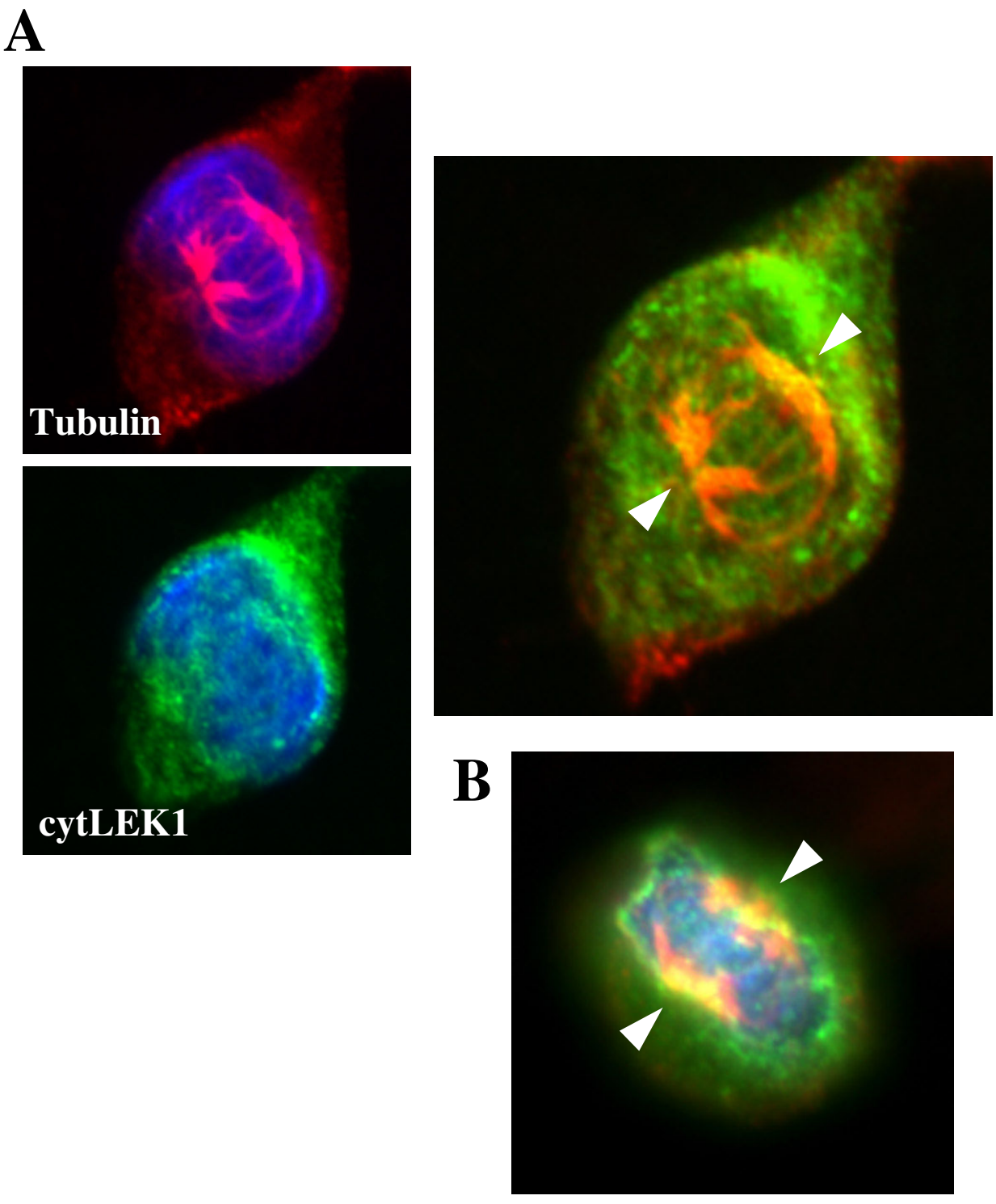

Figure 13. **CytLEK1 localizes to the spindle and spindle poles of mitotic murine cells.** CytLEK1 is in green and tubulin is in red. A-B) CytLEK1 is visualized at the spindle poles and the nearby spindle region of dividing 3T3 fibroblasts. Arrowheads indicate general regions of colocalization. DAPI (blue) was used to visualize nuclei.

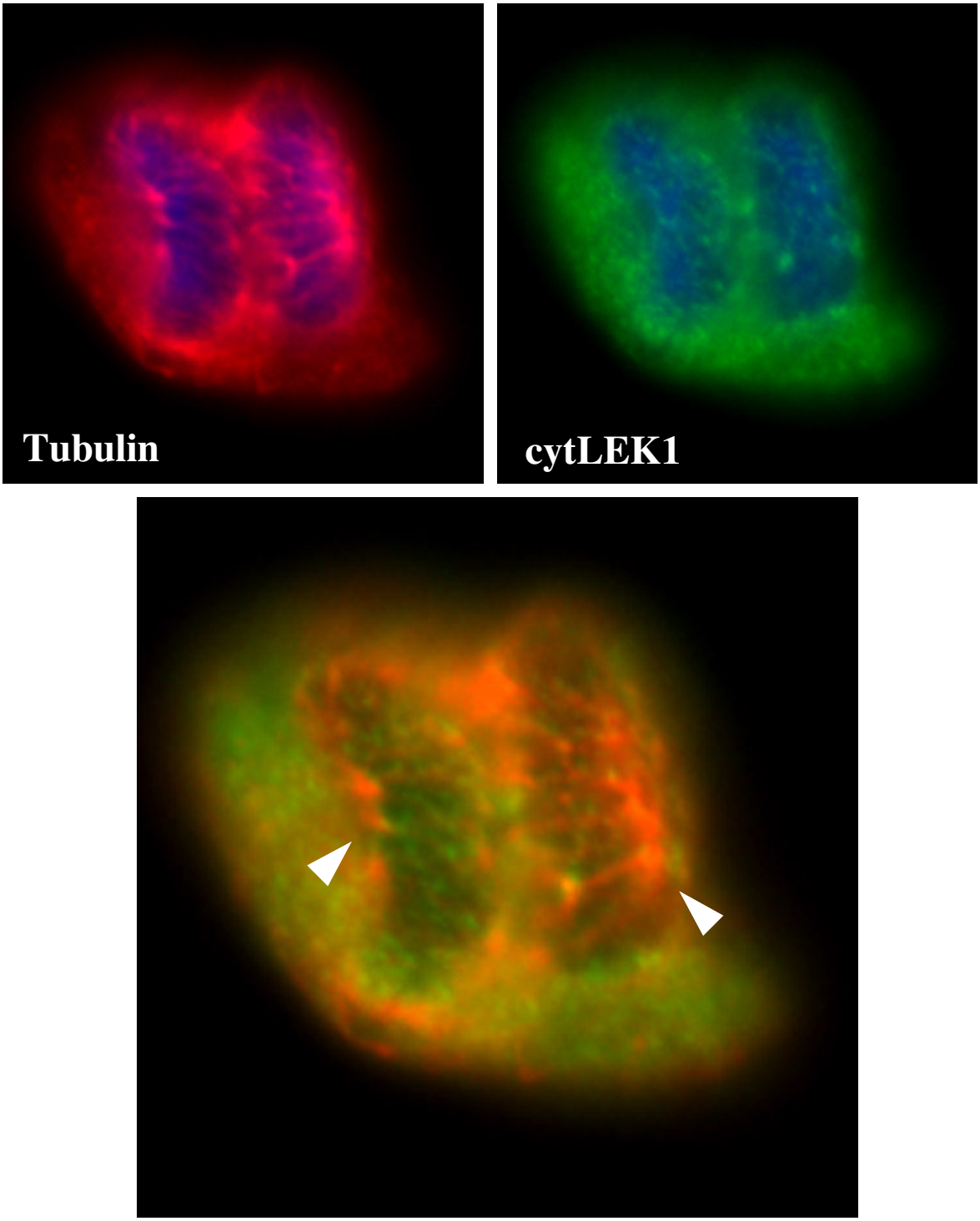

Figure 14. **CytLEK1 localizes to the spindle and spindle poles of dividing murine cells.** CytLEK1 (green) is distributed in distinct puncta along the microtubule spindle (red) in dividing 3T3 fibroblasts. Arrowheads indicate general regions of colocalization. DAPI (blue) was used to visualize nuclei.

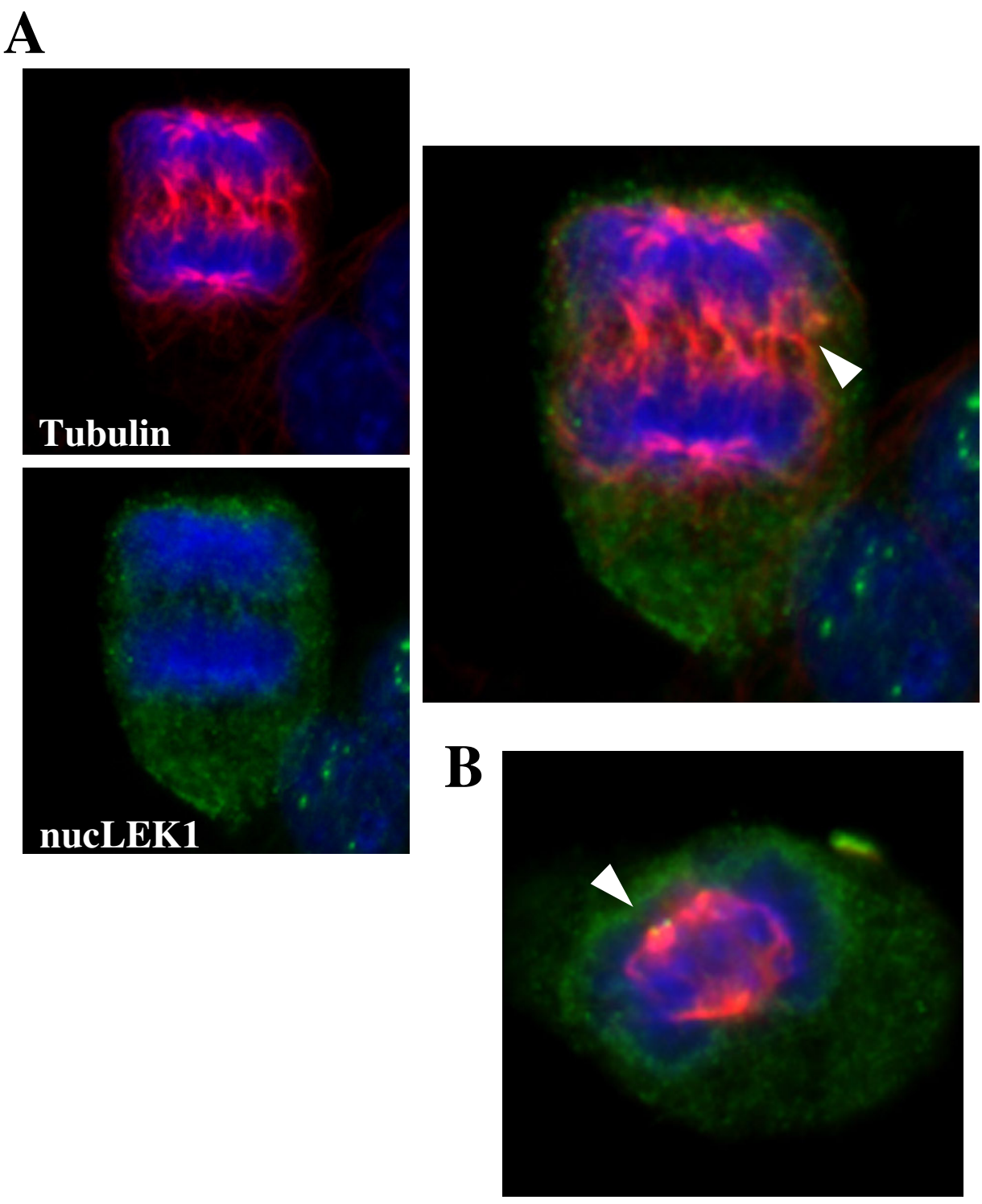

Figure 15. **NucLEK1 localizes to the spindle and spindle poles of mitotic murine cells.** A) NucLEK1 (green) is distributed in distinct puncta along the microtubule spindle (red) in dividing 3T3 fibroblasts. B) NucLEK1 localizes to two distinct puncta at the spindle pole of this mitotic cell. Arrowheads indicate general regions of colocalization. DAPI (blue) was used to visualize nuclei.

Once again, nucLEK1 labeling of the mitotic apparatus is not visible without careful examination, thus likely explaining how it had been missed until now (Goodwin et al., 1999). These results identifying both cytLEK1 and nucLEK1 on the spindle are supportive of LEK1 being a LIS1 family member and playing a role in cell division. Higher resolution confocal deconvolution analysis of mitotic cells will be helpful in better determining the precise localization of cytLEK1 and nucLEK1 on the spindle apparatus.

Examination of cytLEK1 distribution in wounded monolayers

Dynein and its partner proteins have been shown to be important in directed cell movement (Dujardin et al., 2003). Notably, in wounded 3T3 fibroblast monolayers, dynein, dynactin, and LIS1 localize to the leading edge of cells where they assist in reorientation of the microtubule network. We thus examined whether cytLEK1 exhibits a similar change in localization under these conditions. Seven hours after wound formation (utilizing a pipette tip), cytLEK1 is distributed in its usual cytoplasmic pattern (Figure 16). No additional cytLEK1 is present on the leading edge of the presumably migrating cells at the wound border. Additionally, there is no detectable change in the overall level of cytLEK1 protein, as compared to cells located in the unperturbed confluent region of the slide. These results suggest that there is no dramatic shift in cytLEK1 distribution as a consequence of monolayer wounding. However, they do not exclude the possibility that more subtle changes may be occurring, as other researchers have relied on total internal reflection fluorescence microscopy to observe variations (Dujardin et al., 2003).

Characterization of newly-generated LEK1 antibodies

Additional polyclonal antibodies against cytLEK1 and nucLEK1 were generated in order to provide future reagents for the laboratory. Peptide domains were chosen throughout cytLEK1 and nucLEK1 (Figure 17) with the assistance of the manufacturer (Biosynthesis). An effort was made to generate antibodies specific to regions of LEK1 not identified by the current cytLEK1 and nucLEK1 polyclonal antibodies. For reference, the Spec1 antibody to cytLEK1 was generated using a peptide at the 1826 aa region of LEK1. The 863 polyclonal antibody, which has been used extensively for nucLEK1 studies, is directed against a region 2872 aa into LEK1. Three new cytLEK1 antibodies were generated against the following amino acid regions: 264 aa

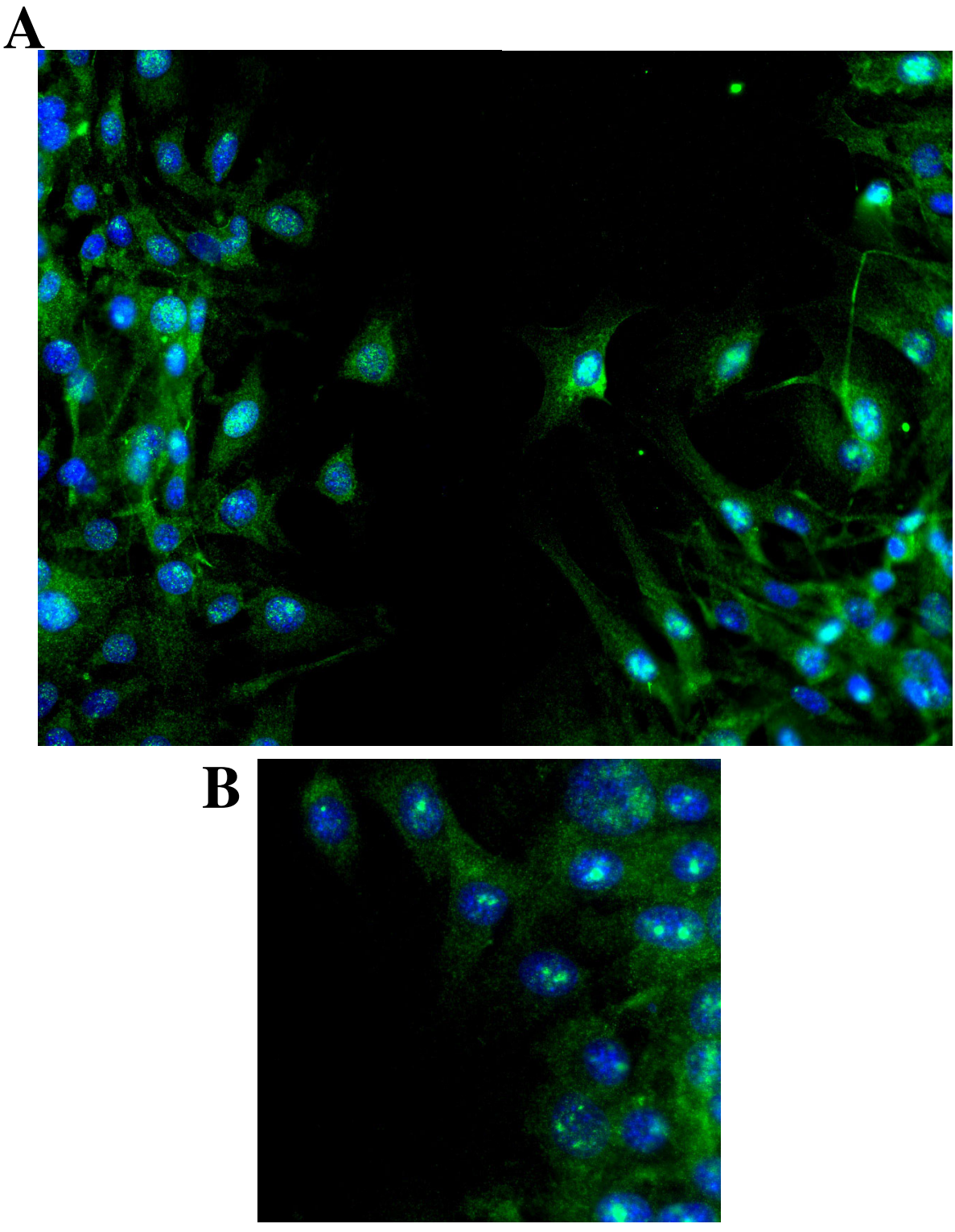

Figure 16. **Examination of cytLEK1 distribution in wounded 3T3 fibroblast monolayers.** No significant change in subcellular localization or expression level of cytLEK1 (green) is detected in cells near the wound border (A), even upon higher power observation (B). DAPI (blue) was used to visualize nuclei.

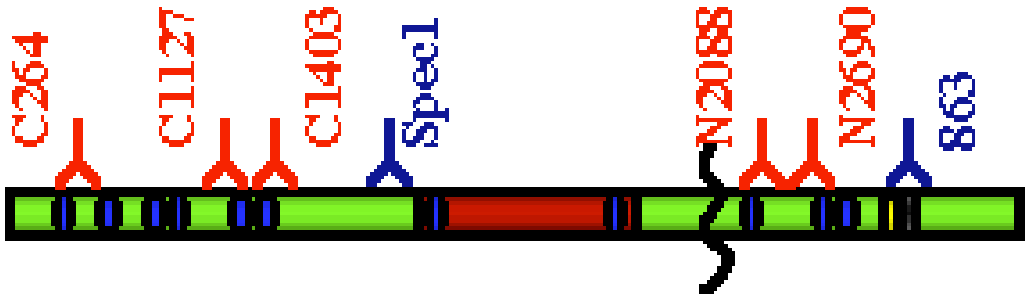

Figure 17. **Binding epitopes for the LEK1 polyclonal antibodies with respect to the LEK1 functional domains and putative cleavage site.** The established antibodies (Spec1 and 863) are shown in blue. The newly-generated antibodies are in red.

(C264), 1127 aa (C1127), and 1403 aa (C1403). Two new nucLEK1 antibodies were created from peptide sequences at the following locations of LEK1: 2088 aa (N2088) and 2690 aa (N2690). Notably, the N2088 antibody recognizes a region of LEK1 that is just C-terminal to the presumed cleavage site of the protein. As the exact location of the cleavage event is not known and may be slightly C-terminal to current predictions, it remained unclear upon design whether this antibody would be specific for endogenous nucLEK1 or, instead, cytLEK1. Two of the antibodies (C264 and N2690) were directed against conserved epitopes among LEK family members to generate potentially cross-reactive reagents that could be used in various species. The remaining antibodies (C1127, C1403, N2088) have epitopes that are relatively specific to LEK1 and thus should not be cross-reactive with other known LEK family members.

After affinity purification as described in the Materials and Methods section, tests were undertaken first to determine the ability of these antibodies to recognize cytLEK1 and nucLEK1 expressed from transfected constructs in COS-7 cells. It is important to note that as currently generated, the cytLEK1 construct extends past the epitope of the N2088 antibody (Figure 18 D). Conversely, the nucLEK1 construct includes the epitope of the Spec1 antibody. When expressed in COS-7 cells, the cytLEK1 protein is properly detected by all expected antibodies based on immunofluorescence: C264, C1127, C1403, Spec1, and N2088 (Figure 18 B). Importantly, the protein is not detected by the N2690 and 863 antibodies, thus providing negative controls for this set of experiments. When nucLEK1 is expressed in COS-7 cells, this protein is recognized by all the appropriate antibodies in immunofluorescence assays: Spec1, N2088, N2690, and 863. However, the C1127 antibody also detects nucLEK1, despite its epitope being absent in this protein. A possible explanation is that there could be a structural similarity between two different epitopes in cytLEK1 and nucLEK1. Alternatively, this antibody may react to some degree with any protein expressed at a high level in cells. Another unexpected observation is that the N2690 antibody results in strong cytoplasmic labeling of non-transfected COS-7 cells (Figure 20 B). As these cells presumably lack murine LEK1, this result suggests that the antibody has additional reactivity for a different protein. It is unknown currently whether this protein would be a LEK family member in this cell type or a completely unrelated molecule. Thus, the usefulness of the N2690 antibody in immunofluorescence assays is limited. All other antibodies, however, do not exhibit any cross-reactivity and do not label non-transfected COS-7 cells (Figure 18 A). In summary, all five new polyclonal antibodies, with the caveats noted above, are able to detect in

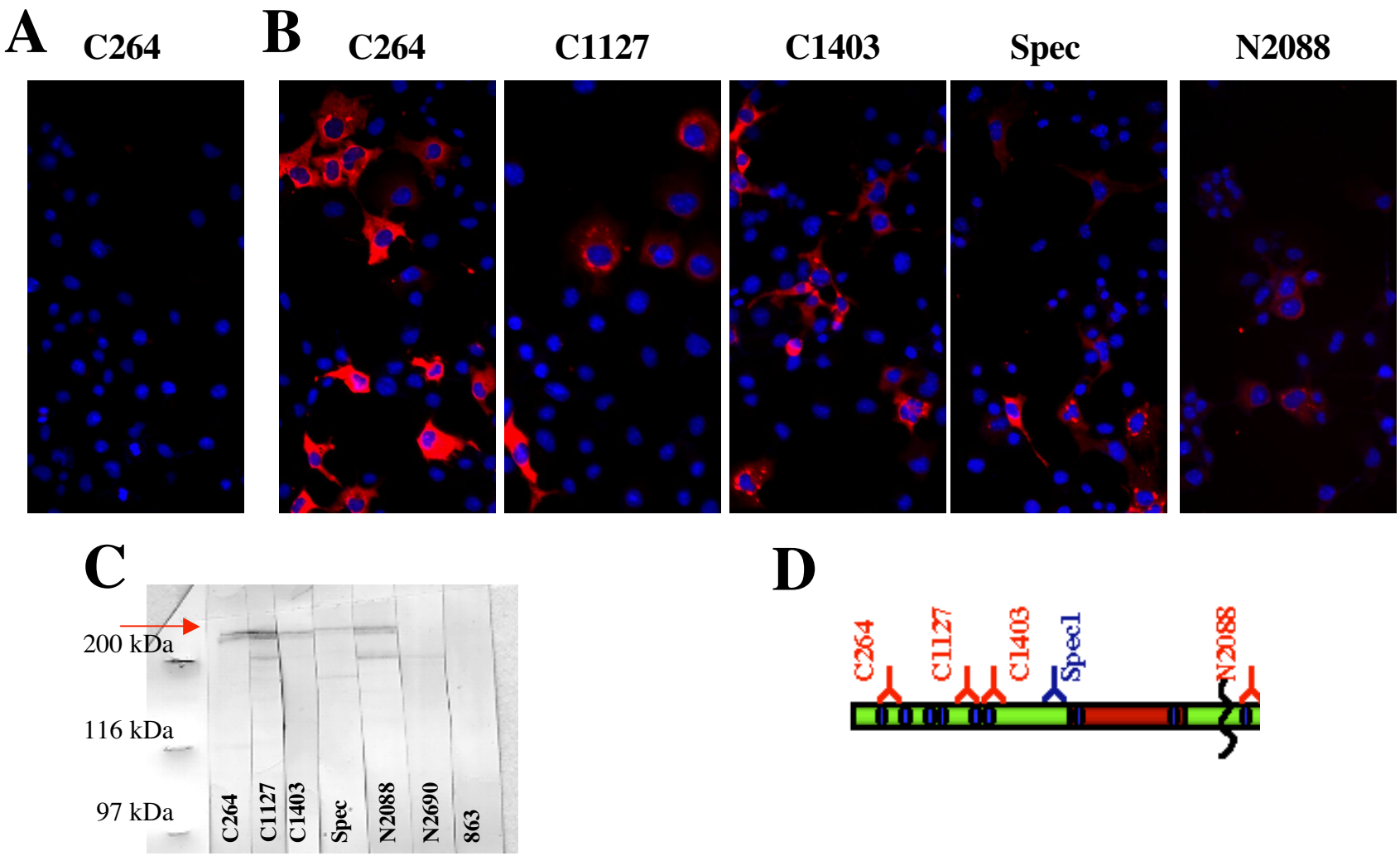

Figure 18. **Reactivity of LEK1 antibodies to transfected cytLEK1 expressed in COS-7 cells.** LEK1 antibodies are in red. A) The antibodies do not exhibit any labeling of non-transfected COS-7 cells. B) All five antibodies whose epitopes are contained within the cytLEK1 construct (see D) detect the protein in transfected COS-7 cells in immunofluorescence assays. C) Western blot analysis confirms detection of the cytLEK1 protein (arrow) by the appropriate antibodies but not by two nucLEK1 antibodies (N2690 and 863). D) Diagram displays antibodies whose epitopes are contained within the cytLEK1 construct. Notably, the sequence extends past the presumed cleavage site. DAPI (blue) was used to visualize nuclei.

immunofluorescence experiments the appropriate LEK1 proteins containing their epitope regions.

Additional experiments were undertaken to determine the ability of these antibodies to detect LEK1 proteins from transfected cells via Western blot (Figure 18 C). COS-7 cells were again transfected with either a cytLEK1 or nucLEK1 construct. All expected antibodies, similar to the immunofluorescence results, were able to detect the cytLEK1 protein: C264, C1127, C1403, N2088, and Spec1. Conversely, a nucLEK1 band was present for all the correct antibodies: Spec1, N2088, N2690, and 863. Interestingly, the unexpected observations seen previously in the immunofluorescence experiments were also observed in these Western blot data. The C1127 antibody yet again detects the nucLEK1 protein, despite the lack of a specific epitope in that protein. Additionally, while the N2690 antibody does identify nucLEK1, it also reveals a large (> 250 kDa) band in non-transfected COS-7 cells. This is likely the same protein product resulting in the cytoplasmic labeling of non-tranfected COS-7 cells by immunofluorescence. Although not conclusively proven, the large size of the detected band suggests that this protein may indeed be a LEK family member in these monkey fibroblast cells, especially since the N2690 epitope was selected to be conserved among all known LEK family members in an attempt to generate an antibody reactive across all species. Once again, all other antibodies do not display any cross-reactivity and do not label non-transfected COS-7 cells. To summarize these data, all five newly-generated polyclonal antibodies can detect cytLEK1 or nucLEK1, as appropriate, in Western blot assays.

The next step in characterization of these antibodies involved examination of their ability to detect endogenous cytLEK1 or nucLEK1 in murine cells. For these experiments, all methods were undertaken in both 3T3 fibroblasts and C2C12 myoblasts, as the subcellular distributions and molecular sizes of cytLEK1 and nucLEK1 in these cell lines have been extensively studied. In immunofluorescence characterizations (Figure 19), there is no gross difference in labeling pattern for any of the LEK1 antibodies between 3T3 fibroblasts and C2C12 myoblasts, as expected. While results are consistent between experiments, the data obtained are not completely in line with expectations for LEK1-specific antibodies. The C264 antibody displays a very faint cytoplasmic distribution with an intense pan-nuclear labeling in approximately one out of every three cells. The remainder of the cells have no nuclear labeling. The C1127 antibody pattern consists of a visible cytoplasmic distribution with the presence of distinct nuclear puncta in all

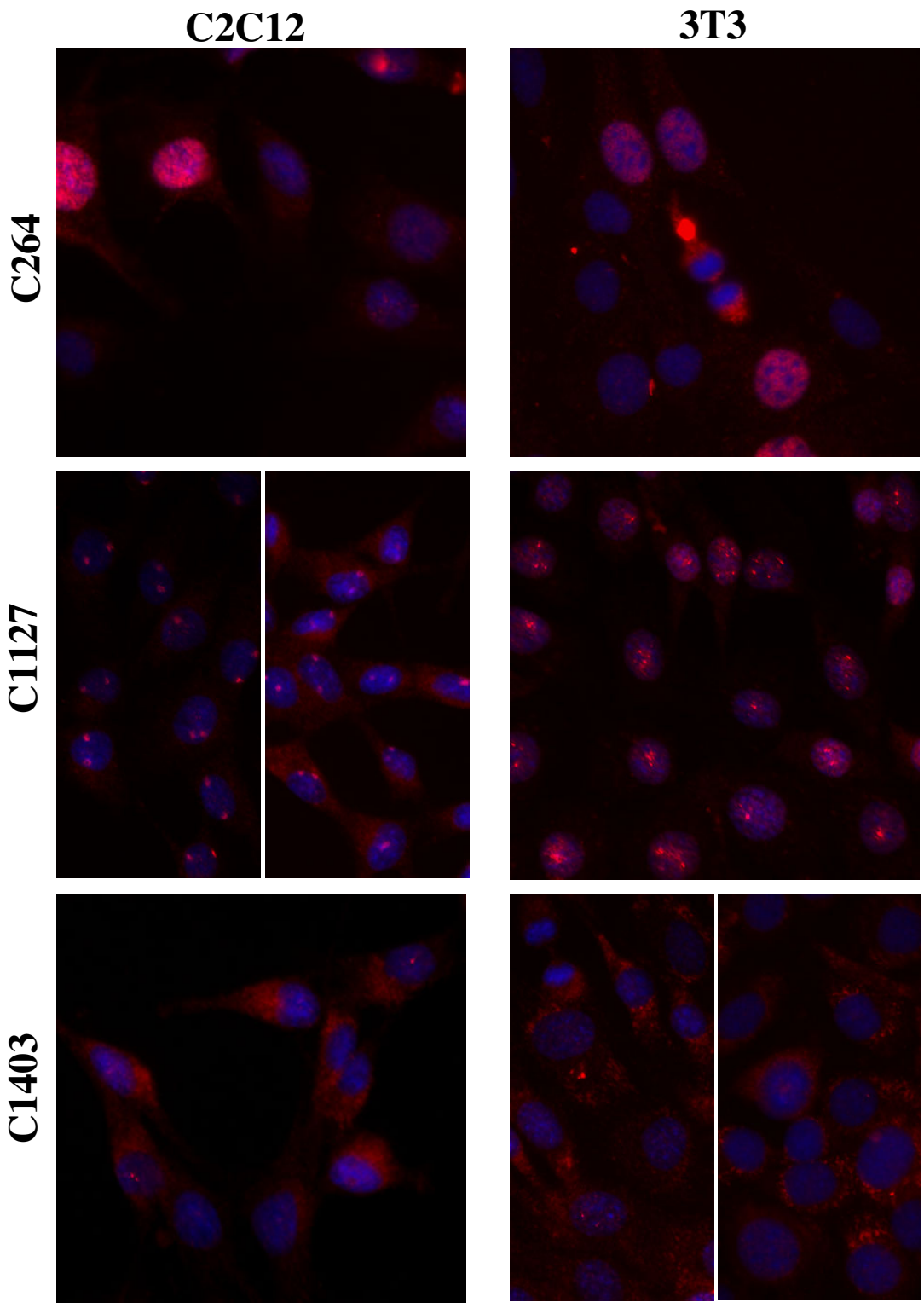

Figure 19. **Distribution of newly-generated cytLEK1 antibodies in murine cells.** The patterns of the three cytLEK1-directed antibodies (red) do not exhibit significant differences between C2C12 myoblasts and 3T3 fibroblasts. C264 is faintly cytoplasmic with an occasional nuclear distribution. C1127 and C1403 are predominantly cytoplasmic, although C1127 also exhibits distinct nuclear puncta. DAPI (blue) was used to visualize nuclei.

cells. In myoblasts, there are usually two uniformly-shaped dots per nucleus. Fibroblast nuclei, conversely, tend to have a larger number of more irregularly-shaped dots. These nuclear puncta are clearly not secondary antibody artifacts, as C1127 is the only primary antibody that visualizes them in combination with the same common secondary antibodies used in all experiments. The C1403 antibody displays a pattern very similar to that established for cytLEK1 with the Spec1 antibody. There is a primarily cytoplasmic distribution with a higher intensity in the perinuclear region. It is worth noting that the C1403 epitope is the closest of the new cytLEK1 antibodies to the Spec1 epitope.

The results from the nucLEK1 antibody studies also present new labeling patterns (Figure 20 A). The distribution of the N2088 antibody is not nuclear but, instead, cytoplasmic. The cytoplasmic staining is most intense near the nucleus, similar to Spec1, as is best visualized in C2C12 myoblasts. As previously mentioned, the epitope of N2088 is very close to the presumed cleavage site of LEK1 and is likely part of cytLEK1 based on our complete LEK1 sequence data. N2088 may, in fact, be an antibody specific to cytLEK1, not nucLEK1. Thus, it is not surprising that the distribution observed is very similar to that of Spec1, whose epitope is only 200 aa upstream. Finally, N2690, surprisingly, results in cytoplasmic labeling very similar to that of Spec1 also. Despite the fact that N2690 can detect nucLEK1 expressed in transfected cells, there is no endogenous nuclear staining visible. A caveat of the N2690 antibody, however, is that it also detects a cytoplasmic protein in non-transfected COS-7 cells, and thus it may have greater affinity for another protein than nucLEK1. Once again, it remains unclear if such a protein would be a LEK family member or an unrelated cytoplasmic protein with a relatively similar distribution to cytLEK1. Clearly, additional factors, such as uncleaved full-length LEK1 and epitope masking, may also be important for better understanding the diverse pattern of labeling seen with the new antibodies. Notably, however, all antibodies do not display substantial colocalization with the DNA material in mitotic cells. This phenotype is consistent with that previously observed for nucLEK1 and cytLEK1 in mitotic cells. Overall, these immunofluorescence results are encouraging since the majority of LEK1 antibodies show a cytoplasmic distribution similar to that of the established cytLEK1 antibody, Spec1.

An initial series of tests was performed to examine the pattern of the new antibodies in tissue sections from murine hearts. The studies were conducted with hearts collected from embryonic day 18.5 and adult mice. Overall, the subcellular labeling of each antibody in E18.5

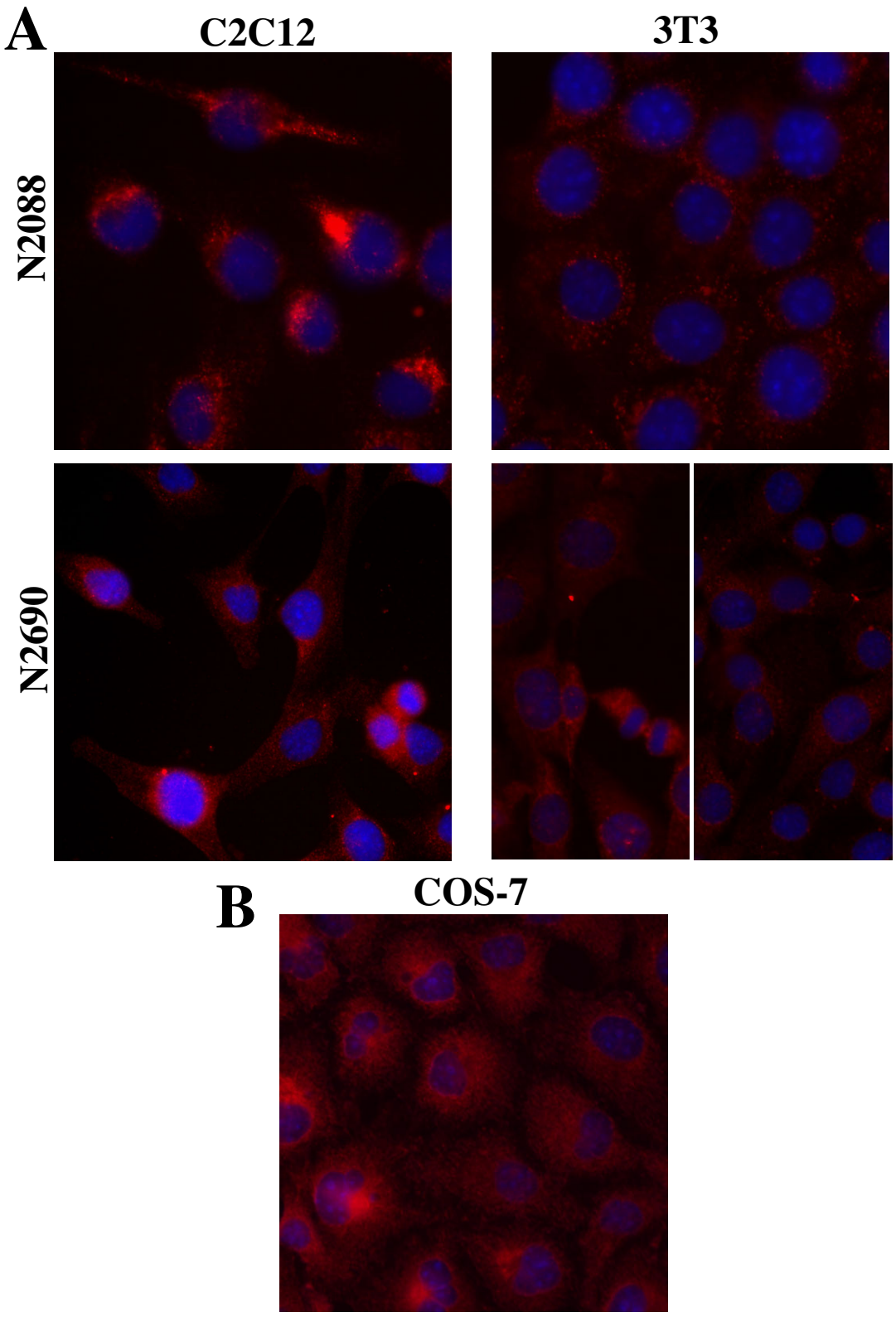

Figure 20. **Distribution of newly-generated nucLEK1 antibodies in murine cells.** A) The patterns of the two nucLEK1-directed antibodies (red) do not exhibit significant differences between C2C12 myoblasts and 3T3 fibroblasts. N2088 and N2690 both exhibit cytoplasmic distributions with no noticeable nuclear labeling. B) N2690 also detects a cytoplasmic protein in non-transfected COS-7 cells. DAPI (blue) was used to visualize nuclei.

hearts is grossly similar to that for cells in culture. C264, for example, stains the nucleus of approximately one out of every twenty cells with a faint cytoplasmic background in all cells. The patterns for C1403 and N2088 are cytoplasmic and similar to Spec1. N2690 labeling is both cytoplasmic and nuclear. The only notable change is that C1127 predominantly labels the nucleus, not the cytoplasm, of cells. Importantly, in adult hearts, all antibodies show substantially decreased fluorescence to near-background levels. Thus, these antibodies detect proteins that are more highly expressed in embryonic tissues, suggesting at least some specificity to LEK1.

These new polyclonal antibodies were also tested for their ability to detect endogenous cytLEK1 and nucLEK1 in Western blot assays. C2C12 myoblasts, 3T3 fibroblasts, and embryonic or adult hearts were used for the studies. However, consistent results were not obtained when utilizing these antibodies. Although at times the new cytLEK1 antibodies produce a band similar to Spec1, they also result in various other bands that differ with each experiment. Additionally, individual tests could not be repeated to generate the same result, unlike with the established Spec1 and 863 antibodies. Peptide competition assays showed, somewhat surprisingly, that all bands disappear with the addition of the original injected peptide. Thus, the antibodies do appear to work specifically on Western blot, although whether this specificity is solely to LEK1 is unclear. In summary, although the new polyclonal antibodies are able to detect transfected LEK1 proteins, they cannot consistently detect in a reproducible fashion the endogenous protein collected from various sources. Since the Spec1 and 863 antibodies are effective in all assays, have been well-characterized, and have been previously tested for specificity through various experiments, including expression library screening, they remain the primary reagents for examination of LEK1.

Distribution of transfected cytLEK1 protein in murine cells

Since certain LIS1 pathway members have been shown to be associated with the microtubule network specifically (Feng et al., 2000; Smith et al., 2000) albeit not always in a reproducible fashion (Faulkner et al., 2000), we wished to examine whether cytLEK1 exhibits similar characteristics. Attempts to examine the potential colocalization of endogenous cytLEK1 with microtubules were unsuccessful for various technical reasons related to specific fixation and extraction conditions required for individual antibodies. Thus, we transfected a FLAG-tagged cytLEK1 construct into cells in order to characterize the distribution of the protein product.

Results were identical in both C2C12 myoblasts and 3T3 fibroblasts. Interestingly, in many, but not all, cells transfected with this cytLEK1 construct, the transfected protein exhibits a very fibrous-like distribution pattern (Figure 21). CytLEK1 is distributed throughout the cytoplasm in long thin tracks separated by gaps lacking any detectable protein.

Colabeling experiments were conducted to determine if these tracks of cytLEK1 coincide with the microtubule network. Indeed, although the microtubule network is not clearly visible throughout the entire cell, the distribution of cytLEK1 is coincident with observable microtubule tracks (Figure 21 A). Except for certain instances on the periphery of cells, nearly every location where a microtubule track is visible it is overlaid with a cytLEK1 track. Thus, it appears that this transfected cytLEK1 protein does distribute along the microtubule network of the cell, suggesting that cytLEK1 has the ability to interact with either microtubules directly or with microtubule-associated proteins. These results are in agreement with the observation that endogenous cytLEK1 exhibits resistance to detergent extraction and is presumably interacting with cytoskeletal structures (Figure 12). Very likely, association with microtubule network structures may be the primary link of cytLEK1 to the cytoskeleton.

However, additional experiments to more precisely examine this colocalization of transfected cytLEK1 and the microtubule network revealed an unexpected result. Pre-extraction to better visualize the microtubule network results in the accumulation of transfected protein into clumps throughout the cytoplasm (Figure 22 A). Notably, there is no clear colocalization between these large cytLEK1 puncta and microtubules. Thus, even though cytLEK1 under normal fixation conditions appears to be distributed along microtubules, the association may not be strong enough to resist detergent pre-extraction. Fixation using cold methanol provides an intermediate phenotype where some cytLEK1 puncta are visualized but there is also a very diffuse cytoplasmic distribution of the transfected protein (Figure 22 B). This highly dispersed nature of cytLEK1 prevents any substantial colocalization analysis. As a whole, these experiments suggest that transfected cytLEK1 protein colocalizes with the microtubule network under certain conditions but such an association has not yet been determined to be definitive and strong.

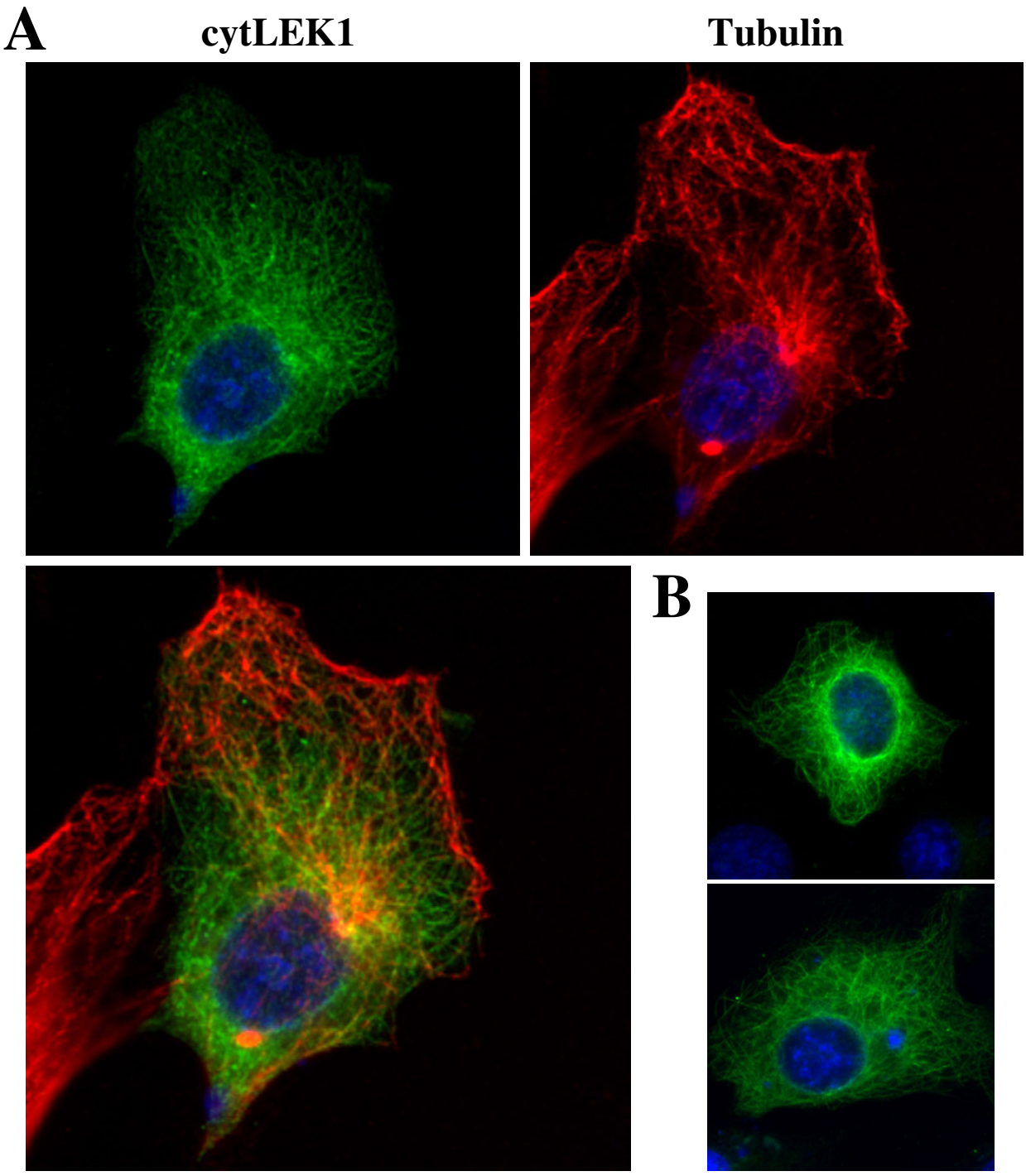

Figure 21. **Transfected cytLEK1 protein colocalizes with the microtubule network in murine cells.** 3T3 fibroblasts were transfected with a FLAG-tagged cytLEK1 construct and colocalization studies were conducted. The cytLEK1 protein (green) exhibits a fibrous distribution in cells (A-B). A) Transfected cytLEK1 colocalizes with the visible microtubule network (red) in these cells. B) A fibrous pattern for transfected cytLEK1 is observed in many cells. DAPI (blue) was used to visualize nuclei.

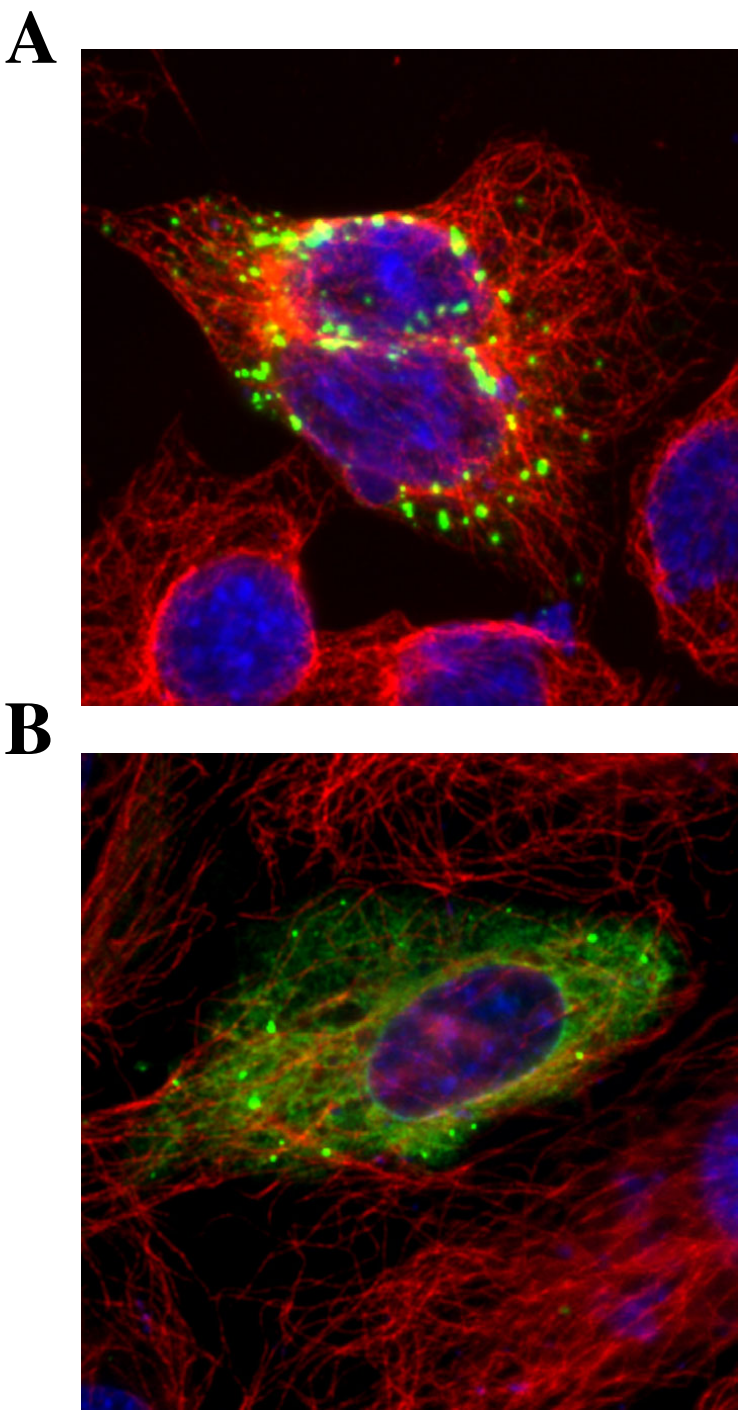

Figure 22. **Distribution of transfected cytLEK1 protein is dependent upon fixation and extraction conditions.** 3T3 fibroblasts were transfected with a FLAG-tagged cytLEK1 construct (green) and colocalization studies with tubulin (red) were conducted. A) Pre-extraction results in large cytLEK1 puncta that exhibit no clear codistribution with the microtubule network. B) Fixation with methanol reveals an intermediate pattern where cytLEK1 is found in both distinct puncta and diffusely in the cytoplasm. DAPI (blue) was used to visualize nuclei.

Discussion

LEK family members share a similar domain structure yet display unique expression patterns and activities (see Introduction). Their specific distributions relate to their putative functions in each different organism. Mitosin/CENP-F is a key component of the chromosomal kinetochore complex and plays an important role in proper completion of mitosis (Liao et al., 1995; Zhu et al., 1995b). As such, the protein is detected in a wide variety of human cells without any known tissue specificity, although available *in vivo* data is limited. It is expressed in a cell cycle-dependent manner with an important phosphorylation event occurring prior to its distribution to the kinetochore (Liao et al., 1995; Zhu et al., 1995b). However, the protein can also be detected on the spindle apparatus itself, suggesting that it may function at more than just the kinetochore. Not surprisingly, given its role in mitosis, Mitosin/CENP-F expression is upregulated in many human cancers (de la Guardia et al., 2001; Esguerra et al., 2004). Farnesylation is being examined as a potentially important post-translational modification in such settings (Russo et al., 2004). In summary, the expression pattern of Mitosin/CENP-F matches its role as a component of the mitotic apparatus in a wide variety of cells.

CMF1, however, has a significantly different distribution than Mitosin/CENP-F, thus providing the first clues of an alternative function. Notably, the protein is localized only to cardiac and skeletal myocytes of the developing chick embryo (Wei et al., 1996; Dees et al., 2000). Its expression is temporally regulated during development with highest levels at early embryonic stages and no protein detected in adult animals (Wei et al., 1996; Dees et al., 2000). Additionally, CMF1 undergoes a change in subcellular localization from the nucleus to the cytoplasm during embryogenesis (Dees et al., 2000), suggestive of a potential alteration in function. These observations imply an important role for CMF1 during development, not adulthood. Indeed, this hypothesis, which is based on distribution pattern, is confirmed by experiments that reveal the importance of CMF1 for myocyte differentiation (Wei et al., 1996; Dees et al., 2000).

Determination of the cytLEK1 expression pattern is thus a critical part of discovering the function of the protein. For this reason, experiments are presented here that uncover for the first time the distribution of this protein in a wide variety of tissues and cells. Previous studies have shown that nucLEK1 is expressed in nearly all cells in the developing embryo (Goodwin et al., 1999). Similar to CMF1, it cannot be detected in adult animals with the exception of the oocyte.

However, its distribution is confined to the nucleus throughout embryogenesis, unlike CMF1. Due to its disappearance in the heart during the critical postnatal period of terminal differentiation of cardiomyocytes, nucLEK1 has been suggested to function in regulating the processes of proliferation and differentiation. Indeed, nucLEK1 binds to all three known Rb family members, and LEK1 depletion results in proliferation and differentiation defects (Ashe et al., 2004). Expression studies have thus yet again aided in the determination of protein function. Therefore, analysis of cytLEK1 localization should provide important clues as to the role of this protein product.

Since the downregulation of nucLEK1 during terminal differentiation of cardiomyocytes is a key event in cardiac development, it is interesting to note that cytLEK1 expression levels also decline during this period (Figure 8). In fact, the decrease appears to be even more abrupt than for nucLEK1, suggesting that the cardiac function of cytLEK1 is confined to events occurring predominantly at embryonic stages. Thus, cytLEK1 may have important effects on the widely-occurring proliferation and migration processes of cardiomyocytes at such developmental stages (Mikawa et al., 1992). These functions would be consistent with those of LIS1 pathway members, including NudE(L), which have been shown to be critical for proper cell division and migration during development (Feng and Walsh, 2004; Shu et al., 2004). However, some cytLEK1 protein still remains at postnatal stages so a direct role in terminal differentiation processes may also be possible. Importantly, the dramatic change in localization of cytLEK1 that occurs by neonatal day 2 is very intriguing and suggests that cytLEK1 may switch to a different function during postnatal stages. As this altered distribution is specific to cytLEK1 and not observed with nucLEK1, such a dual effect may represent a wider role for the larger cytLEK1 peptide than for the smaller nucLEK1 one. Another possibility is that the protein detected in the nucleus is uncleaved LEK1. With currently available reagents, it is difficult to determine if this seemingly nuclear-localized cytLEK1 represents uncleaved protein. It may be that regulation of the cleavage event is a method for specifying the function of LEK1. However, current Western blot evidence does not support this idea, as a ~300 kDa band equivalent to uncleaved LEK1 is not observed. As this may be an issue of detection level, future immunofluorescence studies utilizing LEK1 monoclonal antibodies currently under development will resolve this cleavage event.

An additional intriguing question related to this postnatal change in localization is whether cytLEK1 is truly nuclear or very tightly perinuclear. While the tissue sections are thin (< 7 μm), confocal studies are needed to confirm the exact distribution. If cytLEK1 is truly nuclear at these stages and there is no alteration in cleavage of LEK1, then the protein is likely serving an unknown function in the nucleus at certain developmental stages, similar to CMF1 with its dual subcellular localization (Dees et al., 2000). If instead the confocal analysis reveals that there is a perinuclear localization, then this result is intriguing since this location represents the predominant site of LIS1 pathway proteins (see Introduction; Figures 27-30) and also the area where cytLEK1 is most resistant to detergent extraction (Figure 12). Thus, the pool of cytLEK1 protein that interacts with LIS1 pathway members may persist longer during cardiac development than the subset of protein that serves an as-yet-unknown function at the periphery. Regardless of the exact result, this change in localization suggests a need for distinct cytLEK1 functions at different developmental stages in the murine heart.

Examination of cytLEK1 expression in other tissues yields further clues as to its role during development. In the small intestine, there is a noticeable difference between the fluorescent intensity of the cytLEK1 and nucLEK1 antibodies at all stages inspected. These data suggest that nucLEK1 may possibly play a more important role, or be required at higher expression levels, than cytLEK1 in this tissue. As nucLEK1 is currently postulated to have a primarily proliferative function, this observation may be consistent with the high level of cell division occurring during formation of the intestine. However, another possibility is that the epitope of the cytLEK1 antibody is partially blocked in the intestine, perhaps due to a tissue-specific protein interaction, or that the antibody simply exhibits less affinity for its antigen than the nucLEK1 antibody does. A quantitative Western blot analysis may help confirm these putative expression differences. It is important to note, however, that both cytLEK1 and nucLEK1 are downregulated in the postnatal intestine based on these immunofluorescence data, even though this tissue remains highly proliferative through adulthood (Ross et al., 1995). Thus, we confirm in the intestine that cytLEK1, similar to nucLEK1, plays a specific role in the developing embryo that is not maintained or required during adulthood.

This pattern is also observed in multiple other tissues by an extensive Western blot analysis (Figure 10). In adult animals, cytLEK1 protein, consistent with heart and intestine studies, is not detected in the brain, skeletal muscle, or liver. The intensity of bands in the brain

and liver, especially at late embryonic and early postnatal stages, suggests that these tissues are important sites of cytLEK1 function. The incidence of multiple bands in the brain implies a potentially intriguing oligomerization of cytLEK1. In general, the presence of cytLEK1 in this tissue is of interest, as the brain is a key site of LIS1 pathway member function (see Introduction). It would be unexpected for cytLEK1 regulation of the LIS1 pathway during development to not extend to this organ. The processes of proliferation, migration, and differentiation are occurring throughout this organ during embryogenesis, and we postulate that cytLEK1 is likely required for proper formation of the brain. It will be very interesting for future studies to examine cytLEK1 function in neuronal cells, as well as the effect of a neuronal-specific *LEK1* -/- mouse.

Just as LIS1 pathway members play a role in more tissues than only the brain (see Introduction), we expect cytLEK1 to have a similar function. In fact, the results we present in this chapter and those of previous LEK1 studies (Goodwin et al., 1999) reveal that LEK1, including its cytLEK1 peptide product, shares significant expression similarities with NudE(L). Like cytLEK1, NudE and Nudel proteins are expressed at their highest levels in the brain, heart, and skeletal muscle (Niethammer et al., 2000; Sasaki et al., 2000; Yan et al., 2003). Thus, cytLEK1 has the potential to interact with NudE(L) in the wide range of tissues where the two proteins are coexpressed at high levels. Nudel is first detected in the mouse at embryonic day 13.5 and expression reaches a plateau at neonatal day 5 (Niethammer et al., 2000; Sasaki et al., 2000). While protein data are lacking, *NudE* appears at embryonic day 11 and peaks five days later (Feng et al., 2000). It then begins to decrease to a low level maintained throughout adulthood. Thus, the expression pattern of NudE, especially, suggests that, similar to cytLEK, its presence is most important during development, not adulthood. The fact that Nudel is maintained throughout adulthood differs from cytLEK1, but may partially explain why we have uncovered an interaction of NudE, not Nudel, with cytLEK1 (chapter III). It is possible that cytLEK1 specifically interacts with NudE and that Nudel is not relevant to cytLEK1 function. However, this proposal has not been tested, as direct binding studies have not been conducted and all the cytLEK1 domains are not yet characterized. Nonetheless, it is clear that cytLEK1 and NudE interact and share a similar expression pattern in a time- and tissue-specific fashion. Thus, they are potentially partner proteins in a wide variety of cell types during development. CytLEK1 regulation of the LIS1 pathway may therefore be a critical component of embryogenesis.

Additional studies in chapter IV building upon the expression studies presented here begin to address the role of the cytLEK1-NudE interaction in various tissues and cell types.

Experiments examining the subcellular distribution of cytLEK1 support the idea of an important link between cytLEK1 and the LIS1 pathway. Notably, the perinuclear concentration of cytLEK1 in non-dividing cells (Figure 11) is consistent with the pattern of most LIS1 pathway members (see Introduction). Thus, cytLEK1 is located at the proper position to interact with and regulate these proteins. It is evident that cytLEK1 is not exclusively perinuclear, similar again to many LIS1 pathway members, and this suggests that there may be additional functions of cytLEK1 that have not yet been determined. In fact, the large size and wide cytoplasmic distribution of cytLEK1 make it unlikely that the only role of the protein is to regulate components of the LIS1 pathway near the nucleus. Importantly, a subset of cytLEK1 protein is resistant to detergent pre-extraction, suggesting a link with the cytoskeleton. This is a key observation for a protein postulated to function in the LIS1 pathway. The fact that the resistant cytLEK1 pool is present specifically near the nucleus supports the proposal that cytLEK1 has a LIS1-related role in perinuclear regions and an unknown function at the periphery.

The analysis of LEK1 distribution in mitotic cells is especially exciting, as it marks the first time any significant observation has been made for cytLEK1 or nucLEK1 localization in dividing cells. While they clearly only represent a minority of each total protein population, the cytLEK1 and nucLEK1 proteins present on the spindle itself and the spindle poles are important because they place these molecules at critical locations for regulation of mitotic functions. Once again, this localization pattern matches that of other LIS1 pathway members (Faulkner et al., 2000; Yan et al., 2003; Feng and Walsh, 2004). Considering the dramatic disruption of proliferation resulting from LEK1 depletion (Ashe et al., 2004), these data begin to suggest an additional mechanism for LEK1 regulation of mitosis, independent of any interactions with Rb family members. It may be that cytLEK1 plays a role in spindle formation, similar to its binding partner NudE (Feng and Walsh, 2004), and/or in dynein-directed movement of chromosomes. It will be interesting to see in future studies if cytLEK1, similar to NudE(L), is transported along the spindle through an association with dynein (Yan et al., 2003). Based on its prominent localization at the centrosome of dividing cells, cytLEK1 dysfunction may disrupt spindle attachment to this organizing center, thus inhibiting mitotic progression. The fact that expression of the myc-C dominant negative protein has never been detected in a mitotic cell is an interesting

observation in this context. However, it has also introduced difficulties in designing experiments to examine cytLEK1 dysfunction in dividing cells. Clearly, this is an important area for future studies.

Any discussion of LEK1 localization in mitotic cells requires a comparison with Mitosin/CENP-F, the human kinetochore-binding protein related to LEK1. In our experiments, we cannot detect cytLEK1 or nucLEK1 on chromosomal kinetochores. However, considering the overall low levels of these proteins localized to the mitotic apparatus, a higher resolution detection method, such as confocal deconvolution analysis, in combination with a chromosome spread may be required. There are discrepancies even in the detection of LIS1 pathway members on the kinetochore due to similar issues (Yan et al., 2003; Feng and Walsh, 2004). Mitosin/CENP-F has also been detected on the spindle (Liao et al., 1995; Zhu et al., 1995b), however, and this is in agreement with our observations for LEK1. Examination of the Mitosin/CENP-F and LEK1 protein sequences reveals that the kinetochore-binding domain of the former (Zhu, 1999) appears to be intact in nucLEK1. A large region N-terminal to that domain is absent in nucLEK1, though, which may affect protein conformation and thus mask or disrupt any potential kinetochore-binding domain. Additionally, LEK1 lacks the homodimerization region of Mitosin/CENP-F (Zhu, 1999). It thus appears that while LEK1 and Mitosin/CENP-F do share some similarities, such as presence on the spindle apparatus, their functions and domains are significantly divergent. Our expression studies confirm the substantial differences between the two proteins. Most importantly, cytLEK1 and nucLEK1, unlike Mitosin/CENP-F (Liao et al., 1995; Zhu et al., 1995a), are present in non-mitotic cells and do not appear to be significantly upregulated prior to cell division. It is currently unknown what human protein may serve to compensate for the function of LEK1 and vice-versa. Answering this question will likely be very difficult due to the inherent problems in examining the role of a protein during human embryonic development.

Our final examination of endogenous cytLEK1 localization consists of studying fibroblasts *in vitro* during monolayer wound healing. The results do not reveal any substantial change in cytLEK1 distribution or expression in these cells, despite one previous study revealing an alteration for some LIS1 pathway members (Dujardin et al., 2003). At this point, it is difficult to discern whether there truly is no change in cytLEK1 localization or whether we are unable to detect it using current techniques. It is worthwhile to note that the previous study required total

internal fluorescence microscopy to observe the alterations (Dujardin et al., 2003). Based on its interaction with NudE, it is highly likely that cytLEK1 plays a role in cell migration, although a redistribution of the protein may not be required for this function. Future live imaging studies examining the effects of cytLEK1 dysfunction on migration will help provide a more direct assay for determining such a role for the protein.

As evidenced from the results in this chapter, the two antibodies we currently use for cytLEK1 and nucLEK1 detection have been useful in a wide range of assays. Previous work in our laboratory, in addition to experiments here, has shown that these antibodies are capable of specifically detecting the LEK1 peptide products in immunofluorescence assays, Western blots, expression library screens, and *in vitro* translation studies (Pabon-Pena et al. unpublished data; Figures 4-5). Additionally, morpholino studies of LEK1 knockdown serve as additional controls for specificity (Ashe et al., 2004; Figure 38). However, the new sets of antibodies we generate and characterize here are not as robust. The fact that the majority of new antibodies reveal a pattern similar to that previously observed for cytLEK1 is reassuring for the cytLEK1 studies that are the main focus of this document. We are surprised, though, at the inability of any newly-designed antibody to detect a localization pattern similar to that of our current nucLEK1 antibody. There are several potential explanations for this result. First, it appears that only one antibody (N2690) is truly directed against an epitope in nucLEK1. The N2088 antibody near the putative cleavage site likely detects cytLEK1 based on our results. Thus, this discrepancy may simply be the result of a single unsuccessful antibody design. Second, epitope masking is always a potential issue, so we may have designed the antibody against a region of nucLEK1 that is not exposed endogenously. Third, the N2690 antibody may have additional specificity for another protein. Notably, it is able to detect protein in non-transfected COS-7 cells. It is currently unknown whether this effect is due to a completely unrelated protein or, in fact, a LEK family member in primates.

An additional issue is the strange localization detected by certain of the new cytLEK1 antibodies. The occasionally nuclear distribution of the C264 antibody is intriguing, as it suggests the possibility that cytLEK1 may sometimes enter the nucleus of cells. However, as such a localization is not observed with any other antibody, we are hesitant to place much value on such a scenario. Another possibility is that the extreme N-terminus of cytLEK1 is additionally cleaved and thus has a different and unique distribution. Unfortunately, the inability of these

newly-designed antibodies to consistently work on a Western blot prevents a thorough testing of this hypothesis. As we have shown in this document, cytLEK1 is at least partially associated with the cytoskeleton and resistant to detergent extraction. Thus, the amount of endogenous cytLEK1 present in the soluble fraction of cell lysate may be low and require an antibody with very high affinity on Western blot for consistent detection. Finally, with regard to the C1127 antibody, the nuclear puncta detected are intriguing due to the observation of cytLEK1 puncta in the nucleus during postnatal heart development (Figure 7). However, the fact that the C1127 antibody is also able to detect transfected nucLEK1 protein suggests that its specificity is not high and may explain this result. Additional studies are required to resolve these discrepancies with the new antibodies, and the ongoing generation of a *LEK1* -/- mouse will be of great assistance.

The final observations on cytLEK1 localization come from studies of transfected cytLEK1 protein. The fibrous-like distribution of the protein in many cells is very suggestive of a cytoskeletal link. Even with the limited resolution obtained in these experiments due to fixation issues, it is clear that this transfected cytLEK1 is located on microtubule tracks and is generally absent from other areas. While we are unable to unambiguously detect endogenous cytLEK1 on the microtubule network, this is primarily the result of fixation/extraction incompatibilities with the cytLEK1 antibody and is not a conclusive result. Thus, these transfection experiments overcome such restrictions. However, the dramatic change in localization of transfected cytLEK1 protein with alteration of the fixation and extraction protocol is somewhat puzzling. The results from methanol fixation are inconclusive due to the widespread distribution of the protein. However, the large cytLEK1 puncta that appear with detergent pre-extraction do not exhibit any colocalization with the clearly-detected microtubule network. A partial explanation is that the transfected cytLEK1 protein does indeed associate with microtubules but that this link is not strong. Thus, the pre-extraction conditions are harsh enough to disrupt this interaction and remove any transfected cytLEK1 from the cytoskeleton. The lack of strong binding may be a consequence of the fact that the full length cytLEK1 protein expressed is not the same size as the endogenous protein due to the unknown location of the cleavage site. Thus, this transfected protein may not be able to properly fold and interact with the same structures as endogenous cytLEK1. An additional possibility, which is difficult to directly test, is simply that inherent artifacts in each fixation/extraction technique are obscuring similarities between the results. Such

an artifact issue may explain the large cytLEK1 puncta that accumulate after pre-extraction, as they have not been seen under any other conditions. It may be that the high amount of transfected protein aggregates during the pre-extraction procedure and thus appears as clumps.

In conclusion, the results on the localization and expression of cytLEK1 presented in this chapter provide important clues as to the nature of cytLEK1 function. It is evident that cytLEK1 has the potential to interact with LIS1 pathway members in many tissues and cell types in the developing mouse. The heart and brain remain the most intriguing organs for future study. These data suggest that the subcellular location of any interactions between cytLEK1 and LIS1 pathway members is likely near the nucleus in non-dividing cells. In mitotic cells, cytLEK1 may play a role in spindle formation and function. Additionally, cytLEK1 associates with the cytoskeleton predominantly around the nucleus, consistent with its role as a regulator of the LIS1 pathway. This interaction likely specifically involves the microtubule network of cells based on our results. Experiments in later chapters elaborate further on the function of cytLEK1 in these various tissues and subcellular locations.

CHAPTER III

EXAMINATION OF CYTLEK1 PROTEIN BINDING PARTNERS

Introduction

Previous studies on LEK1 suggest that it plays a role in proliferation and differentiation processes in the developing embryo (Goodwin et al., 1999; Ashe et al., 2004). This hypothesis was initially based on the observation that disruption of CMF1, the chick member of the LEK family, inhibits myocyte differentiation (Wei et al., 1996; Dees et al., 2000). This was supported by the observation that, in the heart specifically, *LEK1* mRNA is detected until neonatal day 4 and then abruptly disappears (Goodwin et al., 1999). We show in chapter II that the cytLEK1 protein undergoes an interesting change in localization during this same time period. This alteration in cytLEK1 distribution and subsequent reduction in LEK1 expression coincide with the period when cardiomyocytes are undergoing permanent cessation of mitosis and terminal differentiation (Soonpaa et al., 1996; Soonpaa and Field, 1998). Additional studies have shown that nucLEK1 binds to all three known Rb family members (Rb, p107, p130) both *in vitro* and *in vivo* (Ashe et al., 2004). Through such interactions, nucLEK1 has the potential to be a critical regulator of proliferation and differentiation. Indeed, depletion of LEK1 expression in murine cells results in a disruption of proliferation and differentiation (Ashe et al., 2004). However, the distinct roles of cytLEK1 and nucLEK1 in these important cellular processes are not clear. In fact, no function at all had been attributed to the cytLEK1 protein prior to the work presented here. Thus, we wished to examine the role of cytLEK1 by first determining its key binding partners.

We initially hypothesized that cytLEK1 may have a cytoskeletal role due to its cytoplasmic distribution pattern (Figure 11) and the presence of a spectrin repeat, a domain shown in other proteins to be involved in cytoskeletal functions (Djinovic-Carugo et al., 2002). Thus, we utilized the spectrin repeat region of cytLEK1 as bait in a yeast two-hybrid screen. The major interacting protein identified in this assay is NudE, a member of the LIS1 pathway (Feng et al., 2000). LIS1 pathway members function in dynein-related processes of the microtubule network (see Introduction). This interaction with NudE supports our hypothesis of a cytoskeletal role for cytLEK1 through the spectrin repeat region. We define the exact binding domains within

each protein and reveal that an 80 aa "C domain" in cytLEK1 is critical for the cytLEK1-NudE interaction to occur. Co-immunoprecipitation studies of cytLEK1 and NudE confirm the validity of the yeast two-hybrid results. Also, these two protein products colocalize after cotransfection. We show that the C domain alone is capable of directing the interaction with NudE, especially at the centrosome, as determined by localization studies in COS-7 cells. Finally, extensive confocal deconvolution analysis of endogenous proteins in murine cells reveals that cytLEK1 colocalizes with NudE, in addition to LIS1 and dynein, the two known binding partners of NudE. In summary, these data show that cytLEK1 binds to NudE and codistributes with several key members of the LIS1 pathway. Thus, cytLEK1 has the potential to regulate critical interactions between LIS1 pathway members.

Materials and Methods

Yeast two-hybrid screen

The yeast two-hybrid (Y2H) screen was conducted by utilizing the Matchmaker Y2H System 3 (BD Biosciences Clontech). The spectrin repeat region (SRR) of cytLEK1 (aa 1906-2149) was PCR amplified on an iCycler PCR machine (Bio-Rad) using Pfu Turbo polymerase (Stratagene) from a full-length cytLEK1 vector (aa 1-2210) with primers containing a 5' NcoI and 3' EcoRI site. The pGBKT7 vector (BD Biosciences Clontech) and the resulting SRR fragment were digested with NcoI/EcoRI and ligated to generate pGBKT7-SRR. This plasmid was transformed into AH109 yeast per manufacturer's instructions and tested for toxicity and growth on SD/-Trp/X-α-Gal, SD/-His/-Trp/X-α-Gal, and SD/-Ade/-Trp/X-α-Gal. Mating efficiency of the pGBKT7-SRR-containing yeast was comparable to controls. The AH109 yeast containing this bait plasmid were subsequently mated per manufacturer's instructions with Y187 yeast pretransformed with a whole mouse embryonic day 11 cDNA library (BD Biosciences Clontech). The mating reaction was grown overnight at 30˚C with gentle swirling (50 rpm). The colonies were then plated onto TDO without Gal (SD/-His/-Leu/-Trp; first screen performed) or QDO without Gal (SD/-Ade/-His/-Leu/-Trp; second screen performed) 150 mm plates and grown for 4 days (TDO) or 7 days (QDO) at 30˚C. Library mating mixtures and negative controls were also conducted in parallel per manufacturer's instructions. Colonies were replica plated manually onto QDO plates (SD/-Ade/-His/-Leu/-Trp /X-α-gal) a minimum of three times

to retest phenotypes. Segregation was observed upon streaking, and only blue colonies were selected for further analysis.

Bait and prey plasmids were simultaneously isolated from these yeast using the Yeastmaker Yeast Plasmid Isolation Kit (BD Biosciences Clontech) per manufacturer's instructions. Successful isolation of prey plasmid was confirmed via Taq polymerase (Promega) PCR amplification using the Matchmaker AD LD Insert Screening Amplimer Set (BD Biosciences Clontech). Plasmids were then electroporated into XL-1 Blue Electrocompetent *E. coli* (Stratagene), and prey plasmid-containing bacteria were selected for by growth on ampicillin LB plates. Plasmids were isolated from the bacteria via Wizard Plus SV MiniPreps (Promega) and sequenced using the GAL4 AD Sequencing Primer (BD Biosciences Clontech). Resulting sequences were identified via NCBI Blast (Altschul et al., 1990). To confirm the validity of interactions, false positive tests were conducted per manufacturer's instructions. Briefly, each unique prey clone was transformed into AH109 yeast and mated with Y187 yeast containing pGBKT7-SRR, pGBKT7-53, or pGBKT7 before plating onto QDO medium. Only yeast that grew with pGBKT7-SRR but not the other two plasmids were deemed to be true positives and considered candidates for further biochemical examination.

Deletion constructs

In order to determine precisely which region of the SRR of cytLEK1 interacts with NudE, a deletion approach was followed in the yeast two-hybrid system. The SRR was further divided into the N domain (aa 1906-64), the repeat (R) domain (aa 1964-2071), and the C domain (aa 2071-2149). Deletion constructs were created by Pfu Turbo polymerase PCR amplification and subsequent cloning into pGBKT7 using NcoI/EcoRI. Variations of these domains were created as shown in Figure 23. AH109 yeast were transformed with each SRR deletion construct. Conversely, NudE deletion constructs were created as shown in Figure 23. After cloning into pGADT7 using EcoRI/XhoI, the plasmids were transformed into Y187 yeast. Matings of the various SRR and NudE deletion construct-containing yeast were conducted and grown on QDO plates while being tested for Gal expression to determine viable interactions.

In order to confirm results by co-immunoprecipitation (co-IP) in mammalian cells, the relevant cytLEK1 and NudE yeast plasmid inserts were cloned, respectively, into pCMV-myc and pCMV-HA mammalian expression vectors (BD Biosciences Clontech). The SRR and N+R

cytLEK1 fragments were ligated into pCMV-myc using MscI/SalI. NudE was ligated into pCMV-HA using SfiI/XhoI. Since pCMV-HA-NudE did not yield high-level expression, GFP-mNudE (Feng et al., 2000) was used for transfection studies.

Cloning of dysbindin

The murine dysbindin coding sequence was PCR amplified on an iCycler PCR machine (Bio-Rad) using Pfu Turbo polymerase (Stratagene) from an IMAGE dysbindin cDNA clone (Invitrogen) with primers containing a 5' EcoRI site and 3' XhoI site. The resulting insert was then cloned into pGADT7 and transformed into AH109 yeast. Additionally, the insert was ligated with the mammalian expression vector pEGFP-C1 (BD Biosciences Clontech) to create a GFP-dysbindin fusion.

Cell culture

COS-7 and NIH 3T3 cells (ATCC) were maintained in Dulbecco's Modified Eagle's Medium (DMEM; Cellgro) supplemented with 10% fetal bovine serum, 100 □g/mL penicillin/streptomycin, and L-glutamine. C2C12 cells (ATCC) were grown in Dulbecco's Modified Eagle's Medium (DMEM) supplemented with 20% fetal bovine serum, 100 □g/mL penicillin/streptomycin, and L-glutamine. All cell lines were maintained in a 95% air-5% CO_2 humidified atmosphere at 37˚C.

Transfections

COS-7 cells were grown to 40-60% confluency and transfected using FuGENE6 (Roche) per manufacturer's instructions. Briefly, FuGENE was added to a tube containing OptiMEM medium (Cellgro) and gently mixed. DNA was then added and gently mixed. After a 15 min incubation, the FuGENE-DNA mixture was pipetted into plates containing cells and fresh medium. For each 10 cm plate, 3 □g of total DNA was utilized for transfection. Cells were grown for 24-48 h prior to collection for further examination.

Co-immunoprecipitation

COS-7 cells grown on 10 cm plates were harvested 48 h after transfection for use with the ProFound Mammalian c-Myc Tag Co-IP Kit (Pierce) according to manufacturer's protocol.

Briefly, cells were washed once with ice-cold TBS, incubated with gentle shaking in M-PER™ (Pierce) plus protease inhibitor (Sigma), and spun down at 16,000 x *g* for 20 min at 4˚C. Protein concentration was determined using a bicinchoninic acid solution assay (Smith et al., 1985) from Pierce. Lysates (250 μg/column) were incubated overnight with 10 μL anti-c-myc agarose slurry with gentle end-over-end mixing at 4˚C. After 3 washes with TBS-Tween, protein was eluted with 2X non-reducing sample buffer (Pierce) at 95˚C. 2-mercaptoethanol was added to the eluate for SDS-PAGE analysis followed by immunoblotting. Lysate (10 μg/lane) was used to confirm protein expression.

Western blotting

Lysates were incubated with 5X sample buffer (0.312 M Tris-HCl pH 6.8, 10% sodium dodecyl sulfate, 25% 2-mercaptoethanol, 0.05% bromophenol blue) for 5 min at 95˚C. After boiling, samples were separated by sodium dodecyl sulfate-polyacrylamide gel electrophoresis (SDS-PAGE). Proteins on the gel were transferred overnight on ice to 0.45 μm pore size Immobilon-P PVDF transfer membrane (Millipore). Membranes were blocked with 2% BSA in TBST for 1-2 h at room temperature. Primary antibody was then applied for 1-2 h with shaking. After three washes with TBST, the membrane was incubated with alkaline phosphatase-conjugated secondary antibody for 1 h with shaking. This was followed with three TBST washes and one alkaline phosphatase buffer wash. Membranes were developed using NBT-BCIP (Roche) in alkaline phosphatase buffer and scanned into digital format (Hewlett-Packard).

Immunocytochemistry and microscopy

Cells grown on glass chamber slides (Nalge Nunc) were gently washed with PBS and fixed with Histochoice (Amresco), 70% ethanol (for Spec1), or -20˚C methanol (for β-tubulin) for 20 min. Cells were then washed briefly in PBS, permeabilized with 0.25% Triton X-100 in PBS for 10 min, and blocked in 2% BSA in PBS for a minimum of 1 h. Primary antibodies in 1% BSA in PBS were applied overnight at 4˚C. After three PBS washes, secondary antibodies were applied for 1 h at room temperature. The slides were washed three times with PBS and twice with water before cover slips were attached with Aqua Poly/Mount (PolySciences). Cells were visualized by fluorescence microscopy on an AX70 (Olympus) or, for confocal analysis, an LSM510 (Zeiss) microscope. Digital images were captured and processed using Magnafire

(Optronics), Metamorph (Universal Imaging), and Photoshop (Adobe) software. Deconvolution analysis was performed on confocal Z stacks (0.5 μm optical thickness) using a blind 3-D deconvolution algorithm (AutoQuant Imaging).

Antibodies

Polyclonal antibodies against LIS1 and dynein were purchased from Santa Cruz. Anti-GFP and anti-myc monoclonal antibodies were from BD Biosciences. A polyclonal anti-myc antibody was acquired from Novus. The monoclonal antibodies against β-tubulin, vimentin, and desmin were manufactured by Sigma. The MF20 antiserum to sarcomeric myosin heavy chain was a generous gift of Donald A. Fischman at Cornell Medical College. Polyclonal antibody Spec1 to a cytLEK1 peptide (aa 1826-45) was generated in rabbits (Biosynthesis) and affinity purified using the injected peptide (Smith et al., 1985). The N-terminal 14 residues of murine NudE protein were synthesized, coupled to KLH, and used to immunize chicken. IgY from egg yolks was purified to > 90% purity (QED Bioscience) and screened for specific immunoreactivity against both recombinant and endogenous murine NudE protein (antibody obtained from Dr. Christopher A. Walsh at Harvard University; Feng and Walsh, 2004). Alexa 488 and Alexa 568 conjugated secondary antibodies, as well as Phalloidin-488, were obtained from Molecular Probes. Anti-mouse alkaline phosphatase conjugated secondary antibodies for Western blot were purchased from Sigma. DAPI was used to visualize nuclei (Boehringer Mannheim).

Results

Identification of cytLEK1-interacting proteins

In order to identify cytLEK1 binding partners and place the protein in a molecular pathway, a yeast two-hybrid approach was utilized. The region chosen as bait was based on sequence analysis and on our hypothesis for a cytoskeletal function of cytLEK1. The spectrin repeat region of cytLEK1 contains both a spectrin repeat, which can serve as a cytoskeletal and signal transduction docking region (Djinovic-Carugo et al., 2002), and numerous leucine zippers, which generally play a role in protein-protein and protein-DNA interactions (O'Shea et al., 1989). For this reason, the spectrin repeat along with ~80 aa flanking sequence on each side (aa

1906-2149; termed SRR for spectrin repeat region) was used as a bait to screen a whole mouse embryonic day 11 cDNA library. The screen was performed twice and yielded 117 and 94 clones, in turn. Of these, 12 and 19 clones, respectively, were found to contain the full coding sequence of NudE. After conducting retransformations to eliminate false positives, all of the NudE clones, unlike the majority of the remaining clones, showed a specific interaction with the SRR of cytLEK1. Two additional proteins pass the false positive test: dysbindin (3 clones) and a hypothetical protein (6 clones). Since the known embryonic and tissue expression, as well as the cytoplasmic distribution and function, of NudE generally coincided with that of cytLEK1 and the hypothesis of a cytoskeletal function for the spectrin repeat region, there was enough evidence to pursue this putative interaction.

Identification of the binding domains of cytLEK1 and NudE

In order to determine precisely which region of the SRR of cytLEK1 interacts with NudE, a deletion approach was followed with the two-hybrid system. The SRR was further divided into the N domain (aa 1906-64), the repeat (R) domain (aa 1964-2071), and the C domain (aa 2071-2149). Deletion constructs were created that combined variations of these domains as shown in Figure 23. Similar myc-tagged plasmids were constructed for mammalian transfection and are referred to by this nomenclature system (myc-SRR, myc-C, myc-N+R). Interestingly, all constructs containing the C domain, not necessarily the R domain itself, were capable of binding to full length NudE. In fact, a construct containing only the C domain was sufficient for interaction. No other proteins were detected during screening that were capable of specifically associating with the C domain alone. Attempting to further truncate the C domain eliminated all binding, suggesting that aa 2071-2149 of cytLEK1 are critical for interaction with NudE. In order to determine the region of NudE binding to the C domain of cytLEK1, deletional constructs of NudE were utilized (Figure 23). These studies revealed that a C-terminal region of NudE (aa 167-290) was required and sufficient for the interaction with the C domain of the SRR. This region in NudE coincides with the dynein-binding domain of its isoform, Nudel, and encompasses a specific region essential for dynein binding (Sasaki et al., 2000; Liang et al., 2004). The homology between NudE and Nudel suggests a conservation of the function of this domain, thus revealing that the cytLEK1-binding domain in NudE partially overlaps the dynein-binding domain.

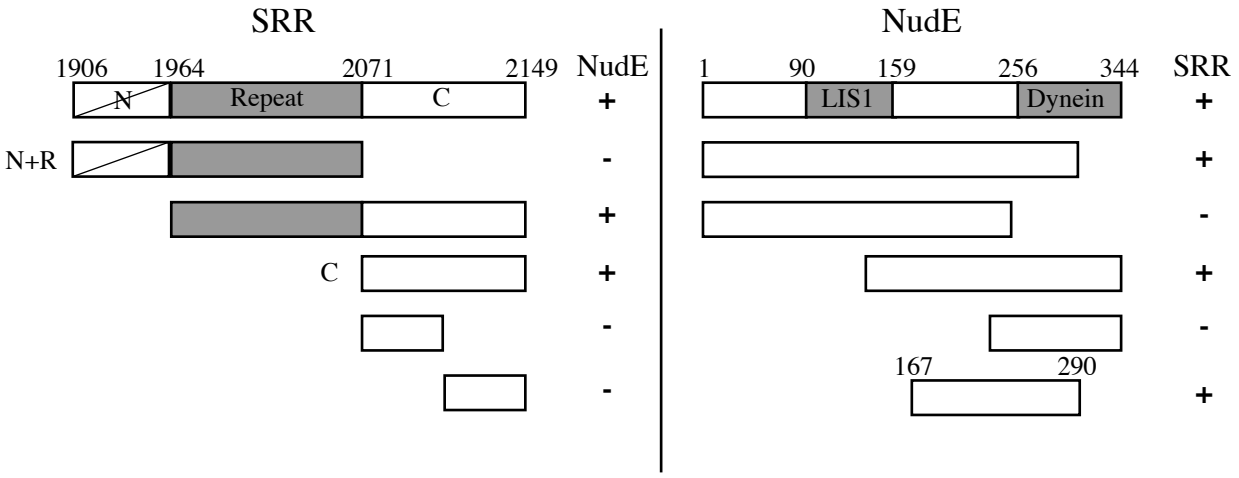

Figure 23. **Examination of cytLEK1-NudE interaction and identification of binding domains.** Deletion constructs of SRR were transformed into yeast and mated with yeast expressing full-length NudE. The spectrin repeat is represented by the gray box while the N and C domains are depicted with hemisected and white rectangles, respectively. Matings that grew on quadruple dropout medium are listed as "+". The C domain of SRR (aa 2071-2149) is required and sufficient for interaction with NudE. Similarly, deletion constructs of NudE were transfected into yeast and mated with yeast expressing SRR. The LIS1- and putative dynein-binding domains of NudE(L) are shown. CytLEK1 binds to aa 167-290 of NudE. These domains were confirmed by mating yeast expressing this region of NudE with yeast expressing the C domain of SRR. The N+R and C constructs used in the dominant negative studies are labeled.

To determine whether cytLEK1 and NudE interact in mammalian cells, COS-7 cells were cotransfected with myc-SRR and GFP-mNudE for co-immunoprecipitation analysis. As seen in Figure 24 A, GFP-mNudE co-immunoprecipates with myc-SRR, confirming the two-hybrid data and demonstrating the interaction between cytLEK1 and NudE. Importantly, GFP-mNudE is unable to be co-immunoprecipitated with myc-N+R, which lacks the C domain (Figure 24 B). Therefore, the C domain is indeed required for the binding of cytLEK1 and NudE. Taken together, these results demonstrate the interaction of cytLEK1 and NudE in mammalian cells and map this interaction to a specific domain.

CytLEK1 colocalizes with NudE and □-tubulin in COS-7 cells

As cytLEK1 and NudE interact on a biochemical level, we next examined whether the proteins colocalize within individual cells. Initially, COS-7 cells were cotransfected with either myc-SRR or myc-C and GFP-mNudE to examine their cellular distribution. As seen in Figure 25 A, myc-SRR and GFP-mNudE exhibit extensive overlap in staining, predominantly in distinct cytoplasmic puncta, previously shown to be related to the centrosome (Feng et al., 2000). Importantly, presence of the C-domain alone is sufficient to direct this colocalization to a cytoplasmic spot in both COS-7 and 3T3 fibroblasts (Figure 25 B). We confirmed that myc-C indeed does localize most intensely to the centrosome based on □-tubulin staining (Figure 26 A). Additionally, myc-C colocalizes with endogenous NudE protein present at the centrosome (Figure 26 B), reiterating the specificity of the C domain for binding to NudE. Confirming the critical importance of the C domain for NudE colocalization, myc-N+R does not colocalize with GFP-mNudE in COS-7 cells (Figure 25 C).

CytLEK1 colocalizes with NudE binding partners in murine cells

Since cytLEK1 and NudE interact biochemically and have overlapping immunocytochemical distributions after cotransfection (Figures 24-26), we examined the endogenous localization of cytLEK1 with NudE and, additionally, with the known NudE partner proteins, LIS1 and dynein (Feng et al., 2000), using cell lines previously shown to be susceptible to disruption of LEK1, Nudel, and LIS1 (Dujardin et al., 2003; Ashe et al., 2004; Shu et al., 2004). As seen in Figure 27, cytLEK1 displays significant colocalization with dynein in both 3T3 and C2C12 cells. The confocal images reveal a similar and overlapping distribution pattern

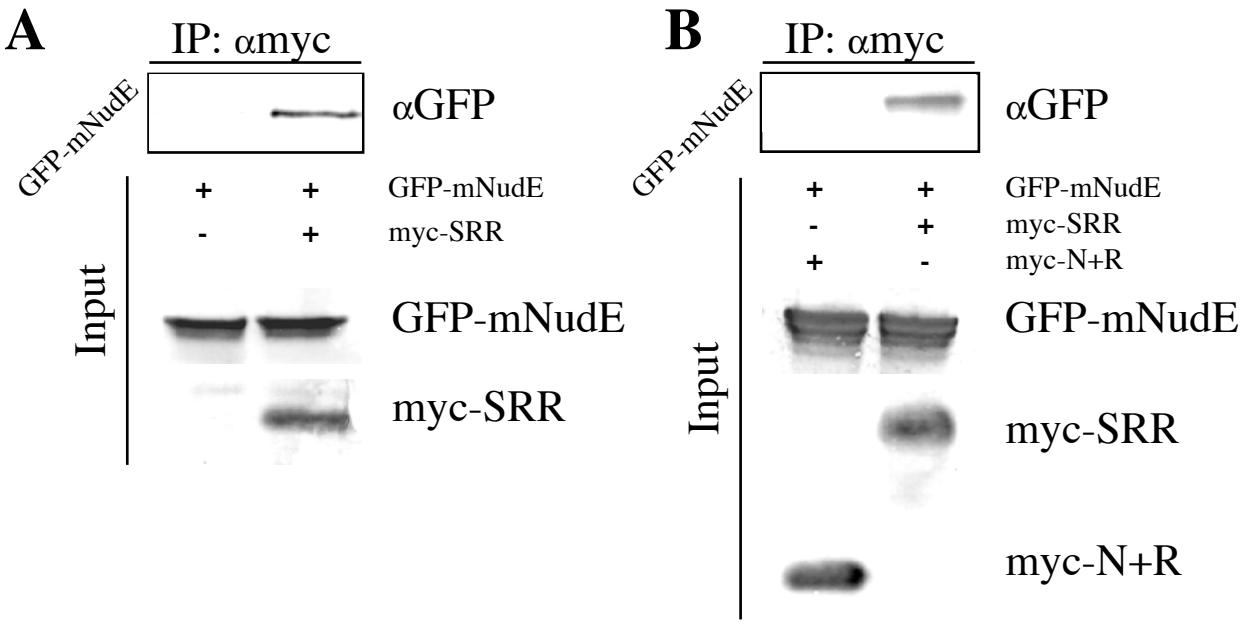

Figure 24. **Examination of cytLEK1-NudE interaction through co-immunoprecipitation.** A) COS-7 cells were transfected with either GFP-mNudE alone or GFP-mNudE and myc-SRR. Lysates were collected and immunoprecipitated with an anti-myc antibody. Blots were then probed with anti-GFP. Protein expression was confirmed by blotting lysate lanes. GFP-mNudE is co-immunoprecipitated with myc-SRR when coexpressed while GFP-mNudE is not co-immunoprecipitated in its absence. B) When COS-7 cells are cotransfected with GFP-NudE and myc-N+R, GFP-mNudE is not detected in the precipitant. Thus, the C domain in myc-SRR is required for the interaction between cytLEK1 and NudE.

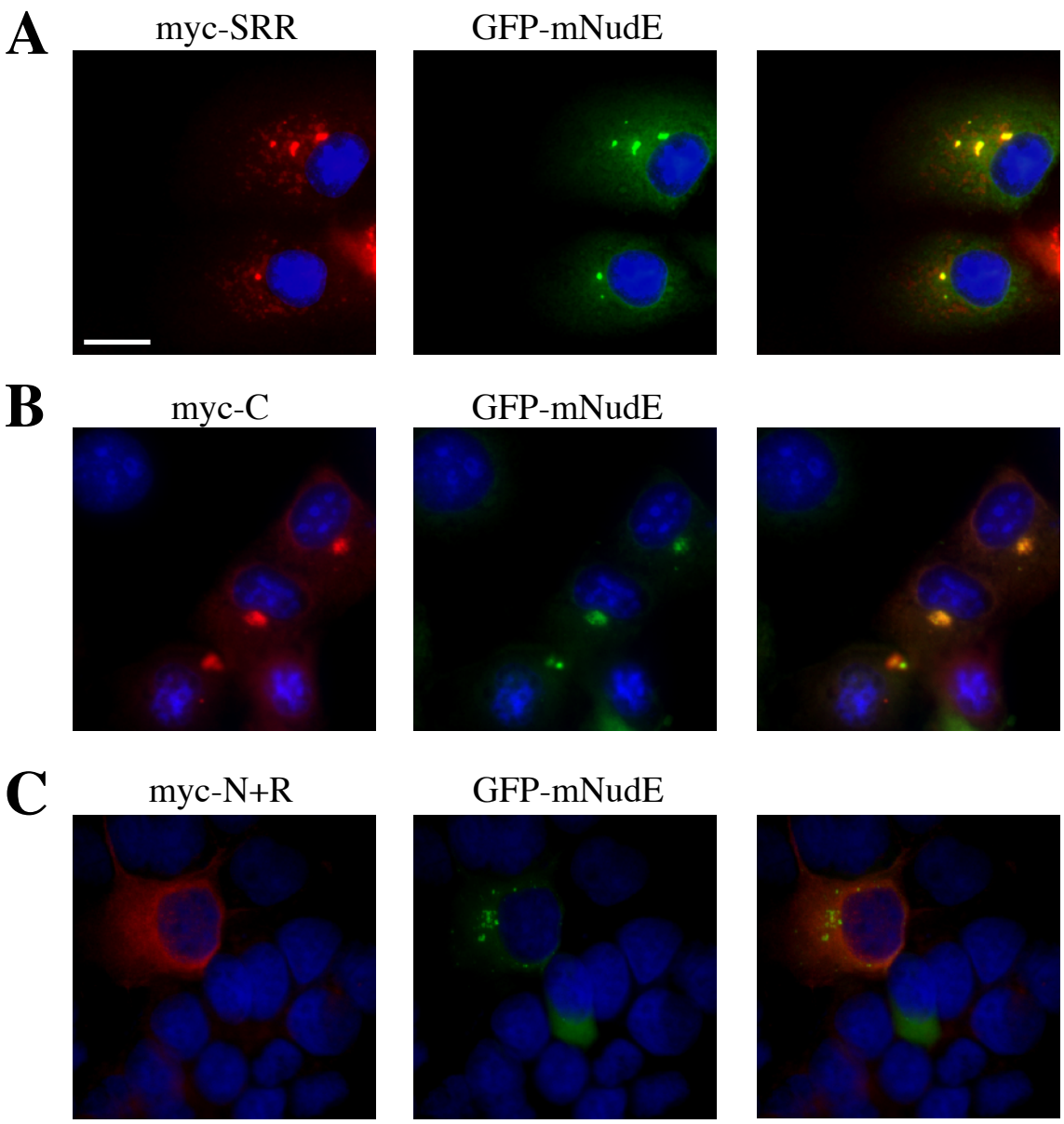

Figure 25. **CytLEK1 colocalizes with GFP-mNudE in COS-7 cells.** GFP-mNudE is in green and myc-tagged proteins are in red. A) COS-7 cells were cotransfected with myc-SRR and GFP-mNudE. The merged image shows clear colocalization of these two proteins. B) COS-7 cells were cotransfected with myc-C and GFP-mNudE. The merged image reveals colocalization of this small cytLEK1 protein containing the NudE-binding domain with GFP-mNudE at a distinct cellular spot. C) Notably, when COS-7 cells were cotransfected with GFP-mNudE and myc-N+R, which lacks the NudE-binding domain, no colocalization can be detected. DAPI (blue) was used to visualize nuclei. Bar, 10 μm.

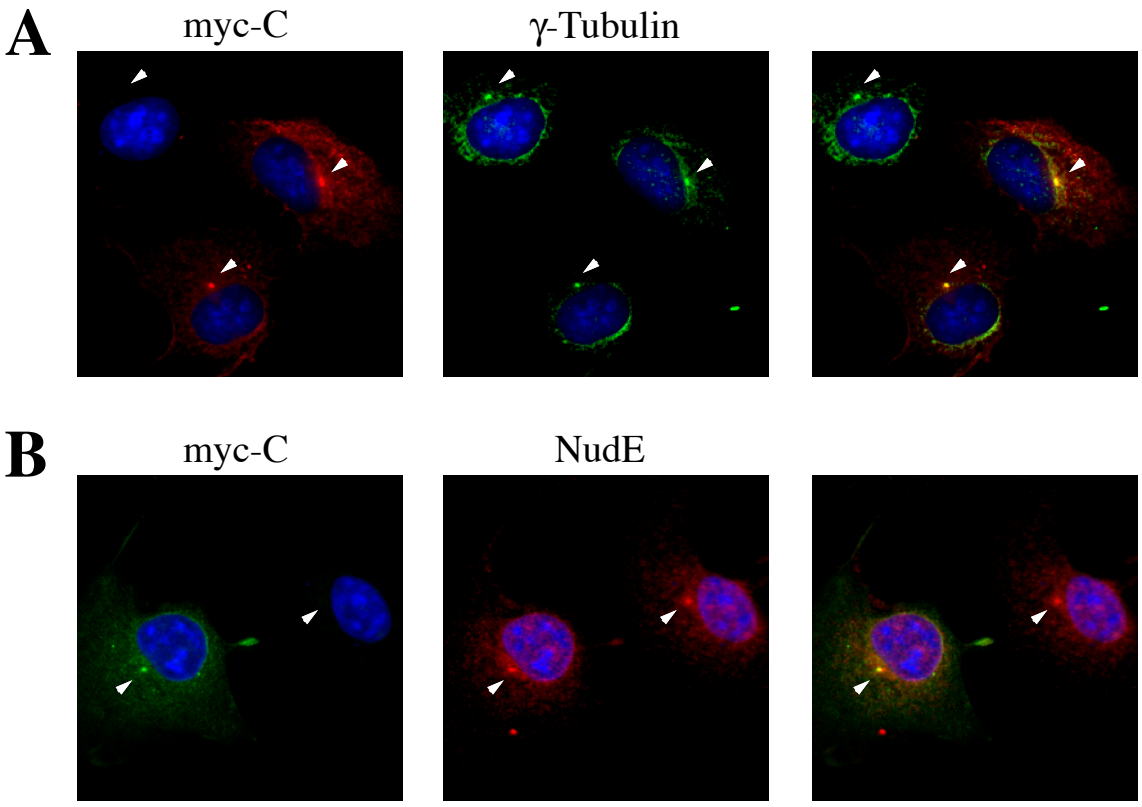

Figure 26. **CytLEK1 colocalizes with NudE and γ-tubulin in COS-7 cells.** Arrowheads mark the γ-tubulin and NudE centrosomal spots. A) Myc-C (red) was transfected into COS-7 cells to examine colocalization with endogenous γ-tubulin (green) at the centrosome. Myc-C localizes most intensely to the centrosome. B) COS-7 cells were transfected with myc-C (green) and the protein colocalizes with endogenous NudE (red) present at the centrosome. DAPI (blue) was used to visualize nuclei.

of cytLEK1 and dynein throughout most of the cell, including perinuclear regions of intense labeling. As will be discussed in detail shortly, the perinuclear staining is not simply an artifact of high protein concentrations in these regions, since colabeling of cytLEK1 with markers for other cytoplasmic proteins does not reveal any noticeable colocalization (Figure 31). We further analyzed the colocalization of dynein and cytLEK1 by conducting deconvolution analysis of confocal images (Figure 27 B). These studies revealed that the codistribution of cytLEK1 and dynein is not absolute. While there is substantial colocalization near the nucleus, it becomes less apparent toward the periphery of cells. This finding is expected as dynein is a protein with a vast array of cellular functions, while the LIS1 pathway is postulated to affect only a subset of these functions (Vallee et al., 2001). Indeed, LIS1 does not colocalize completely with dynein, especially near the cell periphery (Smith et al., 2000). With regard to the distribution between cytLEK1 and LIS1, a high degree of colocalization is observed in both 3T3 and C2C12 cells (Figure 28). Furthermore, deconvolution analysis reveals that the amount of overlap is not complete and is highest in perinuclear regions. Thus, cytLEK1 colocalizes with two key members of the LIS1 pathway predominantly around the nucleus.

CytLEK1 colocalizes with NudE in murine cells

In order to examine colocalization between endogenous cytLEK1 and NudE, a previously-unpublished (at the time) antibody was obtained from Dr. Christopher A. Walsh at Harvard University (Feng and Walsh, 2004). Although extensive assays had been performed by the Walsh laboratory, a series of tests was conducted here to determine its specificity for detection of NudE in immunofluorescence assays. The antibody successfully recognizes GFP-mNudE transfected into COS-7 cells. Additionally, it detects endogenous NudE located at the centrosome in these cells (Figure 26 B), although this localization to the organizing center is not consistently observed and requires following a strict fixation protocol. More often, staining consists of a diffuse perinuclear pattern. Even in those COS-7 cells where centrosomal labeling is observed, there remains a non-centrosomal population, as has been reported in the literature (Feng et al., 2000; Yan et al., 2003; Feng and Walsh, 2004). In summary, this antibody appears to specifically detect both endogenous and transfected NudE protein.

The NudE antibody exhibits a more robust and easily-visualized pattern in 3T3 fibroblasts (Figure 29). Fixation requirements are not as strict and thus allow for colabeling

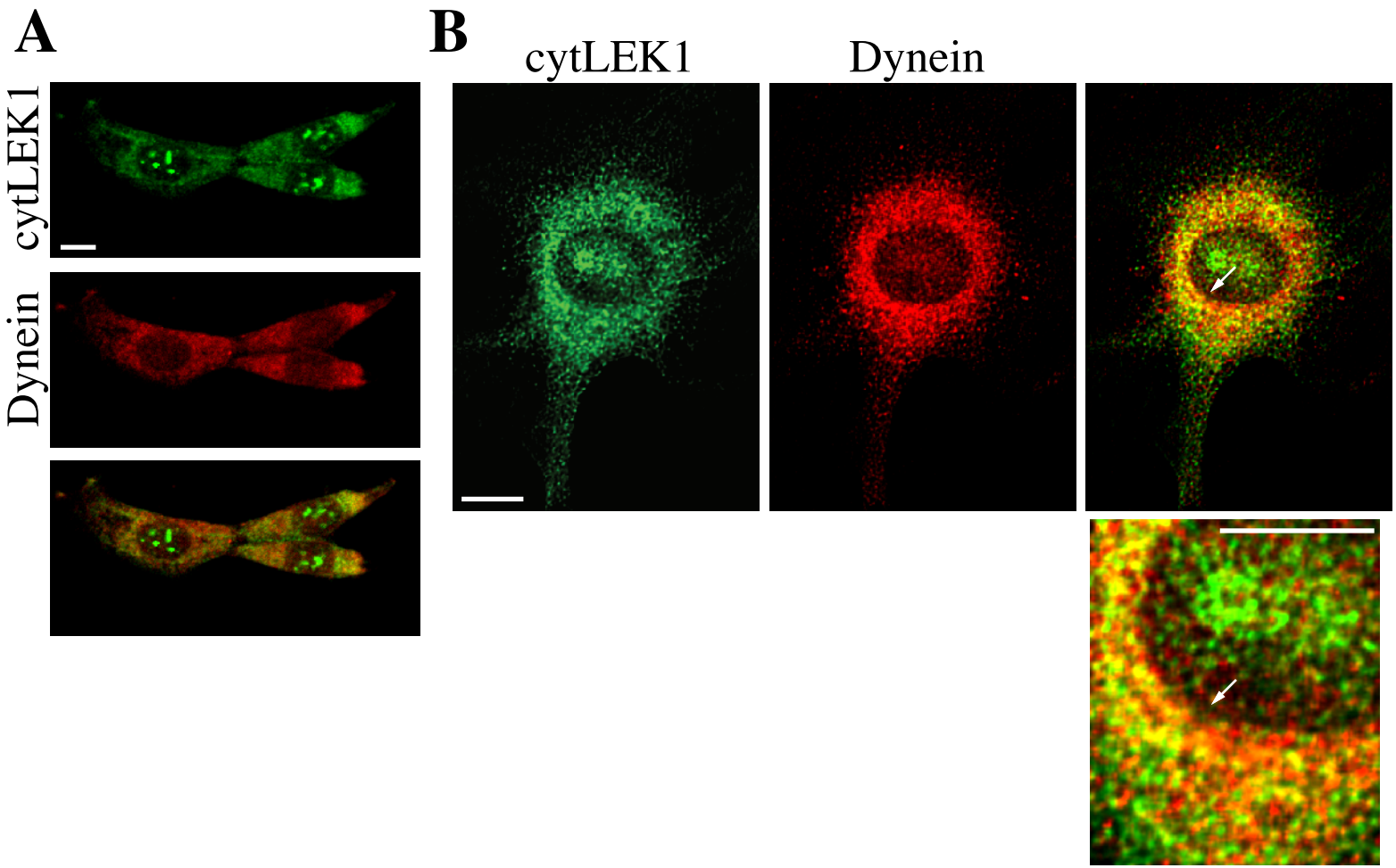

Figure 27. **CytLEK1 colocalizes with the NudE binding partner dynein in murine cells.** Confocal microscopy was utilized to examine colocalization of endogenous proteins in 3T3 fibroblasts. Deconvolution analysis (0.5 mm optical sections) of confocal data was conducted to provide a higher level of detail (B). CytLEK1 is in green and dynein is visualized in red. A) The merged image reveals an overlapping distribution pattern of cytLEK1 and dynein. B) Colocalization is most evident near the nucleus and is less apparent towards the cell periphery. The arrow provides a point of reference for the enlarged image. Intense nuclear puncta are a secondary antibody artifact. Bars, 5 μm.

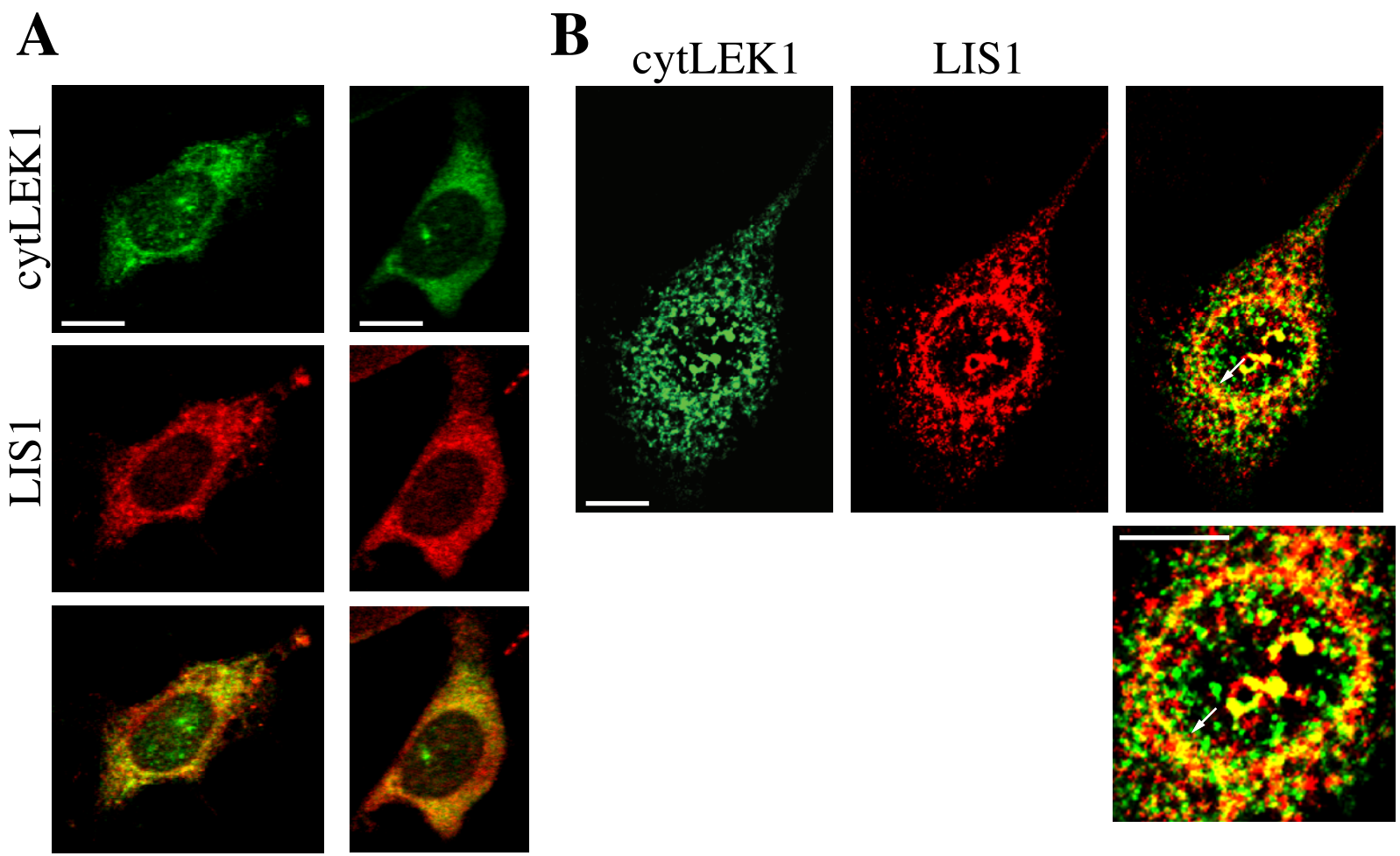

Figure 28. **CytLEK1 colocalizes with the NudE binding partner LIS1 in murine cells.** Confocal microscopy was utilized to examine colocalization of endogenous proteins in 3T3 fibroblasts. Deconvolution analysis (0.5 mm optical sections) of confocal data was conducted to provide a higher level of detail (B). CytLEK1 is in green and LIS1 is visualized in red. A) The merged images display colocalization between cytLEK1 and LIS1 in 3T3 cells. B) Deconvolution analysis confirms a significant perinuclear colocalization of the two proteins. The arrow provides a point of reference for the enlarged image. Intense nuclear puncta are a secondary antibody artifact. Bars, 5 µm.

studies with cytLEK1. This is the first time the distribution of NudE has been specifically examined in this cell line. Our initial studies reveal a perinuclear distribution of NudE in these murine fibroblasts (Figure 29 A), a pattern similar to cytLEK1, other members of the LIS1 pathway, and Nudel in this cell type (Niethammer et al., 2000; Sasaki et al., 2000; Shu et al., 2004). Clearly, NudE is present at more than just the organizing center, as the protein is predominantly perinuclear with no clear centrosomal labeling. CytLEK1 and NudE exhibit a similar distribution in our confocal studies (Figure 29 B). Interestingly, on occasion, there is colocalization of the two proteins seemingly on the cell membrane or periphery (unpublished data). Deconvolution analysis (Figure 30) further defines the highest amount of colocalization to be near the nucleus, as described above for the two other LIS1 family members. Taken together, our results here suggest that cytLEK1 has the potential to influence dynein-mediated processes, such as microtubule regulation, through the LIS1 pathway.

Colocalization studies with cytLEK1 and additional cytoplasmic proteins

Since cytLEK1 is a protein with a cytoplasmic distribution and a putative cytoskeletal role, colocalization experiments were conducted with antibodies against various potential partner proteins unrelated to the LIS1 pathway. In total, components of the thick, thin, and intermediate filament networks were studies in myoblasts and other cell types, since their general cytoplasmic pattern could coincide with that of cytLEK1. First, various intermediate filament proteins were examined. Vimentin clearly does not colocalize with cytLEK1 in 3T3 fibroblasts. Additionally, although there is at times slight overlap, the overall distribution of cytLEK1 does not coincide with that of desmin in C2C12 myoblasts (Figure 31 A). High concentrations of one protein do not match areas with large quantities of the other protein. For visualization of actin networks, a component of thin filaments, phalloidin was utilized. There is no correlation between the punctate cytLEK1 pattern and the actin network within 3T3 fibroblasts and C2C12 myoblasts (Figure 31 B). Finally, the MF20 antibody against myosin was utilized for examination of the thick filament network in differentiating myocytes. Once again, there is no colabeling of cytLEK1 and myosin of myofibrils. These results are in agreement with previous studies examining the distribution of CMF1 in cardiac myocytes (Pabon-Pena et al., 2000). While negative in nature, these data here provide an important control for our positive colocalization

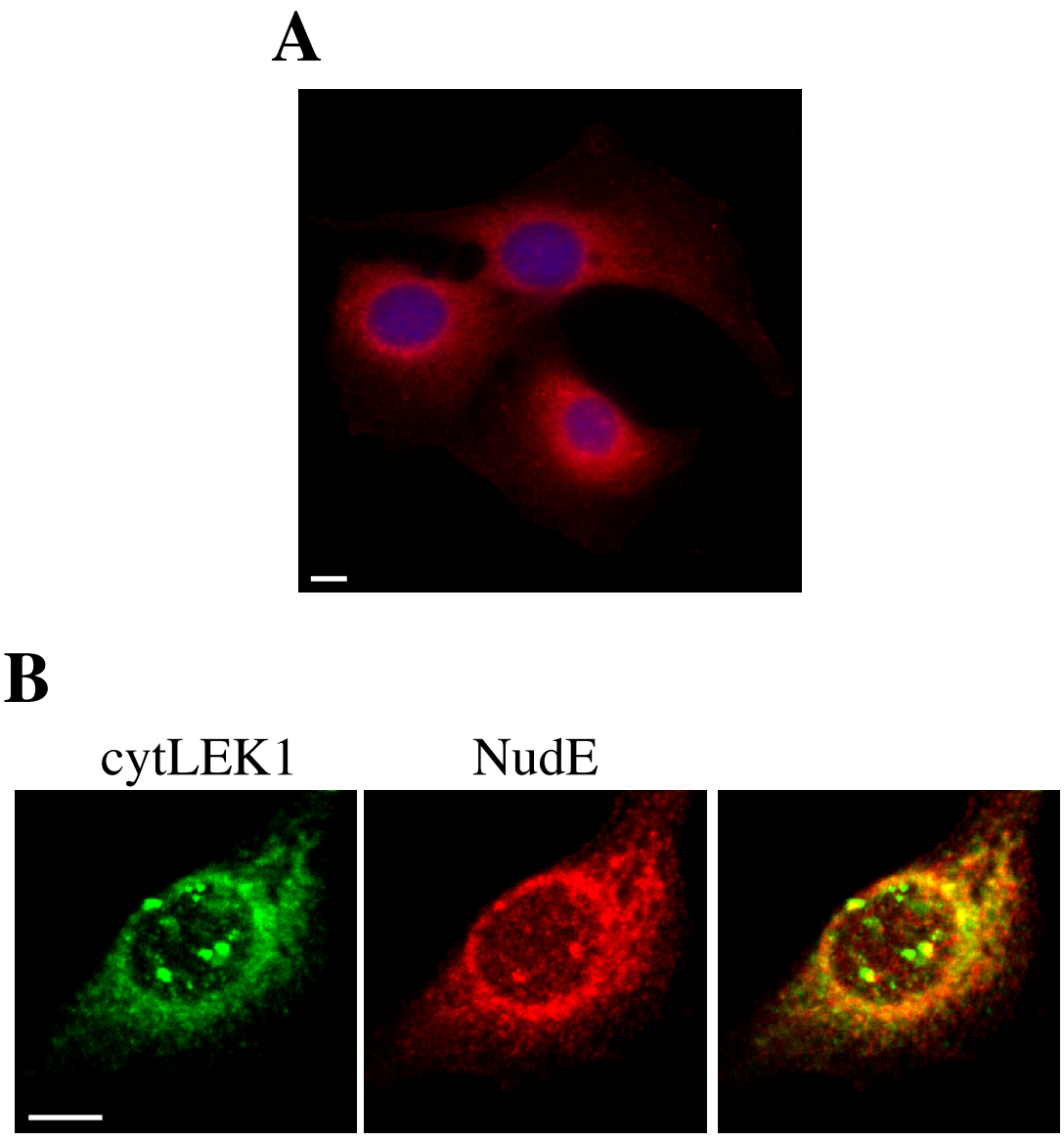

Figure 29. **Examination of NudE localization in murine cells.** Confocal microscopy was employed to examine colocalization of endogenous proteins in 3T3 fibroblasts (B). CytLEK1 is in green and NudE is visualized in red. A) NudE is distributed in the cytoplasm of 3T3 fibroblasts and is concentrated more highly around the nucleus. B) The merged image reveals a similar and overlapping distribution pattern of cytLEK1 and NudE. Intense nuclear puncta in (B) are a secondary antibody artifact. Bars, 5 μm.

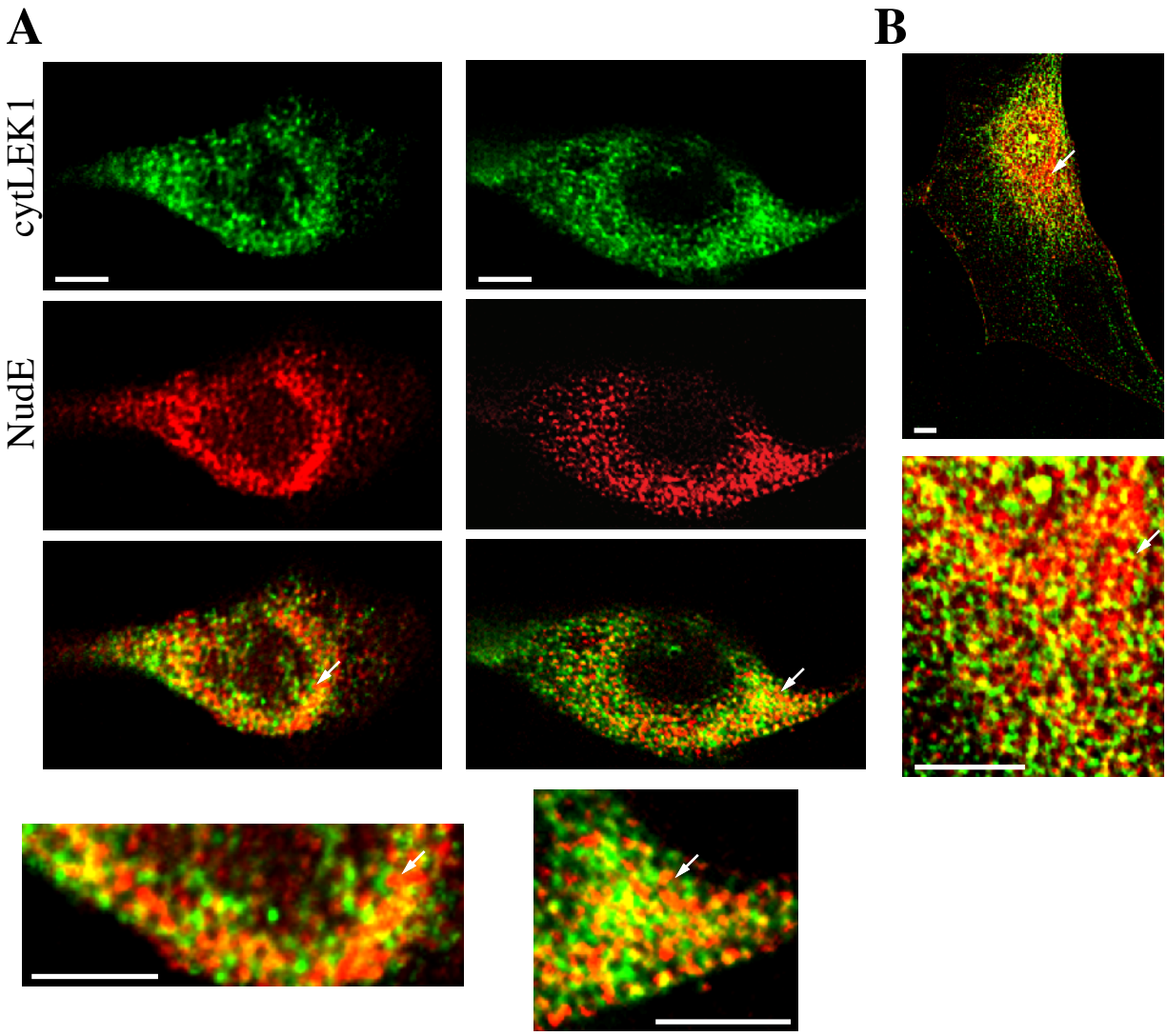

Figure 30. **CytLEK1 colocalizes with NudE in murine cells.** Confocal microscopy was employed to examine colocalization of endogenous proteins in 3T3 fibroblasts. Deconvolution analysis (0.5 mm optical sections) of confocal data was utilized to provide a higher level of detail. CytLEK1 is in green and NudE is visualized in red. A) Deconvolution analysis confirms signficant colocalization of cytLEK1 and NudE in perinuclear regions. B) Colocalization becomes less evident away from the nucleus. The arrows provide reference points for the enlarged images. Intense nuclear puncta are a secondary antibody artifact. Bars, 5 µm.

studies with LIS1 pathway components. Clearly, cytLEK1 distribution exhibits a similarity specifically related to LIS1 family members, not just any cytoplasmic protein.

Examination of putative cytLEK1-dysbindin interaction

The other putative interacting protein to cytLEK1 discovered through the yeast two-hybrid screen is dysbindin (dystrobrevin-binding protein). This result is interesting due to the similarities in expression of dysbindin and LEK1. Both are most highly expressed in heart, skeletal muscle, and brain (Goodwin et al., 1999; Benson et al., 2001). They also play important roles during development. Dysbindin interacts with dystrophin and dystrobrevin, both of which are members of the dystrophin-associated protein complex in muscle (Benson et al., 2001). This complex is involved in membrane scaffolding for muscle integrity and in signal transduction pathways, and its dysfunction results in Duchenne muscular dystrophy (Blake and Martin-Rendon 2002). Additionally, dysbindin has also been associated with abnormalities in brain function as related to schizophrenia (Numakawa et al., 2004). More recently, roles for dysbindin outside of the dystrophin complex in muscle have been suggested. The protein appears to regulate vesicular trafficking to organelles as part of the BLOC-1 (biogenesis of lysosome-related organelles) complex (Li et al., 2003). While the actions of dysbindin relate broadly to the proposed hypothesis for cytLEK1 function, the localization of dysbindin to the muscle sarcolemma does not match the observed distribution of cytLEK1 in such tissues. However, since dysbindin is a recently discovered protein that has not been thoroughly studied yet, its localization in cardiac myocytes and the possible existence of a cytoplasmic pool of protein remain unknown.

Since we were unable to obtain an antibody to dysbindin for localization studies, we utilized commercial antibodies to its primary binding partner, dystrobrevin. Experiments were conducted to examine the localization of □- and □-dystrobrevin in muscle cells and tissues (Figure 32). In general, both proteins exhibit similar patterns with □-dystrobrevin having a more diffuse distribution. To confirm the efficacy of the antibodies, they were first used on adult mouse skeletal muscle tissue sections, and they successfully label the muscle sarcolemma, as well as the cytoplasm for □-dystrobrevin. Experiments then proceeded to examine C2C12 myoblasts, which have not been carefully studied in the past for dystrobrevin localization. Interestingly, in undifferentiated C2C12 myoblasts, dystrobrevin is cytoplasmic and localizes

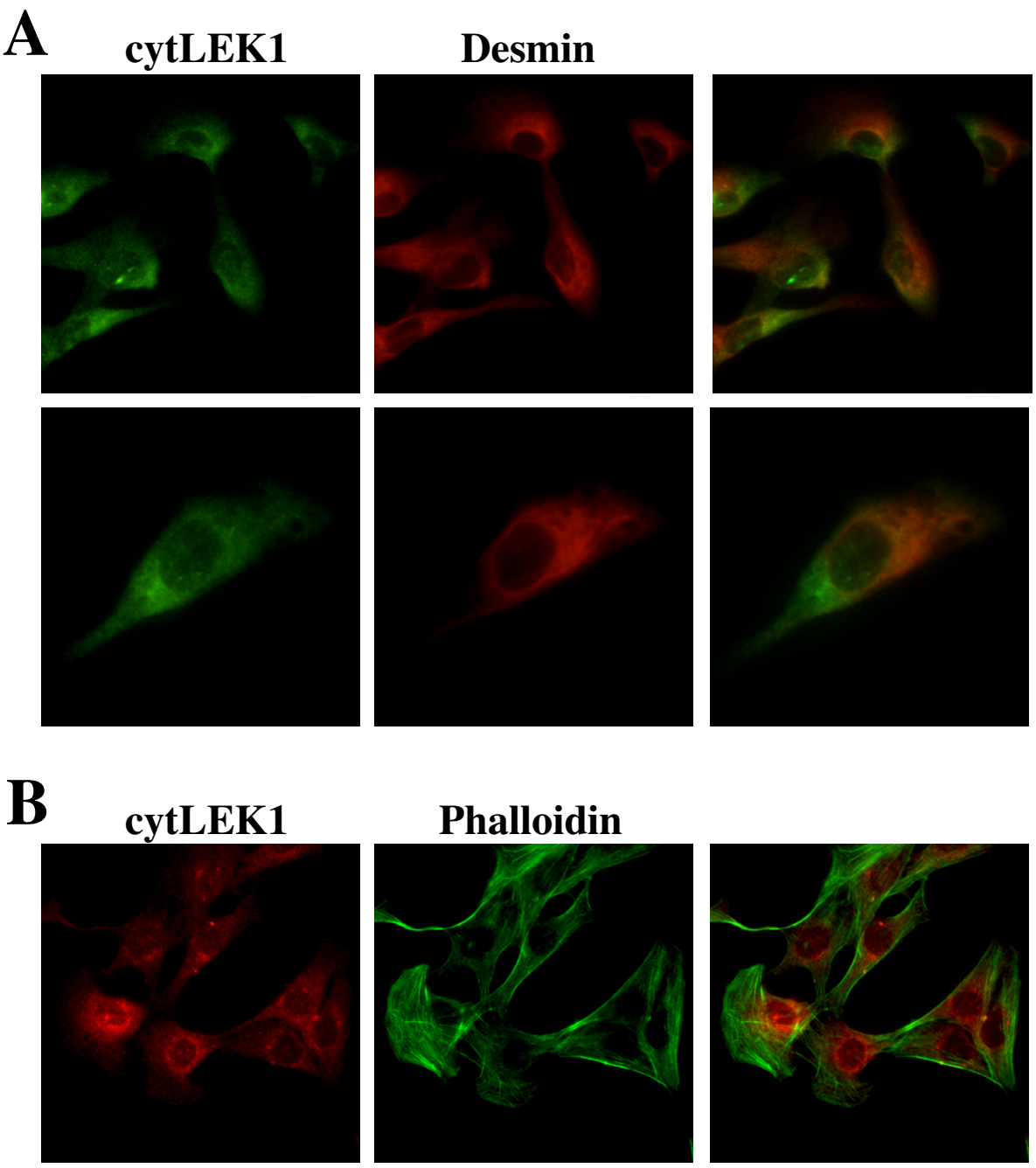

Figure 31. **CytLEK1 does not colocalize with several cytoplasmic proteins in murine cells.** A) CytLEK1 is visualized in green and desmin is in red. No colocalization is observed between these two cytoplasmic proteins in C2C12 myoblasts. B) CytLEK1 is in red and the actin network is visualized with phalloidin (green). No colocalization is observed in C2C12 cells.

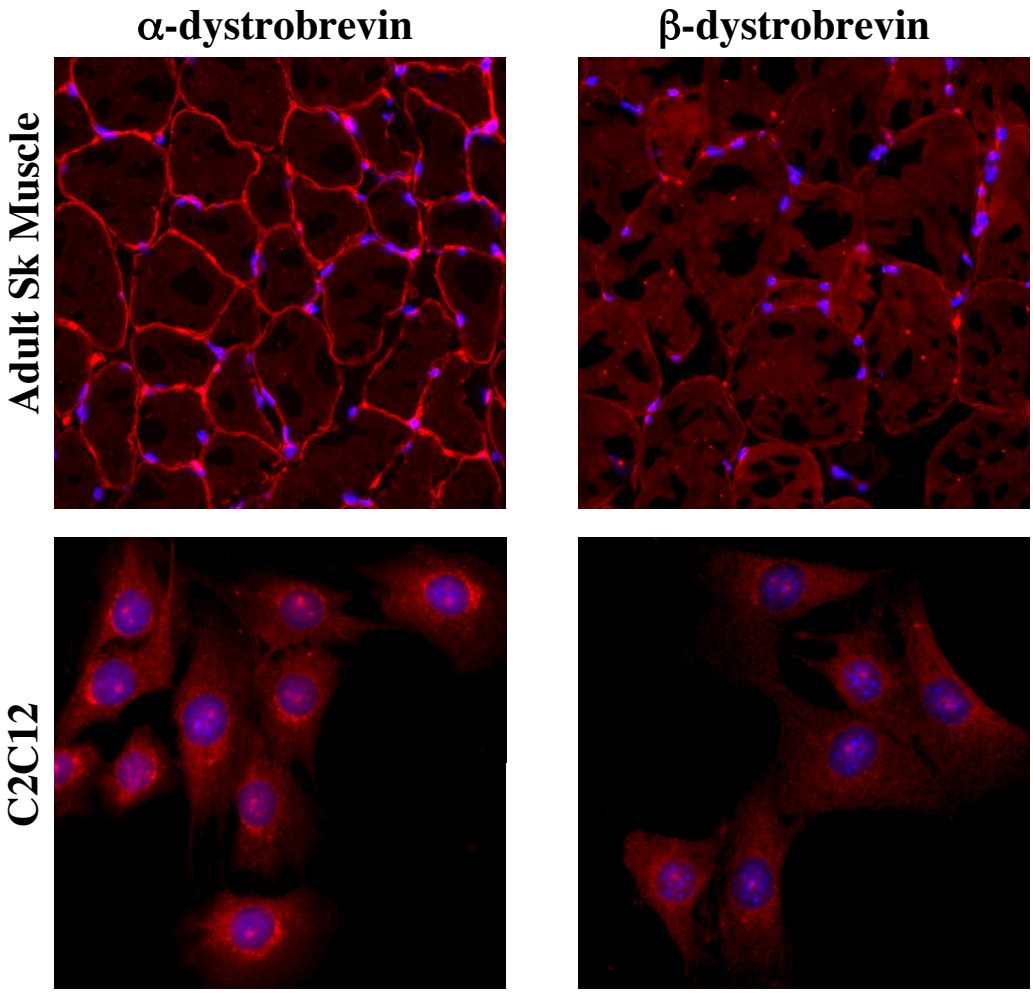

Figure 32. **Distribution of dystrobrevin in murine skeletal muscle and myoblasts.** Dystrobrevin is visualized in red. In adult skeletal muscle, α-dystrobrevin is predominantly localized to the muscle sarcolemma, while β-dystrobrevin has a wider distribution throughout the cytoplasm. In C2C12 skeletal myoblasts, α- and β-dystrobrevin are both cytoplasmic and exhibit a perinuclear concentration, especially with regard to the former. DAPI (blue) was used to visualize nuclei.

primarily to a perinuclear region. Very little membrane labeling is observed. In differentiated C2C12 myocytes, dystrobrevin is distributed in a similar cytoplasmic pattern. Interestingly, a few cells express very high levels of dystrobrevin, although the significance of this observation is unknown. Since dystrobrevin and dysbindin have not been well-characterized in muscle cells in culture, these results revealing a cytoplasmic population of dystrobrevin suggest that there may be potential for interaction of dystrophin-related proteins with cytLEK1 based on an overlap in distribution.

During the course of false positive screening for dysbindin in the yeast two-hybrid assay, it was observed that all three obtained clones contained extraneous DNA within the dysbindin coding region. Thus, while each of these dysbindin clones passed the false positive test, the interaction could not be truly verified until an error-free dysbindin clone was generated and used in a yeast mating experiment. To achieve this, a cDNA clone (Invitrogen) was utilized to create a proper dysbindin-expressing yeast colony. Surprisingly, mating of this yeast with the SRR-expressing yeast results in only minimal growth on QDO plates. However, control experiments conducted in parallel using the incorrect dysbindin clones exhibit a similar phenotype, despite previously showing robust growth under such conditions. Colocalization studies conducted with myc-SRR and a newly-generated GFP-dysbindin construct in COS-7 cells do not yield useful additional data. GFP-dysbindin is distributed throughout the cytoplasm and thus does not exhibit any specific codistribution with myc-SRR. Notably, since the interaction of dysbindin with cytLEK1 cannot be properly confirmed in a yeast two-hybrid setting, experiments studying this interaction have been delegated to a lower priority than the NudE studies. The initial results are promising enough though to warrant additional examination in the future.

Discussion

Despite their functional differences, LEK family members share a similar domain structure (see Introduction). In the cytLEK1 portion of LEK1, the key conserved domains consist of numerous leucine zippers and a spectrin repeat. As leucine zippers are a generic protein-protein interaction motif found in many different proteins (O'Shea et al., 1989), we decided to focus instead on the spectrin repeat region of cytLEK1 for our studies. Notably, this repeat region contains several leucine zippers of its own. It does not, however, share any significant sequence homology with the spectrin repeats of other LEK1 family members, although these

repeats are likely structurally similar due to their coiled-coil assembly. In general, spectrin repeats have been shown to serve as binding sites for various proteins involved in cytoskeletal and signal transduction functions (Djinovic-Carugo et al., 2002). As cytLEK1 is a cytoplasmic protein that is partially resistant to detergent extraction (chapter II), we hypothesized that the repeat region of cytLEK1 may mediate a cytoskeletal role for the protein.

Thus, we utilized the spectrin repeat region (SRR) as bait in a yeast two-hybrid screen of an embryonic whole mouse cDNA library. Since cytLEK1 is present in most tissues in early murine development (Goodwin et al., 1999; chapter II), a whole mouse library enables detection of all potential interacting proteins in various embryonic locations. Two separate screens were conducted to ensure the detection of putative interactions. The positive hits are consistent among both screens, confirming the reproducibility of our results. While the false positive rate, as determined by control matings, is surprisingly high, this factor does not influence the importance of our true positives. The interaction with NudE is by far the most prevalent positive hit with 31 total clones isolated. While all the clones contain the full length NudE sequence and thus do not provide any information on the specific cytLEK1 binding site within NudE, the high number of hits is nonetheless reassuring. The two other positive hits are a hypothetical protein (6 clones) and dysbindin (3 clones). It is difficult to determine whether the lower number of clones obtained with these molecules is the result of a weaker interaction with cytLEK1 or simply an indication of a lower abundance of these specific cDNAs in the library. We focus our efforts here on the interaction with NudE for several reasons. First, NudE is the most prevalent positive result in our screen. Additionally, NudE(L) is expressed at highest levels in the brain, heart, and skeletal muscle, similar to cytLEK1 (Niethammer et al., 2000; Sasaki et al., 2000; Yan et al., 2003). The *NudE* mRNA is most abundant at embryonic stages and decreases during postnatal development, yet again like *LEK1* (Goodwin et al., 1999; Feng et al., 2000). NudE is a cytoplasmic protein with a predominantly perinuclear distribution around the centrosome (Feng et al., 2000). This localization is similar to that described for cytLEK1 in various cells in chapter II. Finally, NudE has a cytoskeletal role due to its association with LIS1 pathway members, and this pathway plays a role in proliferation, migration, and differentiation processes during development (see Introduction). Thus, this function is analogous to our hypothesis of a cytoskeletal role for cytLEK1 in such cellular processes.

Our additional studies in this chapter primarily focus on the characterization of the cytLEK1-NudE interaction. The importance of the discovery cannot be overstated, as this is the first time that a binding partner of cytLEK1 has been identified. The cytLEK1 protein can thus be placed in a molecular pathway. Detailed cytLEK1 functional studies conducted in chapter IV are a direct result of the data presented in this chapter. Characterization of the exact binding domains within cytLEK1 and NudE is a key result. The yeast two-hybrid deletional analysis reveals, somewhat surprisingly, that the region C-terminal to the cytLEK1 spectrin repeat itself (C domain) is necessary and sufficient for binding to NudE. The repeat does not play a direct role in this interaction, although it may possibly be important for binding to a different protein. In fact, the cytLEK1-dysbindin association appears to require the entire spectrin repeat region. Thus, the repeat region may indeed bring together another protein with cytLEK1 and NudE. Proteins of the Dbl family contain spectrin repeats that act in conjunction with a neighboring Rho-GEF domain, for example (Alam et al., 1997; Estrach et al., 2002). Another possibility is that the spectrin repeat of cytLEK1 is simply providing a tertiary structure conducive to binding of proteins at the neighboring C domain. Additional studies are required to test these various ideas. It is clear, however, that the small (80 aa) C domain of cytLEK1 is critical for the interaction with NudE. This discovery enables the dominant negative studies in chapter IV that separate this C domain from all other regions of the intact cytLEK1 molecule. In this way, the function of the cytLEK1-NudE interaction can be isolated from any other currently-unknown roles of the cytLEK1 protein.

Conversely, determination of the cytLEK1-binding domain within NudE also yields an interesting result. This region in NudE partially overlaps the putative dynein-binding domain of its isoform, Nudel (Sasaki et al., 2000; Liang et al., 2004). While the specific dynein-related studies have not yet been conducted with NudE, the high degree of homology between NudE and Nudel, including in this region, suggests a conserved function for this domain. Thus, the overlap between the cytLEK- and dynein-binding domains within NudE presents the interesting possibility of a complex regulation of protein-protein interactions. Given the large size of cytLEK1, it is possible that its association with NudE may block the dynein-NudE interaction. Thus, cytLEK1 would control the binding of NudE to one of its key partner proteins. Alternatively, cytLEK1 may in fact bind dynein itself through a different domain and play a role in bringing cytLEK1, dynein, and NudE together into a functional complex. In either scenario,

cytLEK1 has an important function in directing interactions of LIS1 pathway members. Disrupting the association of Nudel with dynein has been shown to affect many cellular processes (Liang et al., 2004). Interestingly, only mutants that lack either the dynein- or LIS1-binding domain, but not both, exhibit a phenotype. Given our results, deletion of the dynein-binding region would also potentially disrupt any association with cytLEK1. Thus, these Nudel data suggest that proper coordination of the interactions occurring at each of these domains is critical. CytLEK1 may specifically be involved in regulating the association of NudE(L) with dynein, as it has not yet been found to interact with the LIS1-binding domain of NudE. Detailed biochemical studies in the future will help reveal the exact role of cytLEK1. An additional complicating factor, however, is the unclear nature of the differences between NudE and Nudel (see Introduction). In our experiments, cytLEK1 has been shown to associate with NudE, but an interaction with Nudel has not been examined. Given the homology between the NudE and Nudel sequences and their similarities in known binding partners (LIS1 and dynein), a cytLEK1-Nudel interaction seems likely. However, no Nudel clones were obtained in our yeast two-hybrid screens, although this is likely due to the lack of *Nudel* transcription at the embryonic day 11 stage of our screening library (Sasaki et al., 2000). Directed binding studies are needed in the future to directly test for any potential association.

The cytLEK1-NudE interaction is confirmed by co-immunoprecipitation (co-IP) studies of cotransfected proteins in COS-7 cells (Figure 24). These results clearly show that GFP-mNudE co-immunoprecipitates with myc-SRR. We further define this interaction by confirming the importance of the C domain identified in the yeast two-hybrid deletion studies. Removal of this C domain eliminates the ability of GFP-mNudE to co-immunoprecipitate with the resulting myc-N+R protein. This result is of high value, as the primary challenge in co-IP studies is to differentiate between specific and non-specific binding. Whereas simply looking for co-immunoprecipitation of GFP-mNudE and myc-C may result in identification of a non-specific band as a positive result, determining the absence of any band in a co-IP with myc-N+R is more challenging and experimentally relevant. Ideally, we would like to confirm these co-IPs using endogenous proteins from murine cell lysates. However, there are numerous technical challenges that cannot yet be overcome. The NudE antibody from the Walsh laboratory is ineffective in both immunoprecipitation and Western blot assays (Yuanyi Feng, personal communication). We thus have no way to collect or detect endogenous NudE within a protein complex, and this makes a

co-IP impossible. If at a later stage a different NudE antibody becomes available, there will likely still be additional challenges. Both cytLEK1 and NudE are associated with the cytoskeleton, and an endogenous complex between the two proteins may thus not be soluble. In fact, endogenous NudE is very difficult to isolate from cell lysates due to its lack of solubility (Yuanyi Feng, personal communication). Additionally, our current cytLEK1 antibody has never been tested in immunoprecipitation experiments and may be ineffective in such assays. An alternative method for examining interaction between full length cytLEK1 and NudE is to conduct a co-IP using transfected full length cytLEK1 and NudE proteins. However, this presents different challenges, as the transfection efficiency of our very large cytLEK1 construct is low. It is also important to note that this construct is not the same size as endogenous cytLEK1, since the exact endogenous molecular weight is unknown due to the lack of specific cleavage site data. Thus, this discrepancy may possibly inhibit fully proper protein-protein interactions. Regardless, an additional result using transfected proteins yet again would not substantially add to the co-IP and detailed colocalization data we already have.

To support our biochemical data, codistribution experiments were conducted that initially focus on transfected proteins in COS-7 cells. We chose this approach for two reasons. First, it allows us to confirm our co-IP results using the same transfected proteins in a substantially different assay. Second, COS-7 cells are uniquely suited for visualization of the centrosome and any proteins located at this structure. Our results reveal that myc-SRR colocalizes with GFP-mNude in these cells, confirming our co-IP data. Importantly, this colocalization occurs at distinct dots that we show to be related to centrosomes. This pattern is identical to that observed for cells transfected with GFP-mNudE alone, suggesting that the SRR directs a specific interaction with NudE. It is worthwhile to note that the amount of GFP-mNude localizing to the centrosome appears to be directly related to the level of expression. High amounts of protein within a cell result in a more pancytoplasmic distribution. Thus, while NudE is located more preferentially at the centrosome in these cells, it is not exclusively there. Deletion of the C domain once again eliminates any relationship with NudE, as seen in the myc-N+R studies.

Importantly, the myc-C protein also colocalizes with GFP-mNudE in transfected COS-7 cells. In fact, it appears to exhibit an even higher codistribution with NudE than seen in the myc-SRR experiments. These data are consistent with the biochemical studies showing that the C domain alone directs a specific and apparently exclusive interaction with NudE. Further analysis

of the distribution of myc-C reveals that the protein also colocalizes with endogenous NudE present at the centrosome. This result is very important due to the inability to co-immunoprecipitate endogenous NudE for reasons already noted. Thus, these data show that the C domain is capable of directing a codistribution with, not just transfected NudE protein, but also endogenous NudE. It is interesting to note that even in specific COS-7 cells where the centrosome can be easily visualized, endogenous NudE exhibits a predominantly perinuclear distribution with a somewhat higher abundance at the centrosome. It is clear that NudE has a localization and, thus, likely, function at both centrosomal and non-centrosomal areas. The propensity of myc-C to similarly be perinuclear with a concentration at the centrosome, as evidenced by □-tubulin staining, coincides with its strong affinity for NudE. Since studies conducted in murine cells make centrosome visualization difficult, these data in COS-7 cells importantly show that myc-C is specifically directed to the centrosome and perinuclear regions and colocalizes with NudE. Thus, this protein has the potential to disrupt key NudE-related functions in this subcellular area in a dominant negative fashion, as discussed in chapter IV.

In order to also test the association of endogenous cytLEK1 and NudE, we conducted colocalization experiments in murine cells. Since the two known binding partners of NudE are important members of the LIS1 pathway, the distributions of dynein and LIS1, as well as NudE, were examined in relation to cytLEK1 in C2C12 myoblasts and 3T3 fibroblasts. For each of these proteins, we observe a general similarity in localization pattern when compared to cytLEK1. All of the proteins are cytoplasmic with somewhat perinuclear distributions, as has been previously observed (see Introduction). Since the resolution of confocal microscopy alone is not sufficient to clearly detect colocalization among such cytoplasmic proteins, deconvolution analysis was performed to provide unambiguous results. These data reveal substantial colocalization between each of the LIS1 pathway members (dynein, LIS1, NudE) and cytLEK1 in 3T3 cells. This codistribution is most evident in the perinuclear region of cells, which is an interesting result for two reasons. First, this is the subcellular area where the known LIS1 family members most commonly associate and colocalize (Smith et al., 2000). Second, endogenous cytLEK1 near the nucleus is detergent resistant and presumably linked to the cytoskeleton. This association may in fact be a direct consequence of its interaction with LIS1 pathway members in the perinuclear region. As has been noted previously, examining the colocalization of proteins at the centrosome is difficult in murine cells. However, the importance of achieving this is minimal,

as these specific LIS1 pathway members have been repeatedly shown to be present at and important in a wide perinuclear region (Niethammer et al., 2000; Sasaki et al., 2000; Smith et al., 2000; Shu et al., 2004). Even NudE(L), which has the strongest centrosomal localization of any LIS1 pathway member, is observed in these referenced studies to not exhibit a substantial distribution at the centrosome of murine cells. Thus, our results are in complete agreement with the literature. We also occasionally witness colocalization of cytLEK1 with LIS1 pathway members near the plasma membrane, although this is not consistently detected. This observation should be more carefully examined in the future, however, to discern if cytLEK1 functions in leading edge processes. Additionally, LIS1 pathway members play important roles in mitotic cells at various locations on the spindle and kinetochores (Faulkner et al., 2000; Yan et al., 2003; Feng and Walsh, 2004). CytLEK1 has a similar distribution, as described in chapter II. It will be interesting in future studies to examine colocalization of pathway members and cytLEK1 at such structures in dividing cells.

Our data here do not reveal a complete colocalization of cytLEK1 with LIS1 pathway members. In fact, such a result would be unexpected and troubling. None of the pathway members have previously been shown to completely codistribute with each other. For example, LIS1 does not fully colocalize with dynein, especially near the periphery of the cell (Smith et al., 2000). This result is attributed to the fact that the LIS1 pathway is postulated to affect only a subset of the vast array of dynein functions (Vallee et al., 2001). Similarly, cytLEK1 is a very large protein with presumably several important functional domains. Thus, it likely binds to many different proteins and has roles in various cellular processes and molecular pathways. Interaction with LIS1 pathway members may only be a part of the function of endogenous cytLEK1. In fact, our results support this idea, as cytLEK1 does not substantially colocalize with pathway members near the periphery of cells. We have shown in chapter II that the resistance to detergent extraction of cytLEK1 at the periphery is different than for perinuclear protein, thus implying distinct functions for these subpopulations. Even near the nucleus, the codistribution of cytLEK1 and LIS1 pathway members is high but not exact, suggesting that other interactions of cytLEK1 are important in this region of the cell. Additionally, cytLEK1 may not immediately bind to NudE in cells due to important regulation of this interaction. This would result in an isolated subpopulation of cytLEK1 molecules that either have been temporarily sequestered or are simply newly-translated. Such proteins would not colocalize with LIS1 family members.

Nonetheless, in order to be certain of the importance of the high but partial colocalization that we observe, we conducted experiments with many other cytoplasmic proteins unrelated to the LIS1 pathway. These studies examined the distribution of cytLEK1 in relation to vimentin, desmin, actin, and myosin in various cell lines. Notably, no significant colocalization can be observed between cytLEK1 and any of these proteins. In fact, even the general pattern of protein distribution within the cell is highly divergent from that of cytLEK1 and LIS1 pathway members. Importantly, no clear perinuclear localization is observed for these other proteins. Regions of high concentration of desmin, for example, are unrelated to similar areas of high cytLEK1 levels. These studies provide important negative controls and reveal that our colocalization results are specific to cytLEK1 and LIS1 family members.

Although experiments are in a preliminary stage, a short discussion of the potential interaction between cytLEK1 and dysbindin is warranted. Detailed examination of this interaction was postponed due to various technical difficulties. The existence of extraneous DNA within each unique clone obtained from the screening library required the creation of a separate dysbindin cDNA clone for use in yeast two-hybrid assays. Surprisingly, this new dysbindin clone does not exhibit a strong interaction with the SRR of cytLEK1 in such assays. However, the original clones containing the extraneous DNA also do not associate with the SRR in parallel experiments, despite our previous results. As dysbindin clones have been isolated from two separate yeast two-hybrid screens and subject to numerous successful independent false positive tests, there is a distinct possibility that the inability to replicate the interaction at this later timepoint is due to issues with the growth and maintenance of yeast. Thus, additional examination of this interaction is likely necessary.

Initial published experiments on dysbindin do not reveal characteristics suggestive of a cytLEK1-interacting protein (Benson et al., 2001). Dysbindin is part of the dystrophin-associated protein complex in muscle. While it is highly expressed in brain, heart, and skeletal muscle, similar to cytLEK1, its localization to the sarcolemma of myocytes *in vivo* does not match the predominantly cytoplasmic distribution of cytLEK1 within such cells (Benson et al., 2001). However, our studies with dystrobrevin, the primary binding partner of dysbindin, reveal that this protein is primarily distributed in the cytoplasm of myocytes in culture (Figure 32). Even in skeletal muscle of adult mice, certain dystrobrevin isoforms have a partially cytoplasmic distribution. Additionally, more recent studies have suggested further roles for dysbindin outside

of the dystrophin complex in muscle. The protein functions in regulation of vesicular trafficking to organelles as part of the BLOC-1 (biogenesis of lysosome-related organelles) complex (Li et al., 2003). This is an intriguing role as it shares similarities to the effects of the LIS1 pathway on movement of organelles, lysosomes, and endosomes (see Introduction). Additionally, abnormalities in dysbindin are associated with brain dysfunction, including schizophrenia (Numakawa et al., 2004). LIS1 pathway members are critical for the proper development of this organ (see Introduction). Thus, relating the function of dysbindin to that of the LIS1 pathway through cytLEK1 is an intriguing scenario.

Unfortunately, such studies are complicated by various technical challenges. There is only one known antibody to dysbindin, and we have been unsuccessful in obtaining it from the relevant laboratory. Without the receipt or generation of such a dysbindin antibody, it is impossible to conduct any co-IP or colocalization studies of endogenous proteins. Additionally, transfection of GFP-dysbindin into COS-7 cells results in a pan-cytoplasmic distribution of the protein with no evident pattern. Co-transfection with myc-SRR does not alter this result. Without an antibody to dysbindin, it is difficult to tell whether this result is due to improper trafficking of the transfected GFP-tagged protein or to dysbindin itself not having a distinct cytoplasmic pattern. This problem is compounded by the lack of published data examining the localization of dysbindin in cultured cells. Future transfection studies in myocytes may result in a more distinct distribution of the protein. However, as myc-SRR causes a severe morphological phenotype in C2C12 myoblasts, colocalization experiments are necessarily limited. Nonetheless, the potential interaction between cytLEK1 and dysbindin is intriguing enough to warrant future investigation. Our initial result that the entire SRR is required for binding to dysbindin suggests that this interaction may interfere with or facilitate the cytLEK1-NudE association occurring at the C domain within the SRR. Perhaps binding to dysbindin is important for the role of cytLEK1 at the cell periphery. Further yeast two-hybrid screens utilizing different regions of cytLEK1 as bait have revealed putative interactions with proteins related to vesicular transport, a dysbindin function (Pooley et al. unpublished data). Additional experiments in the future will hopefully reveal the exact nature of any cytLEK1-dysbindin association.

In summary, the results in this chapter reveal and characterize a novel interaction between cytLEK1 and NudE. This association with NudE marks the first time any cytLEK1 binding partner has been identified. It thus places cytLEK1 within the LIS1 pathway and

provides a context for understanding its distribution and function. In chapter II, we describe the expression pattern of cytLEK1 in various tissues and cells. The results in this chapter here now reveal a purpose for such a cytLEK1 localization in the context of being a member of the LIS1 pathway. CytLEK1 appears to associate with proteins of this pathway predominantly near the nucleus, including at the centrosome. Thus, it is situated in the primary location of LIS1 pathway function, and its colocalization with dynein, LIS1, and NudE implies that it has the ability to widely regulate multiple components of the pathway. Notably, the overlap of the cytLEK1- and dynein-binding domains within NudE suggests the potential for a complex regulation of multiple protein-protein interactions, perhaps directed by cytLEK1 itself. Clearly, functional analyses are the next step in determining the importance of the cytLEK1-NudE association. Isolation of the critical C domain within cytLEK1 provides a powerful tool for conducting such studies. This region of cytLEK1 is able to specifically direct localization to a perinuclear region, including the centrosome, and an interaction with NudE. At the same time, the myc-C protein isolates any other functional domains in the full length cytLEK1 from the NudE-binding region. Thus, it serves as a powerful tool for examining, in a dominant negative fashion, the role of cytLEK1 within the LIS1 pathway in chapter IV.

CHAPTER IV

ANALYSIS OF CYTLEK1 FUNCTION AND REGULATION OF THE LIS1 PATHWAY

Introduction

Data presented in chapter III reveal an important interaction between cytLEK1 and NudE. Additionally, cytLEK1 protein is shown to be present in many developing tissues and key subcellular locations in chapter II. Thus, cytLEK1, through its interaction with NudE, has the potential to be a significant regulator of the LIS1 pathway in multiple cell types. The LIS1 pathway is critical for many important cellular functions, as described in the Introduction. Briefly, members of the pathway play a role in dynein-related processes occurring with the microtubule network. Thus, events such as organelle positioning, cytoskeletal organization, cell shape, migration, and mitosis are directly regulated by the LIS1 pathway (Hirotsune et al., 1998; Faulkner et al., 2000; Sasaki et al., 2000; Smith et al., 2000; Dujardin et al., 2003; Liang et al., 2004; Shu et al., 2004). Disrupting the function of pathway members results in perturbation of these processes. As cytLEK1 interacts with NudE and colocalizes with other key components of the LIS1 pathway, we wished to examine whether cytLEK1 is critical for pathway actions. More specifically, we focused on the C domain of cytLEK1 that binds NudE. We postulated that isolation of the C domain from any other functional domains in the intact cytLEK1 molecule would produce a dominant negative effect.

In this chapter, we present data characterizing the role of cytLEK1 on LIS1 pathway functions. We primarily use the dominant negative myc-C protein to examine the effects of disrupting cytLEK1 activity in various murine cells lines. Expression of the NudE-binding domain alone produces severe effects on cell morphology and the microtubule network in a proposed dominant negative fashion. These cells quickly adopt a dramatically rounded shape. Interestingly, microtubules are tightly focused around the nucleus, consistent with previous studies disrupting LIS1 function (Smith et al., 2000). Importantly, these cells expressing the dominant negative cytLEK1 protein are strongly inhibited in microtubule repolymerization after treatment with the depolymerizing agent nocodazole. Additional experiments examining the effects of LEK1 knockdown in cells reveal a similar alteration of the microtubule network. Our data also show that the C domain confers resistance to detergent extraction, suggesting that it

mediates interaction with cytoskeletal components. We expand on this by examining the unique subcellular localization of the myc-C protein in cells. Finally, overexpression of full-length cytLEK1 causes a tight clustering of the Golgi apparatus near the nucleus, consistent with the role of other LIS1 pathway members (Sasaki et al., 2000; Smith et al., 2000; Liang et al., 2004). Examination of additional results of cytLEK1 overexpression is also presented here. In summary, the experiments in this chapter characterize the effects of cytLEK1 dysfunction on key cellular events. The severity of the defects in microtubule organization and repolymerization imply a critical and novel role for cytLEK1 in the LIS1 pathway, which regulates microtubule function in important cellular processes.

Materials and Methods

Cell culture

NIH 3T3 cells (ATCC) were maintained in Dulbecco's Modified Eagle's Medium (DMEM; Cellgro) supplemented with 10% fetal bovine serum, 100 □g/mL penicillin/streptomycin, and L-glutamine. C2C12 cells (ATCC) were grown in Dulbecco's Modified Eagle's Medium (DMEM) supplemented with 20% fetal bovine serum, 100 □g/mL penicillin/streptomycin, and L-glutamine. All cell lines were maintained in a 95% air-5% CO_2 humidified atmosphere at 37˚C.

Transfections

3T3 and C2C12 cells were grown to 40-60% confluency and transfected using FuGENE6 (Roche) per manufacturer's instructions. Briefly, FuGENE was added to a tube containing OptiMEM medium (Cellgro) and gently mixed. DNA was then added and gently mixed. After a 15 min incubation, the FuGENE-DNA mixture was pipetted into wells containing cells and fresh medium. For each well of a 4-well slide, 0.25 □g of total DNA was utilized for transfection. Cells were generally grown for 24-48 h prior to collection for further examination.

Immunocytochemistry and microscopy

Cells grown on glass chamber slides (Nalge Nunc) were gently washed with PBS and fixed with Histochoice (Amresco) or 70% ethanol (for Spec1) for 20 min. For pre-extraction to

visualize microtubules (Toomre et al., 1999; Bennin et al., 2002; Giodini et al., 2002), cells were additionally washed with PHEM buffer (60 mM PIPES, 25 mM HEPES, 10 mM EGTA, 3 mM $MgCl_2$ pH 6.8) and treated with 0.5% Triton X-100 in PHEM for 1 min prior to fixation. Cells were then washed briefly in PBS, permeabilized with 0.25% Triton X-100 in PBS for 10 min, and blocked in 2% BSA in PBS for a minimum of 1 h. Primary antibodies in 1% BSA in PBS were applied overnight at 4˚C. After three PBS washes, secondary antibodies were applied for 1 h at room temperature. The slides were washed three times with PBS and twice with water before cover slips were attached with Aqua Poly/Mount (PolySciences). Cells were visualized by fluorescence microscopy on an AX70 (Olympus) or, for confocal analysis, an LSM510 (Zeiss) microscope. Digital images were captured and processed using Magnafire (Optronics), Metamorph (Universal Imaging), and Photoshop (Adobe) software.

Nocodazole treatment

Cells were transfected with the appropriate plasmid using FuGENE. Six hours post-transfection, they were exposed to nocodazole (Sigma), a microtubule depolymerizing agent, at a final concentration of 5 □g/mL for 3 h in the appropriate medium for the cell type. After washing out the drug three times with medium, the cells were grown for an additional 0, 10, or 20 min before pre-extraction and fixation as described above.

Morpholino antisense oligomer treatment

Morpholino oligomers (MO; GeneTools) are composed of a nucleic acid base, a morpholine ring, and a non-ionic intersubunit linkage. This structure prevents them from being degraded inside cells by nucleases. They also have minimal interactions with proteins, thus avoiding non-specific effects associated with other antisense technologies. Morpholinos inhibit translation of a target RNA through a steric block of the translational machinery. Morpholinos specific to the 5' untranslated region of the *LEK1* mRNA had previously been constructed and tested for specificity (Ashe et al., 2004). The L50 morpholino was most effective at knocking down LEK1 protein expression and was used in all studies. Its sequence was as follows: 5'-AGCTCCTCACAGAACCTGGCTCCG-3'. A standard control morpholino with no detectable biological target or activity was provided by the manufacturer and utilized in experiments. Its sequence was as follows: 5'-CCTCTTACCTCAGTTACAATTTATA-3'. Non-confluent cells

were treated with morpholinos per manufacturer's Special Delivery instructions. Briefly, 0.5 mM Special Delivery morpholino/DNA stock solution was added to H_2O and gently mixed. EPEI Special Delivery solution was pipetted into this mixture and vortexed immediately. This was followed by a 20 min incubation during which time cells were rinsed three times with PBS. Serum-free medium (Cellgro) was then added to the Morpholino/EPEI solution and immediately vortexed. This final delivery medium was added to the cells. After 3 h incubation, the delivery medium was removed and replaced with fresh medium. Cells were then assayed 72 hours post-treatment. When confirming cytLEK1 knockdown, special attention was taken to ensure that all antibody concentrations, camera exposure times, and Photoshop preparations were identical and conducted in parallel.

WGA endosomal assay

TRITC-labeled wheat germ agglutinin (WGA) was obtained from Sigma for use in an assay to test trafficking of endosomes containing WGA-binding sites. Cells were transfected with the appropriate plasmid using FuGENE. Six to eight hours after transfection, cells were incubated in the dark with 10 □g/mL TRITC-WGA in PBS for 30 min at 4˚C. Cells were then either immediately washed two times with PBS before fixation (0 min) or incubated with the appropriate medium for 1 h (60 min) at 37˚C before fixation. Cells were fixed and processed as described above. No primary or secondary antibody was needed to visualize the WGA since it was TRITC-labeled.

Antibodies

The monoclonal anti-myc and GM130 antibodies were from BD Biosciences. A polyclonal anti-myc antibody was acquired from Novus. The antibodies against □-tubulin and FLAG were manufactured by Sigma. Polyclonal antibody Spec1 to a cytLEK1 peptide (aa 1826-45) was generated in rabbits (Biosynthesis) and affinity purified using the injected peptide (Backstrom and Sanders-Bush, 1997). Alexa 488 and Alexa 568 conjugated secondary antibodies, as well as Phalloidin-488, were obtained from Molecular Probes. DAPI was used to visualize nuclei (Boehringer Mannheim).

Results

Disrupting cytLEK1 function alters cell shape and microtubule network organization

Since cytLEK1 interacts with NudE and colocalizes with key components of the LIS1 pathway, we postulated that alteration of cytLEK1 function would disrupt cellular processes regulated by these proteins. Alterations in LIS1 pathway function have previously been demonstrated to cause abrupt changes in cell morphology and the microtubule network (Feng et al., 2000; Smith et al., 2000; Cahana et al., 2001). We tested the ability of the myc-C protein to act in a dominant negative fashion on the LIS1 pathway by uncoupling the NudE-binding site in cytLEK1 from other functions in the intact molecule.

Expression of myc-C in 3T3 fibroblasts results in a severe alteration of cell shape (Figure 33 A), a phenotype that previously has been reported with a dominant negative LIS1 protein (Cahana et al., 2001). Transfected cells round up, and their microtubule networks become tightly focused around the nucleus and lose their regular broad cytoplasmic distribution (Figure 33 C), which has also been observed in *LIS1*-heterozygous fibroblasts (Smith et al., 2000). This change in morphology of 3T3 cells is visible as soon as 8 hours after transfection. Notably, the cells do not detach from the plate even 72 hours post-transfection, and thus this effect is not likely to be a simple cell death response. Similar changes in morphology and the cytoskeleton were observed in C2C12 myoblasts. Although the myoblasts were initially more resistant to the expression of myc-C, extending the time of post-transfection incubation resulted in similar changes in morphology as seen in 3T3 cells. Examination of the rounded myc-C-expressing cells suggests that endogenous LIS1 and dynein are tightly packed around the nucleus. Expression of myc-SRR causes similar rounding of cells, but transfection of full-length cytLEK1 does not reveal any such phenotype (Figure 33 D). The myc-N+R construct, which lacks the NudE-binding domain, was transfected into 3T3 cells to examine possible changes in phenotype. Importantly, expression of myc-N+R in these cells results in no change in morphology or cytoskeletal organization (Figure 33 A), suggesting that this phenotype is specific to the presence of the cytLEK1-NudE interaction domain. Cell counts determined that 88 ± 3% of the myc-C-transfected cells have rounded up after 24 hours, whereas only 7.7 ± 2% of the myc-N+R-transfected cells are similarly affected (Figure 33 B, $p<0.0001$). Examining the small number of cells that are initially resistant to disruption by myc-C allowed us to analyze the subcellular distribution of the SRR constructs

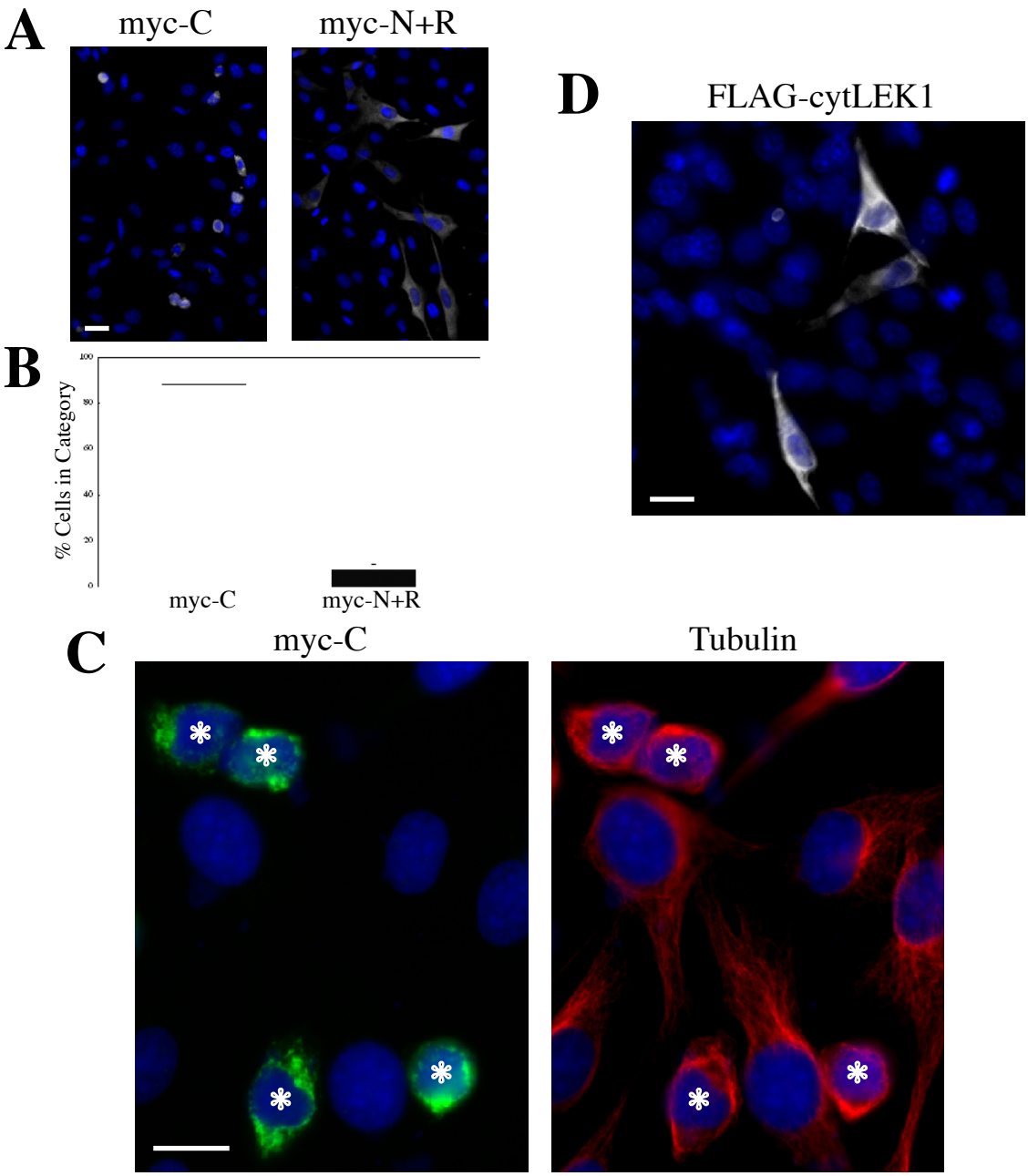

Figure 33. **Disrupting cytLEK1 function alters cell shape and microtubule network organization.** A) 3T3 cells were transfected with either myc-C or myc-N+R and examined for changes in cell morphology. Fluorescence of transfected cells here and in (D) was converted to grayscale and thus appears white. The majority of cells expressing myc-C round up within 24 h post-transfection, unlike myc-N+R-expressing cells, where morphology is unchanged from non-transfected cells. B) When quantified, 88% of myc-C-expressing cells round up versus 7.7% of myc-N+R-expressing cells, a statistically significant difference ($p<0.0001$ by Mann-Whitney U-test, Prism 3.0, Graphpad Software). C) 3T3 cells were transfected with myc-C and examined 24 h post-transfection. myc-C is visualized in green while tubulin is in red. Transfected cells (marked by asterisks) adopt a rounded morphology and have an altered microtubule network. The microtubule network becomes tightly focused around the nucleus and loses its regular broad cytoplasmic distribution pattern. D) C2C12 cells were transfected with a construct of intact cytLEK1 and examined 24 h post-transfection. Transfected cells do not show any abnormalities in cell morphology. DAPI (blue) was used to visualize nuclei. Bars: (A) 20 μm; (C-D) 10 μm.

prior to severe changes in morphology. In this minority population of cells, a differential distribution of myc-C and myc-N+R is observed. Whereas myc-C, similar to LIS1 (Smith et al., 2000), is distributed more tightly around the nucleus, myc-N+R is uniformly expressed diffusely throughout the cytoplasm (Figure 34). By 72 hours post-transfection, nearly all cells transfected with myc-C have adopted the rounded morphology and perinuclear microtubule network.

To determine whether detergent resistance is conferred by the C domain, we utilized a detergent pre-extraction protocol, which allows for examination of proteins associated with the cytoskeleton (Sapir et al., 1997; Toomre et al., 1999; Giodini et al., 2002). Interestingly, pre-extraction of cells before fixation results in the washing out of myc-N+R, while myc-C is resistant to detergent treatment and remains in the insoluble cytoskeletal pool (Figure 35). Considering the role of the LIS1 pathway in microtubule function, the presence of the C domain of cytLEK1 with detergent-resistant subcellular structures, along with the morphologic changes observed, provides further evidence of a role for cytLEK1 in microtubule function.

Disrupting cytLEK1 function inhibits microtubule repolymerization

The present data demonstrate that the myc-C protein has a strong effect on the organization of pre-existing, intact microtubule networks. Additionally, LIS1 overexpression has been shown to cause altered microtubule polymerization and localization after nocodazole treatment (Smith et al., 2000). Thus, we next wished to determine whether myc-C inhibits nascent microtubule polymerization. Cells were transfected with the myc-C construct, cultured for 6 hours in order to minimize the severe rounding of cells observed with prolonged exposure to the protein, and then treated for 3 hours with nocodazole. After a 10 min washout of nocodazole, cells were pre-extracted and the microtubule network analyzed. Remarkably, both C2C12 and 3T3 cells transfected with myc-C show a nearly complete inability to repolymerize their microtubule networks after nocodazole washout (Figure 36). While surrounding non-transfected cells have long microtubule networks emanating from their organizing centers, the transfected cells lack microtubule segment formation. Even after a 20 min washout, the microtubule network remains unformed in these cells, suggesting that the defect is both severe and long-lasting (Figure 37 A). The myc-N+R protein was used as a control since it is unable to bind NudE and thus would not be expected to affect microtubule repolymerization. For this experiment, pre-extraction was impossible because it washes out the transfected protein (Figure

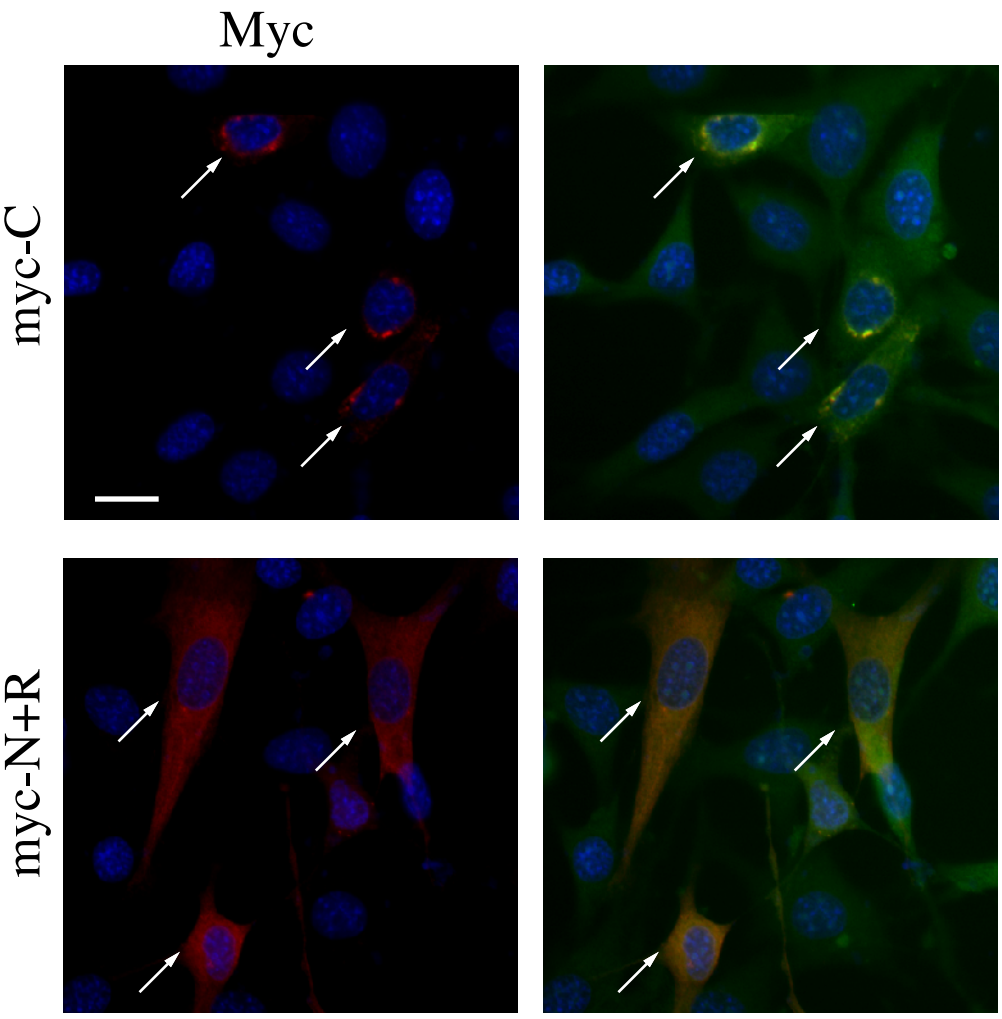

Figure 34. **Myc-C exhibits a distinct subcellular localization in murine cells.** Disrupting cytLEK1 function alters cell shape and microtubule network organization. 3T3 cells were transfected with myc-C or myc-N+R and any non-rounded cells, which were a small minority of the total myc-C population, were examined. Myc proteins are in red (arrows) while a cytoplasmic label (phalloidin) is in green. The myc-C protein is distributed in a perinuclear fashion in these cells while the myc-N+R protein shows no such specific localization and is instead found throughout the cytoplasm. DAPI (blue) was used to visualize nuclei. Bar, 10 μm.

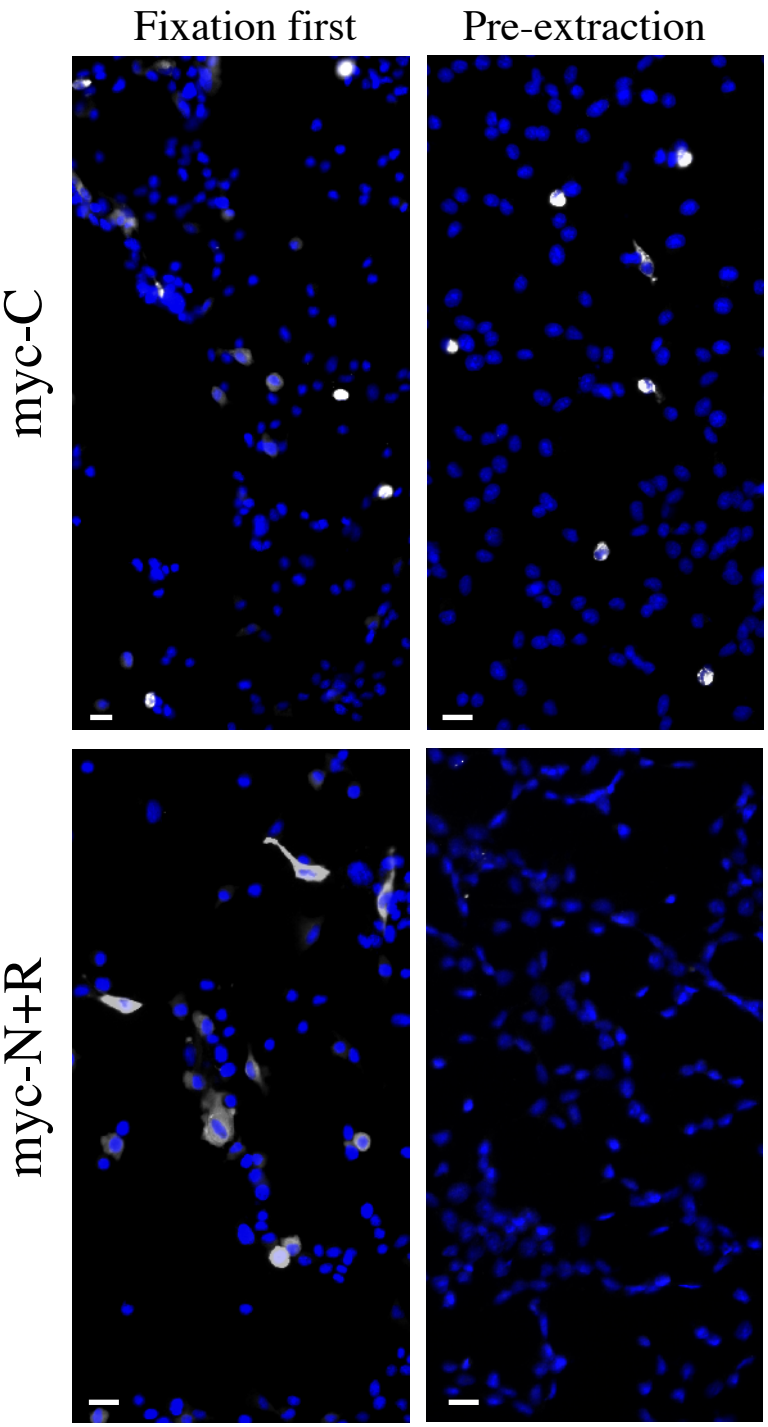

Figure 35. **The C domain of cytLEK1 confers resistance to detergent pre-extraction.** C2C12 cells were transfected with myc-C or myc-N+R (both white) and then fixed before or after Triton extraction. The myc-C protein is resistant to pre-extraction and thus likely attached to the detergent-resistant cytoskeletal network. The myc-N+R protein is washed out, however, so it is not bound to the cytoskeletal network. DAPI (blue) was used to visualize nuclei. Bars, 20 µm.

35). As expected, expression of myc-N+R does not lead to any changes in microtubule repolymerization after nocodazole treatment (Figure 37 B), and both transfected and surrounding cells have microtubule networks attached to organizing centers. Taken together, these experiments demonstrate that the presence of the NudE-binding domain of cytLEK1 causes nearly complete inhibition of microtubule repolymerization and may explain the intense effects on cell morphology and the cytoskeleton that occur with expression of the myc-C protein.

LEK1 knockdown alters microtubule network organization

To further confirm the role of cytLEK1 in the LIS1 pathway, we examined the effects of knockdown of the LEK1 protein using morpholino antisense oligomers. These LEK1 morpholinos had previously been utilized by our laboratory and confirmed to effectively and specifically knock down LEK1 protein expression (Ashe et al., 2004). We verified that cytLEK1 protein expression is indeed knocked down by LEK1 morpholino versus standard control morpholino treatment in 3T3 fibroblasts (Figure 38 A). As previously reported (Ashe et al., 2004), LEK1 knockdown induces apoptosis in cells after several days and this was observed here also. Not surprisingly, LEK1-knockdown cells are very susceptible to environmental stress and experiments to examine their response to nocodazole treatment resulted in massive cell death and detachment from the slide surface. While a severe change in morphology to a rounded phenotype was not observed in LEK1-knockdown cells, their microtubule networks are significantly altered. Notably, there is a substantial accumulation of microtubules around the nucleus (Figure 38 B-C). Whereas control-treated cells display a uniform distribution of microtubules throughout the cytoplasm, LEK1-knockdown cells exhibit a tight perinuclear focusing of microtubules, similar to that observed with expression of the myc-C dominant negative protein and consistent with inhibition of microtubule transport to the cell periphery. Since the LIS1 pathway is critical for this transport process, inhibition of the function of any member of the LIS1 pathway has consistently resulted in accumulation of microtubules around the nucleus (Ahmad et al., 1998; Smith et al., 2000; Shu et al., 2004). This result thus provides additional evidence that cytLEK1 expression is critical for LIS1 pathway function.

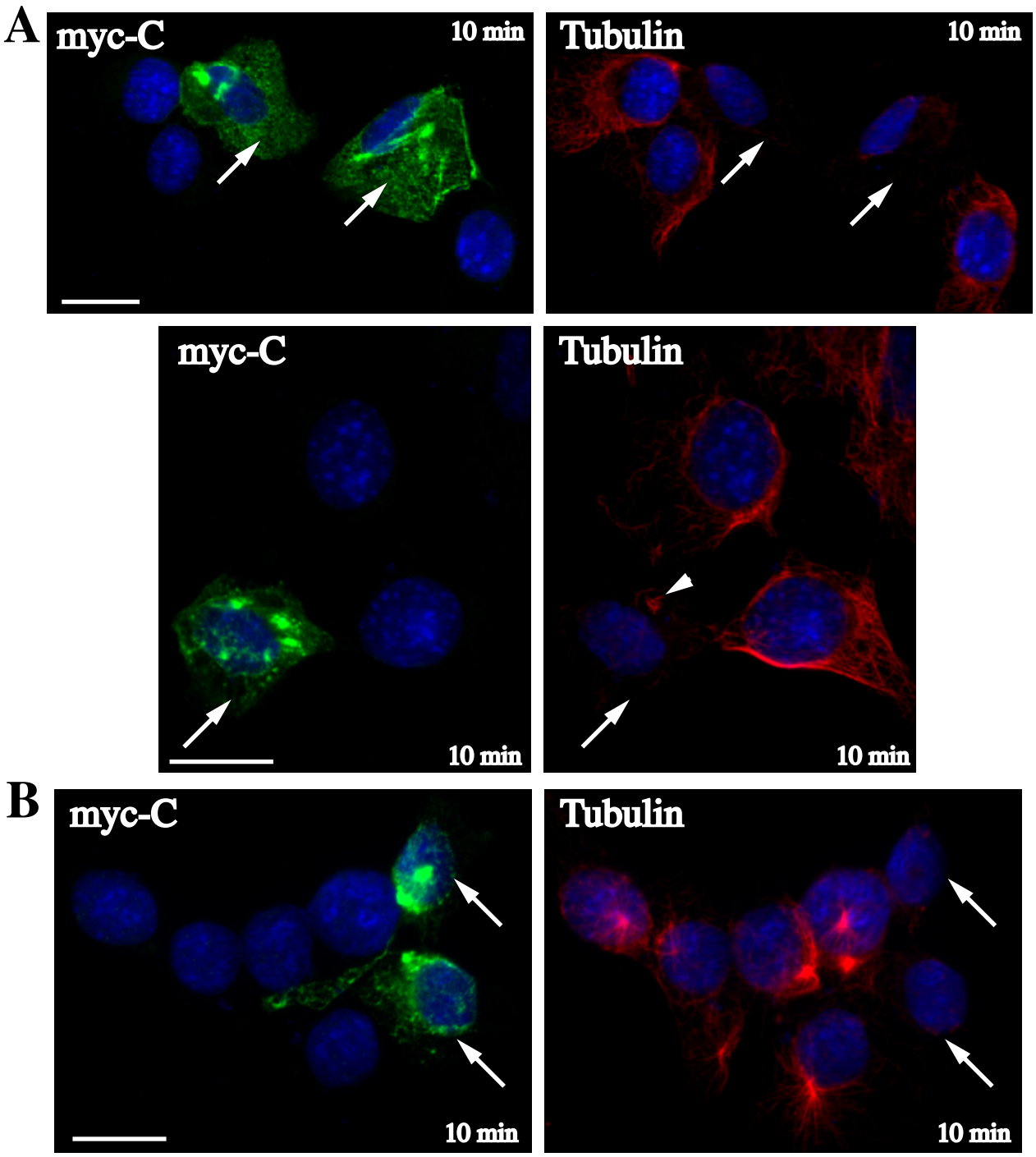

Figure 36. **Disrupting cytLEK1 function inhibits microtubule repolymerization after nocodazole challenge in murine cells.** Cells were treated with 5 mg/mL nocodazole for 3 h followed by 10 min washout before pre-extraction and fixation. Myc-tagged proteins are in green (arrows) and tubulin is in red. A) Myc-C expressed in C2C12 myoblasts causes a severe inhibition in microtubule repolymerization after nocodazole washout. While surrounding untransfected cells have clearly visible microtubule networks, such networks are almost completely absent in transfected cells. Very small, disorganized networks may be forming in some cells (arrowhead). B) Myc-C expression in 3T3 fibroblasts causes severe inhibition of polymerization in these cells also. Microtubules are seen associated with the organizing center in untransfected cells while no such organized repolymerization is visible in transfected cells. DAPI (blue) was used to visualize nuclei. Bars, 10 μm.

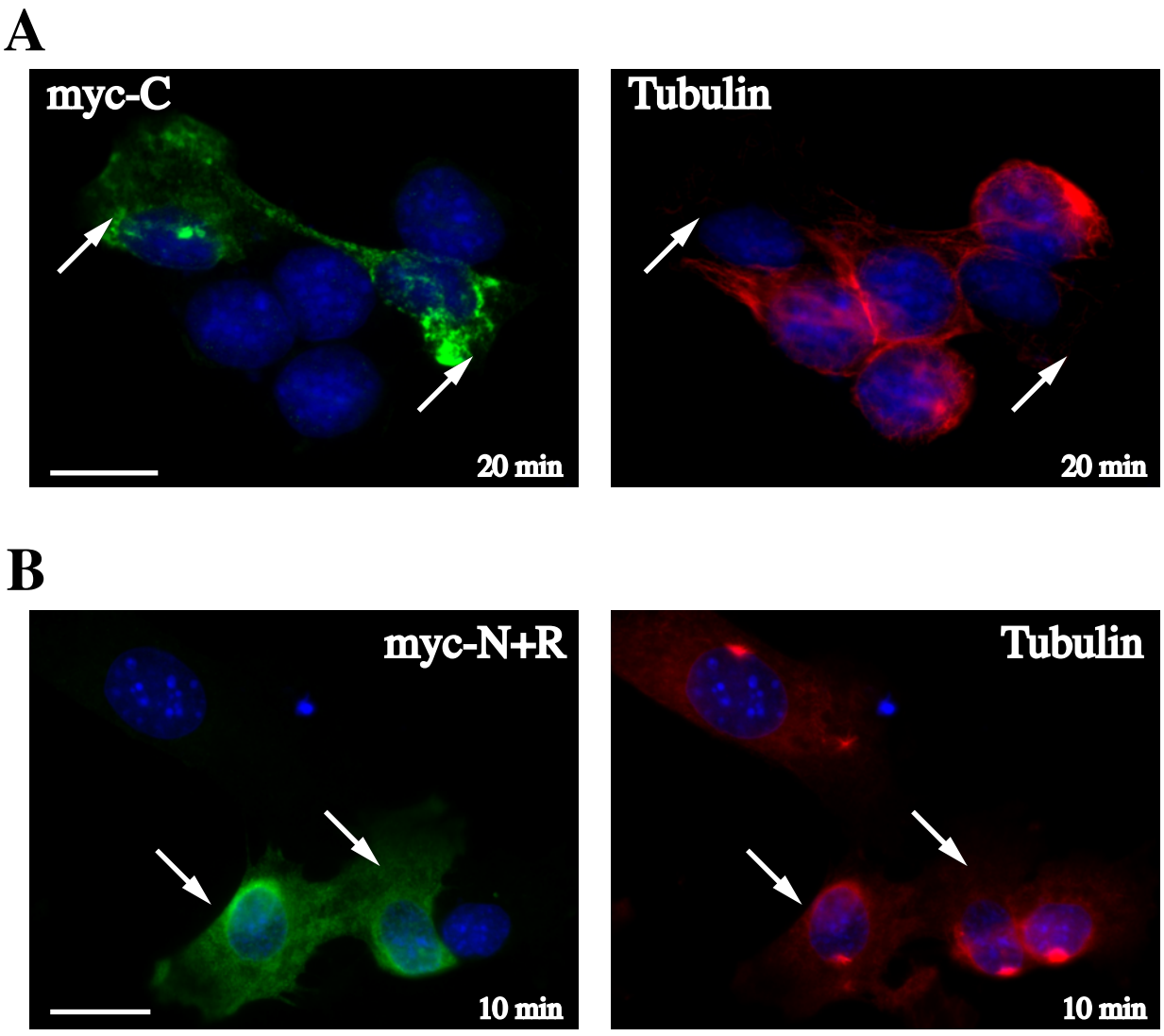

Figure 37. **Disruption of microtubule repolymerization caused by cytLEK1 dysfunction is long-lasting and specific.** Disrupting cytLEK1 function inhibits microtubule repolymerization after nocodazole challenge in murine cells. Cells were treated with 5 mg/mL nocodazole for 3 h followed by 10 (B) or 20 (A) min washout before pre-extraction and fixation. Myc-tagged proteins are in green (arrows) and tubulin is in red. A) Even after 20 min of nocodazole washout, 3T3 cells transfected with myc-C have not reformed their microtubule networks. B) 3T3 cells transfected with myc-N+R were visualized without pre-extraction to prevent washing out of the myc-N+R protein. Cells that express this protein do not show any noticeable inhibition in microtubule repolymerization. DAPI (blue) was used to visualize nuclei. Bars, 10 μm.

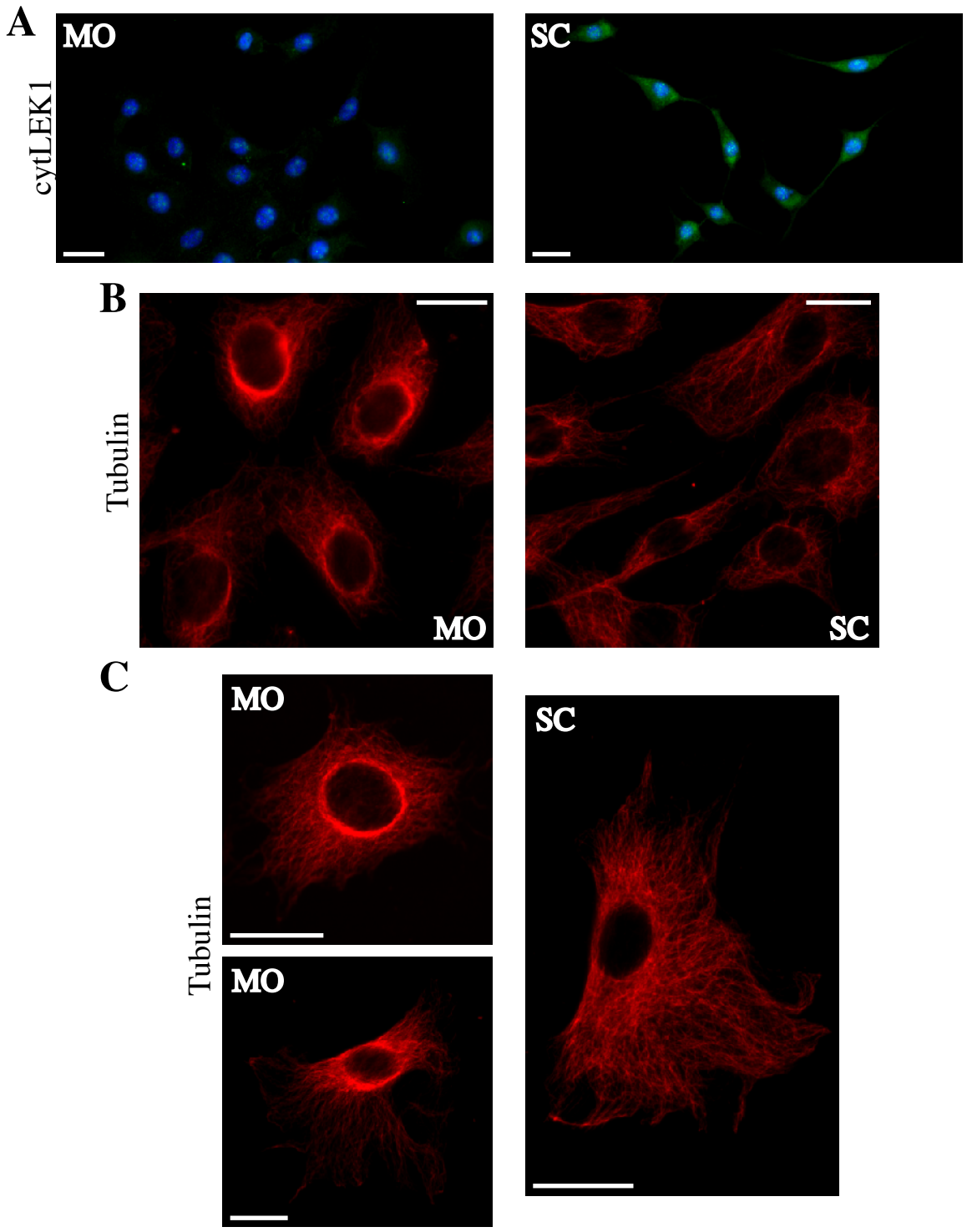

Figure 38. **LEK1 knockdown alters microtubule network organization.** 3T3 cells were treated with either LEK1-specific morpholinos (MO) or standard control morpholinos (SC) and examined 72 hours post-treatment. A) MO-treated cells show a substantial, but not complete, knockdown of cytLEK1 protein (green) compared to controls. B) The microtubule networks (red) of MO-treated cells are tightly focused around the nucleus when compared to control cells. C) Despite not exhibiting a rounded morphology, knockdown of LEK1 clearly results in a perinuclear accumulation of microtubules (red). DAPI (blue) was used to visualize nuclei. Bars: (A) 20 µm; (B-C) 10 µm.

Examination of endosome positioning after cytLEK1 disruption

Since the LIS1 pathway has been shown to be involved in the process of membrane trafficking (Liang et al., 2004), experiments were conducted to examine whether expression of the dominant negative myc-C protein disrupts endosomal movement. The approach utilized TRITC-labeled wheat germ agglutinin (WGA) that marks endosomes containing WGA-binding sites. After transfection with the myc-C construct, cells were first incubated at 4˚C to block endocytosis and to leave WGA at the plasma membrane. They were then either immediately fixed or switched to 37˚C for 60 min to examine endosomal transport. The 4˚C incubation successfully blocks endocytosis of WGA, as shown by the immediate (0 min) fixation data (Figure 39 A). However, there is substantial variation among the cell population at 60 min, even in non-transfected samples, such that no clear difference in WGA distribution can be observed between cells expressing myc-C and those expressing myc-N+R (Figure 39 B). Thus, this assay is not very useful for detecting potential changes in endosomal movement resulting from expression of myc-C.

Distribution of the Golgi apparatus is altered after cytLEK1 overexpression

Proper positioning of the Golgi apparatus near the nucleus has been shown to dependent on dynein movement along microtubule tracks (Allan and Vale, 1991; Corthesy-Theulaz et al., 1992). Further experiments have revealed the involvement of additional LIS1 pathway members in this process, although the exact details of this regulation are under dispute (Faulkner et al., 2000; Sasaki et al., 2000; Smith et al., 2000; Tai et al., 2002; Liang et al., 2004). Thus, we first wished to examine whether disruption of cytLEK1 function using the myc-C protein results in an alteration of Golgi localization in 3T3 fibroblasts. An antibody to GM130, a marker of the Golgi apparatus, was used to visualize this organelle. The analysis was made difficult by the severe rounding of cells induced by expression of myc-C and myc-SRR. Therefore, the small number of cells (~10%) that do not exhibit a change in cell shape had to be examined instead. Within this minority population, no significant changes in Golgi positioning are visible. However, additional studies were conducted to examine any effects of expressing full-length cytLEK1 in 3T3 cells. Analysis was more effective in these cytLEK1-transfected cells due to their unaltered fibroblastic shape. Notably, cells overexpressing cytLEK1 at moderate to high levels generally exhibited a tighter clustering of the Golgi apparatus near the nucleus than non-transfected cells (Figure 40

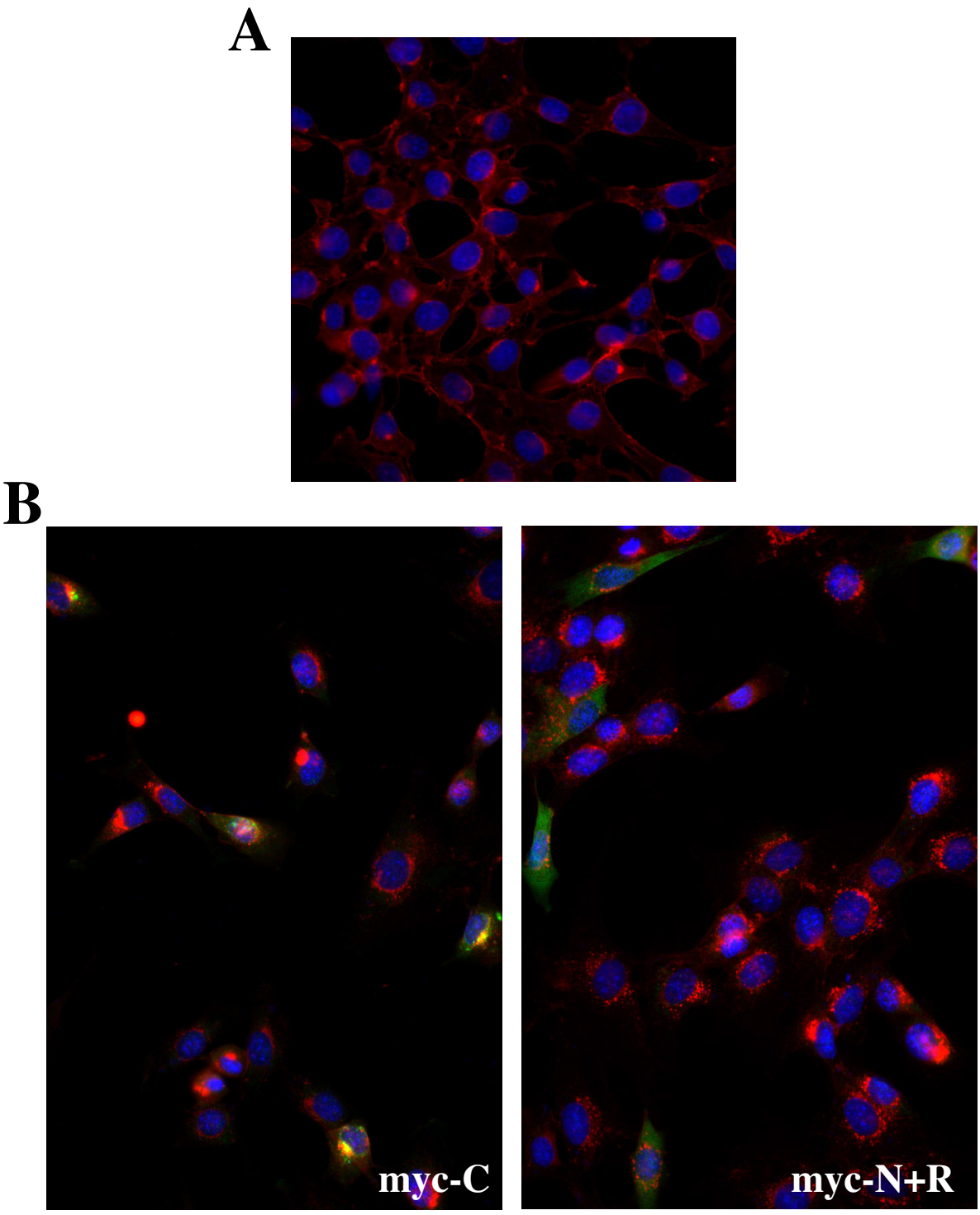

Figure 39. **Examination of endosome positioning in murine cells expressing myc-C.** TRITC-WGA (red) was used to visualize endosomes. A) Immediately after the 4˚C block of endocytosis, few labeled endosomes are detected in the cytoplasm of 3T3 fibroblasts. B) After a 60 min post-block incubation, labeled endosomes have been internalized. Due to substantial variation among the cell population, no clear differences between cells expressing myc-C and myc-N+R (both red) are observed. DAPI (blue) was used to visualize nuclei.

A). Cells transfected with GFP as a control do not exhibit such a dramatic phenotype (Figure 40 B). Thus, these preliminary data suggest that overexpression of cytLEK1 enhances the movement of the Golgi towards the nucleus. This result is consistent with the putative role of the LIS1 pathway in moving such organelles in this direction (Allan and Vale, 1991; Corthesy-Theulaz et al., 1992; Sasaki et al., 2000; Smith et al., 2000; Liang et al., 2004). Further experiments of a more quantitative nature should be conducted to more precisely determine the effect of cytLEK1 on Golgi positioning.

Examination of effects of cytLEK1 overexpression on myocyte differentiation

Since depletion of LEK1 has been shown to induce premature differentiation in C2C12 myoblasts (Ashe et al. unpublished data), we examined whether overexpression of cytLEK1 in these cells also has an effect on this process. As a marker for differentiation after serum deprivation, expression of sMHC was observed. However, these experiments were inconclusive due to an interesting consequence of cytLEK1 expression. During the period required for differentiation to occur, the number of cells expressing the cytLEK1 construct appears to decrease dramatically. This decrease occurs days 2 and 3 post-transfection, whereas sMHC expression is not detected in high numbers until day 4. Thus, there remain too few transfected cells to obtain a significant result regarding cytLEK1 effects on differentiation, as determined by a chi-square analysis. However, further experiments were conducted to better determine the cause of the disappearance of these cytLEK1-expressing cells.

Overexpression of cytLEK1 results in disappearance of cells

In order to examine the effects of cytLEK1 overexpression on a cell line with high transfection efficiency, 3T3 fibroblasts were utilized. Preliminary experiments confirmed a decrease in cytLEK1-transfected cells as initially observed with C2C12 myoblasts, so a more comprehensive analysis was undertaken. These data revealed that these cells undergo a dramatic and significant decline in number between days 2 and 3 post-transfection. In order to confirm that this change cannot be attributed to simply the burden of overexpressing any protein or the shock of the transfection procedure, cells were also transfected with a lacZ construct as a control. Indeed, this decline in transfected cell number is specific to cytLEK1-transfected cells, as it is significantly greater than for lacZ-transfected control cells. Whereas there is a 62.6% decrease in

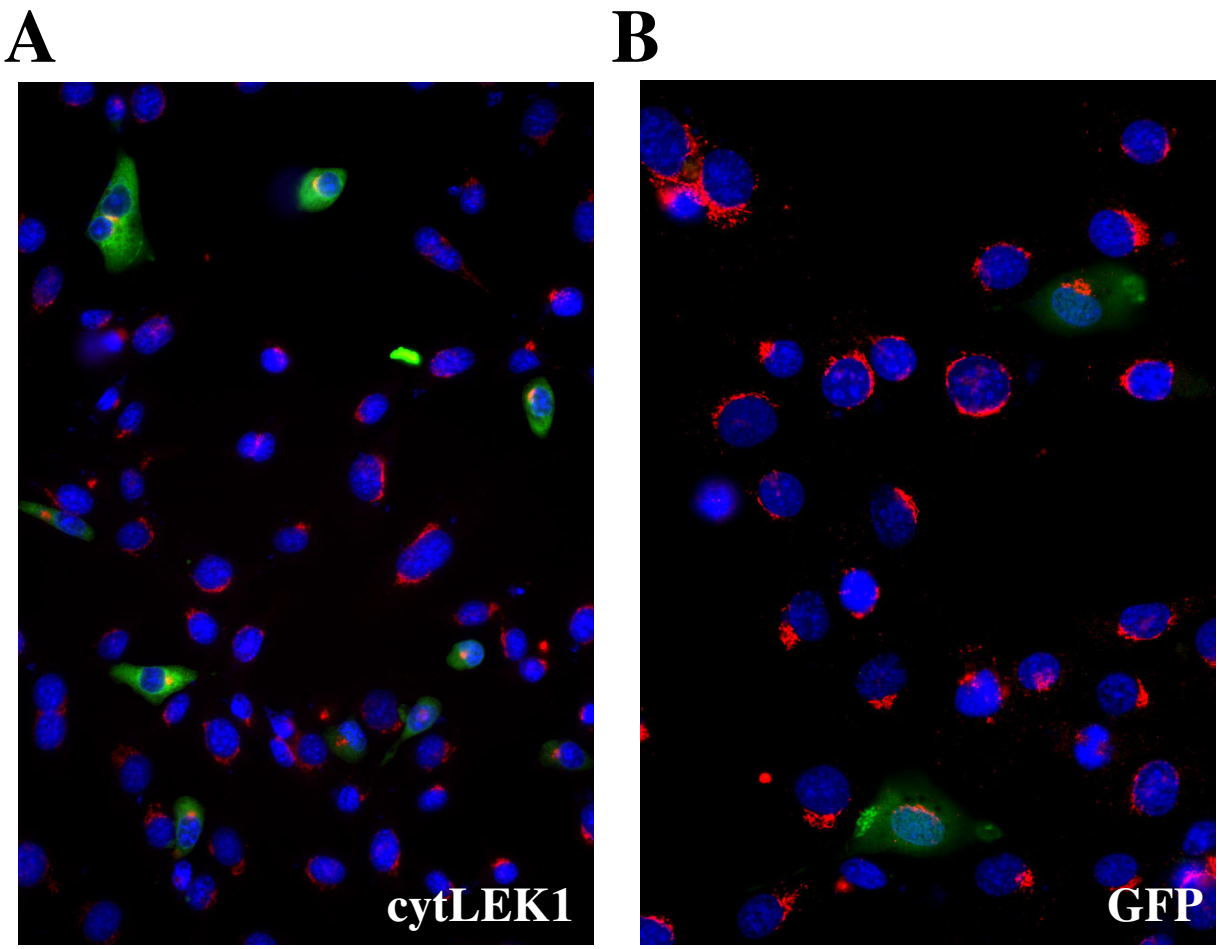

Figure 40. **Overexpression of cytLEK1 in murine cells results in alteration of the distribution of the Golgi apparatus.** The Golgi apparatus of 3T3 fibroblasts was visualized with an antibody to GM130 (red). A) 3T3 cells were transfected with a FLAG-tagged cytLEK1 construct (green) and examined for changes in Golgi localization. Transfected cells appear to have a tighter clustering of the Golgi apparatus near the nucleus than non-transfected cells. B) 3T3 cells were transfected with a GFP construct (green) as a control. No significant effect on Golgi localization was observed. DAPI (blue) was used to visualize nuclei.

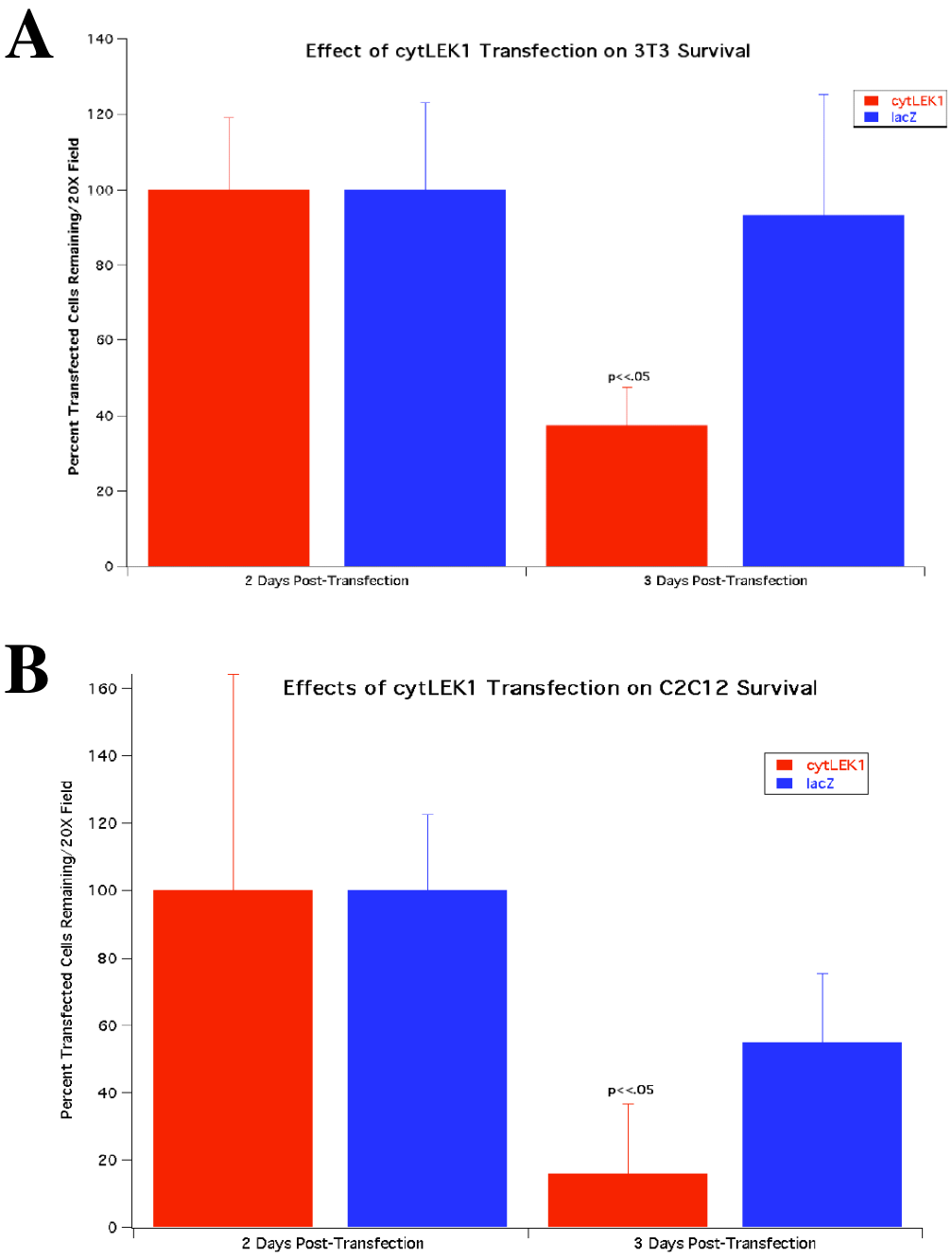

Figure 41. **Overexpression of cytLEK1 in murine cells results in a decrease in transfected cell number.** Cells were transfected with either a FLAG-tagged cytLEK1 construct (red) or a lacZ construct (blue). The number of transfected cells per field was determined at days 2 and 3 post-transfection. The values were averaged based on day 2 numbers and are presented here. A) There is a 62.6% decrease in the number of cytLEK1-transfected 3T3 fibroblasts between days 2 and 3, whereas only 6.8% of the lacZ-transfected cells are absent ($p<0.0001$ by Student's t-test, Microsoft Excel). B) C2C12 myoblasts exhibit a similar decline. Between days 2 and 3 post-transfection, there is an 82.3% decrease in the number of cytLEK1-transfected cells compared to a 45.2% decline for lacZ-transfected cells ($p<0.0001$ by Student's t-test, Microsoft Excel).

the number of cytLEK1-transfected cells between days 2 and 3, only 6.8% of the lacZ-transfected cells are absent (Figure 41 A, $p<0.0001$). This effect does not seem to be cell type-specific, as confirmed by quantitative experiments with C2C12 myoblasts. Although the absolute number of transfected cells is lower, thus increasing the standard deviation, cytLEK1-transfected myoblasts are more affected than control cells. Between days 2 and 3 post-transfection, there is an 82.3% decrease in the number of cytLEK1-transfected cells compared to a 45.2% decline for lacZ-transfected cells (Figure 41 B, $p<0.0001$). The overall higher percentage decline compared to fibroblasts is likely a result of the lower resistance of myoblasts to cellular and environmental perturbations. However, the results clearly indicate that cells overexpressing cytLEK1 decrease significantly in number between 48 and 72 h after transfection. Notably, overexpression of nucLEK1 is associated with a similar phenotype in various cell lines (Ashe et al. unpublished data).

Since overexpression of cytLEK1 results in a dramatic decline in the absolute number of transfected cells, experiments were undertaken to determine if this situation was the result of an increased rate of apoptosis. As a measure of apoptosis, an antibody specific to cleaved caspase 3 was utilized. Immunofluorescence control experiments on UV-treated C2C12 myoblasts reveal an increase in the number of cleaved caspase 3-positive cells, thus confirming the sensitivity of the assay. However, there is no apparent correlation between cytLEK1-transfected cells and the apoptotic marker 2 days post-transfection. While many apoptotic cells are observed, they are distributed equally among the non-transfected and cytLEK1-transfected population. Additional experiments with 3T3 fibroblasts confirm that there is no detectable increase in apoptosis as a result of cytLEK1 overexpression. Thus, the decrease in cytLEK1 appears to be caused by an event other than apoptosis. Two additional possibilities, which are both difficult to test, are that the transfected cells are undergoing necrosis or that the cells are somehow becoming detached from the glass slide. Regardless of cause, the short time span available for observing cytLEK1-transfected cells limits the range of possible experimental analyses.

Discussion

In chapters II and III, we present data characterizing the expression pattern of cytLEK1 and examining its interaction with NudE. These experiments reveal an association with NudE through distinct binding domains and a colocalization of cytLEK1 with key proteins of the LIS1

pathway. The results suggest that cytLEK1 has the potential to interact with and regulate LIS1 pathway members in a wide range of developing tissues and cells. Thus, examination of cytLEK1 function is a logical next step and the focus of this chapter. Experiments were designed to study processes previously shown to be regulated by the LIS1 pathway. Such events include microtubule organization, organelle positioning, spindle formation, and migration (see Introduction). CytLEK1 is well-suited to affect LIS1 pathway functions due to its perinuclear localization, including at the centrosome, and interaction with NudE (chapters II and III). As determination of the role of LIS1 pathway members has generally consisted of conducting loss-of-function or dysfunction studies (see Introduction), the experiments in this chapter are similar in design. In order to examine the specific effects of disrupting the cytLEK1-NudE interaction, a dominant negative approach was utilized for many studies. While we do present some experiments using LEK1 knockdown, this method is not the best approach for our purposes for several reasons. First, LEK1 knockdown results, as confirmed here, in massive cell death several days after treatment with LEK1-specific morpholinos, presumably due to a requirement of LEK1 for cell survival (Ashe et al., 2004). This response both limits the potential assays that can be conducted and also introduces an additional variable into experiments. Also, LEK1 is a relatively unique protein in that it is post-translationally cleaved to yield two peptide products: cytLEK1 and nucLEK1. Any technique that inhibits translation of the LEK1 protein will result in depletion of both peptide products. Thus, it is difficult to ascertain whether the effects seen are predominantly due to cytLEK1 or nucLEK1 depletion, or both. This is the case with previous studies showing an inhibition of proliferation with LEK1 knockdown (Ashe et al., 2004). However, knockdown experiments can serve to confirm results obtained through other techniques, such as dominant negative protein expression, and that is their primary use here.

The dominant negative approach utilized in this chapter allows us to specifically examine the role of the cytLEK1-NudE interaction. By localizing the region of NudE-binding to the small C domain within cytLEK1 (chapter III), we were able to create a protein, myc-C, that isolates this domain from any other functional regions within cytLEK1. Thus, myc-C would be expected to have a dominant negative effect on LIS1 pathway functions. Indeed, the experiments reveal several disruptions resulting from expression of the myc-C protein in murine cells. Our extensive characterization of the cytLEK1-NudE interaction allows us to utilize the myc-N+R protein, which contains the entire SRR except the C domain, as a negative control in these studies. Thus,

the effects we observe are consistently the result of expressing the isolated C domain specifically and examining dysfunction of the LIS1 pathway. Our analysis is somewhat complicated by the lack of knowledge of the direct mechanism of action of most LIS1 pathway members, in addition to the conflicting functional data in the literature (see Introduction). However, the phenotypes we observe are generally consistent with the majority of published studies and the emerging model of LIS1 pathway function.

The most obvious effect of myc-C expression in cells is a dramatic change in cell shape (Figure 33). The cells lose their fibroblast or myoblast morphology and rapidly adopt a rounded shape. This effect is clearly specific to the myc-C protein with its isolated C domain, as expression of myc-N+R does not result in any noticeable change in morphology. Additionally, overexpression of full-length cytLEK1 does not result in any significant alteration of cell shape, although these cells do disappear after several days as has been noted (Figures 33, 41). This result confirms our model for dominant negative function, since it reveals that expression of the C domain with other cytLEK1 regions does not have as severe an effect as expression of the C domain alone. It is also important to note that this rounded phenotype is not an artifact of cell death caused by myc-C expression, as the number of transfected cells does not significantly decline over a 72 hour period. Thus, this effect is specifically a modification of cell shape. Alterations in morphology have previously been noted with a LIS dominant negative protein (Cahana et al., 2001), supporting a role for cytLEK1 in LIS1 pathway function.

As microtubule organization is another key function of the LIS1 pathway (see Introduction), the cells expressing myc-C were also examined for alterations of the microtubule network. Notably, there is a dramatic change in microtubule localization in these cells. Instead of being broadly distributed throughout the cell, the microtubule network becomes tightly focused around the nucleus. Thus, it appears that there is an inhibition of microtubule transport to the periphery. This tight perinuclear distribution of microtubules, observed here with cytLEK1 dysfunction, has previously been detected in fibroblasts from *LIS1*-heterozygous mice, as well as in dynein and Nudel dysfunction studies, and attributed to the role of the LIS1 pathway in dynein-directed outward movement of microtubules in cells (Ahmad et al., 1998; Smith et al., 2000; Shu et al., 2004). Our dominant negative myc-C protein appears to be capable of strongly disrupting this process, indicating the importance of cytLEK1 function in the LIS1 pathway. It is worthwhile to note that it is unclear from these experiments whether the cell shape change

precedes the microtubule network collapse. Clearly, cells that are severely rounded will have microtubules that are tightly focused around the nucleus. Conversely, cells that have a collapsed microtubule network near the nucleus will exhibit an altered morphology. However, distinguishing between these two scenarios is not critical for our purposes here. The microtubule network is partly responsible for determining cell shape, and changes in morphology require cytoskeletal rearrangements. Thus, since the myc-C-expressing cells are rounded, there must have been a change in microtubule organization at some point. If these cells had normal regulation of microtubules, then they would likely be unable to exhibit such a defective cell shape in the first place. Considering the multiple studies noted above that have revealed an important function for LIS1 pathway members in microtubule regulation, as well as our related experiments in this chapter, it is likely that an initial disruption of microtubule transport results in the change in cell shape due to myc-C expression. Indeed, LEK1 knockdown experiments appear to confirm this proposal, as will be discussed shortly.

The speed with which the cells expressing myc-C undergo this alteration of morphology and microtubule network organization is impressive. As soon as 8 hours after transfection, most cells exhibit a rounded phenotype. This suggests that cytLEK1 function is continually required in order for cells to maintain their microtubule network. Presumably, cytLEK1 participates in the LIS1-directed continuous movement of microtubules to the periphery using dynein motors (Ahmad et al., 1998; Smith et al., 2000; Shu et al., 2004). When this transport is disrupted by myc-C, microtubules begin to accumulate around the nucleus and a change in cell shape results. Additionally, since cytLEK1 has been shown to be at the centrosome (chapters II and III), it may be important in stabilizing the microtubule network at this key organizing center. Any disruption of this structure will naturally alter the arrangement of microtubules within cells. As expression of myc-C results in a phenotype in such a rapid fashion, the protein is presumably able to quickly and efficiently replace endogenous cytLEK1 at important subcellular locations. Thus, there is likely a process of cytLEK1 exchange normally occurring at these sites. If instead cytLEK1 were tightly attached to these structures for long periods of time, the ability of myc-C to disrupt its function would be limited and delayed. It seems reasonable to postulate that endogenous cytLEK1 is constantly recruited to newly-created LIS1-related complexes involved in, for example, movement of microtubules to the periphery. Alternatively, myc-C may bypass any regulatory mechanisms that prevent cytLEK1 from interacting with various potential binding

partners in certain locations. An intriguing question is whether cytLEK1 is required for proper localization of LIS1 pathway members to their functional positions in cells. It may be that cytLEK1 serves a structural role in bringing together key proteins, and that myc-C disrupts this complex formation. The overlap of the cytLEK1- and putative dynein-binding domains within NudE suggests a potentially complex regulation of protein-protein interactions. Unfortunately, the severe effect on morphology resulting from myc-C expression limits potential analysis. While endogenous dynein and LIS1 are abnormally tightly packed around the nucleus in these cells, this result may be inevitable due to the shape of the cell. Thus, LIS1 pathway member localization is disrupted in myc-C-expressing cells, but it is impossible to discern whether this effect is the cause of or, instead, result of microtubule network disorganization. Examination of the small subset of cells that express myc-C but do not initially round up does not yield any useful information. The localization of LIS1 pathway members in these cells is unaltered, but they are also unaffected by any cytoskeletal or morphological changes. Thus, there may be no significant change in distribution of pathway members simply due to the fact that the myc-C protein, for whatever reason, is not yet having a dominant negative effect in these cells.

Nonetheless, our results clearly show that expression of myc-C causes dramatic alterations in morphology and microtubule network organization, consistent with disruption of LIS1 pathway function. It is interesting to note that the localization of the myc-C protein supports its cellular effects. In both rounded and non-rounded cells, myc-C exhibits a predominantly perinuclear distribution, thus placing it in the ideal location for interaction with endogenous LIS1 pathway members (see Introduction and chapter III). Additionally, the myc-C protein is resistant to detergent extraction and remains in the insoluble cytoskeletal pool. Thus, the C domain alone is likely capable of interacting with cytoskeletal structures, consistent with its role in directing the cytLEK1-NudE association. Endogenous cytLEK1 is also partially resistant to detergent pre-extraction, especially around the nucleus (Figure 12). The results in this chapter suggest that the C domain is at least partially responsible for conferring this resistance to cytLEK1. Additional experiments are required to determine whether other regions of cytLEK1 may also have such a function. Notably, the N+R region of the SRR does not have such an effect. In fact, this myc-N+R protein lacking the C domain does not exhibit any noticeable localization within cells but instead is distributed throughout the cytoplasm (chapters III and IV).

Thus, the dominant negative myc-C protein causes disruption of cytLEK1 function within the LIS1 pathway through a likely association with cytoskeletal structures.

As the myc-C protein has been shown to have an effect on the organization of pre-existing microtubule networks, we wished to also study its role in nascent microtubule polymerization. To conduct such experiments, nocodazole was first utilized to depolymerize the microtubule network in murine cells, and reformation of the network after drug washout was consequently examined. These studies were conducted with strict time guidelines to minimize the severe rounding of cells observed with prolonged exposure to myc-C. Very interestingly, cells expressing myc-C show a nearly complete inability to repolymerize their microtubule networks after nocodazole challenge. This severe effect is long-lasting and not observed in non-transfected or myc-N+R-expressing cells. In most cells transfected with myc-C, there is no visible formation of microtubules from the organizing center. Conversely, control cells exhibit long microtubule networks emanating from the centrosome. It is interesting to note that, in the few myc-C-expressing cells where there is rudimentary formation of a nascent microtubule network from the organizing center, there is no myc-C protein present near this structure. Although the sample size is not large enough to make a definitive conclusion, this is an intriguing observation suggesting that myc-C may be required at the centrosome in order to have a disruptive effect.

Our repolymerization results here are consistent with previous studies on other LIS1 pathway members. Notably, LIS1 overexpression alters microtubule polymerization and localization after nocodazole challenge (Smith et al., 2000). Overexpression of GFP-mNudE results in the formation of additional microtubule-organizing centers throughout the cell and disrupts normal microtubule organization (Feng et al., 2000). Finally, Nudel knockdown results in an accumulation of microtubules near the nucleus after a combination nocodazole/vinblastine treatment (Shu et al., 2004). In general, the effects we observe here appear to be more severe than those resulting from disruption of other LIS1 family members, such as Nudel. Instead of observing only an inhibition in microtubule transport, we are unable to detect even polymerization of microtubules at the centrosome. Thus, our results suggest that cytLEK1 has an especially critical role in microtubule network formation at the organizing center of cells. This is consistent with the presence of myc-C at this structure (chapter III). Because of its large size, it is possible that cytLEK1 serves as a scaffold at the centrosome, bringing together important

proteins. Proper reformation of centrosomal structures and attachments after nocodazole challenge may require the presence of cytLEK1. Alternative incorporation of myc-C disrupts these normal associations and thus does not allow the centrosome to be effectively used as an organizing center for microtubule repolymerization. It is currently unclear whether cytLEK1 directly binds microtubules or simply associates with other cytoskeletal-binding proteins. An alternative, but related, explanation focuses on the pre-extraction technique used in these experiments to better visualize microtubules. It is possible that microtubule networks are, in fact, partially reformed in transfected cells but are deficient in attachment to a defective myc-C-containing centrosome. Thus, these microtubules easily detach from this structure and are washed out during pre-extraction, whereas normal networks remain strongly bound to the organizing center. This scenario implies, yet again, that cytLEK1 at the centrosome is required for proper formation and function of protein complexes at this structure.

In order to corroborate the dominant negative studies on cytLEK1 function, experiments were conducted to examine the effect of LEK1 knockdown on the microtubule network. As has previously been noted, the primary disadvantages of such studies consist of the resulting cell death and the inability to distinguish cytLEK1- versus nucLEK1-specific actions. Additionally, results are complicated by the fact that the knockdown of LEK1 is incomplete, as evidenced by immunofluorescence labeling of cytLEK1, so some endogenous cytLEK1 remains in these cells. Consistent with this situation, we observe defects in microtubule network organization that are similar, but less severe, than our previous data, confirming our dominant negative studies. Notably, there is yet again a substantial accumulation of microtubules around the nucleus in cells treated with LEK1 morpholinos. However, the cells exhibit a normal morphology, unlike cells expressing myc-C. These data suggest that a change in microtubule organization is the primary event occurring and consequently resulting in alteration of cell shape. Thus, cytLEK1 is critical for movement of microtubules to the periphery of cells, as evidenced by two separate assays. LIS1 pathway members have been shown to be crucial for this transport process, and inhibiting the function of any member consistently results in a perinuclear accumulation of microtubules, as we also observe here (Ahmad et al., 1998; Smith et al., 2000; Shu et al., 2004). Thus, the role of cytLEK1 is similar to those of other LIS1 pathway members.

While LEK1 knockdown does not result in a rounded morphology, this finding is not surprising, as a dominant negative construct specifically examining the NudE-binding domain of

cytLEK1 would likely not have identical effects to knockdown of full-length LEK1 and its resulting cytLEK1 and nucLEK1 cleavage products. In addition, some endogenous cytLEK1 remains even after morpholino treatment, which may be enough to prevent severe changes to the cytoskeleton and cell morphology. Nonetheless, the critical role of cytLEK1 in microtubule network organization is evident in both dominant negative and knockdown experimental models. We also wished to examine whether cytLEK1 knockdown affects microtubule repolymerization after nocodazole challenge. However, such studies were impractical due to the massive cell death response resulting from the apparent sensitivity of LEK1-knockdown cells to environmental stresses. Consistent with previous work (Ashe et al., 2004), it appears that LEK1 expression is required for cell survival and that even incomplete knockdown has highly negative effects on cells. Similarly, Nudel depletion causes rapid apoptosis of cells (Liang et al., 2004), while loss of LIS1 produces proliferation defects (Faulkner et al., 2000; Liu et al., 2000). Additionally, overexpression of cytLEK1 or nucLEK1 results in the eventual disappearance of transfected cells (Ashe et al. unpublished data; Figure 41). These knockdown and overexpression data are not surprising considering the putative role of cytLEK1 and nucLEK1 in key cellular processes, including proliferation. The results we present here reveal the role of cytLEK1 in microtubule transport and organization, including at the centrosome, and imply that cytLEK1 dysfunction disrupts a vast array of cellular processes. However, as cells partially depleted of full-length LEK1 die much faster than cells expressing myc-C, it appears that other regions within LEK1, in addition to the C domain, have important functional roles. This is consistent with our hypothesis that cytLEK1 may bring together key proteins through several independent domains.

As cytLEK1 has been shown to be essential for LIS1 pathway functions related to the microtubule network, experiments were also conducted to examine its role in other processes of this pathway. Our studies focus on examining organelles and endosomes whose movement is dependent on the LIS1 pathway. Experiments are complicated by the fact that the literature is not clear on the exact effects of the LIS1 pathway on such entities (Faulkner et al., 2000; Sasaki et al., 2000; Smith et al., 2000; Tai et al., 2002; Liang et al., 2004) and that results can be highly subjective. These studies innately contain a high degree of variability, as the localization of endosomes, for example, is highly variable among even “identical” cells of a control population. This is likely part of the cause of the inconsistent results often reported in the literature. However, dramatic changes are more easily evident and can be quantified, if necessary. Our

experiments examining the effects of myc-C expression on endosome trafficking are inconclusive due to the caveats listed above. The amount of variation seen in control populations makes it very difficult to detect or quantify any changes due to cytLEK1 dysfunction. Additionally, the rounding of cells expressing myc-C complicates examination of cytoplasmic structures.

Studies were thus conducted instead to look at the localization of the Golgi apparatus in cells transfected with full-length cytLEK1. As these cells do not exhibit a change in morphology, it is far easier to visualize Golgi positioning. Interestingly, cells overexpressing cytLEK1 exhibit a tight clustering of the Golgi apparatus near the nucleus. This effect appears to be significant when compared to non- or GFP-transfected control cells. However, as there is variability among even control cells in this assay, future quantitative analysis is needed to confirm this phenotype. An additional concern based on these preliminary data, which will have to be addressed in the future, is whether the expression level of cytLEK1 affects the phenotype and what the significance of such a result may be. Our current results, though, do suggest that cytLEK1 plays a role in enhancing movement of the Golgi apparatus towards the nucleus. These data are consistent with the putative but disputed role of the LIS1 pathway in moving organelles in this direction (Allan and Vale, 1991; Corthesy-Theulaz et al., 1992; Sasaki et al., 2000; Smith et al., 2000; Liang et al., 2004). While disrupting cytLEK1 function results in inhibition of LIS1 pathway actions, overexpression of cytLEK1 enhances these processes. Thus, our results clearly show that cytLEK1 is a positive regulator of LIS1 pathway functions. Its role appears to extend beyond just microtubule organization into movement of organelles. This is consistent with the significant colocalization of cytLEK1 with several LIS1 pathway members at key subcellular locations (chapter III). It will be interesting to study in future experiments whether cytLEK1 plays a role in additional processes of the LIS1 pathway. Examination of the role of cytLEK1 during mitosis is especially critical, due to the role of pathway members in dividing cells and the localization of cytLEK1 to key mitotic structures (chapter II). Also, no mitotic cells expressing myc-C have ever been detected, suggesting a potential defect in cell division processes due to cytLEK1 dysfunction.

In summary, the data in this chapter reveal a function for cytLEK1 in regulation of the LIS1 pathway. These results are especially exciting as they utilize characterization of a novel cytLEK1-NudE interaction to define, for the first time, a role for cytLEK1. Consistent with its

presence at key subcellular structures (chapter II) and co-IP/colocalization with numerous LIS1 pathway members (chapter III), cytLEK1 has an important function in processes controlled by this pathway. Notably, cytLEK1 dysfunction results in alteration of cell shape and microtubule organization. Our results suggest that cytLEK1 plays a role in a wide range of LIS1 pathway activities, including organelle movement. Additionally, the dominant negative myc-C protein severely inhibits microtubule repolymerization after nocodazole challenge, consistent with the presence of this protein at the centrosome. These data suggest that proper cytLEK1 activity requires the presence of multiple domains within the molecule that bind to several partner proteins. LEK1 is essential for basic cellular functions, as knockdown of the protein results in microtubule disorganization and eventual cell death. Future studies will reveal the exact nature of the role of cytLEK1 within the LIS1 pathway and reveal whether cytLEK1, similar to LIS1, is necessary for correct regulation of the LIS1 pathway during embryonic development.

CHAPTER V

CONCLUSIONS AND FUTURE DIRECTIONS

Conclusions

The studies presented in this document examine for the first time the expression, localization, interaction, and function of cytLEK1. These novel results provide an understanding of the important role of cytLEK1 in key cellular processes through regulation of the LIS1 pathway. In chapter II, we reveal that cytLEK1 is present in the mouse predominantly at embryonic stages, consistent with its putative role in murine development. Its wide pattern of expression suggests that it has the potential to function in several tissues, including the heart and brain where it is highly expressed. In fact, the pattern observed for cytLEK1 is very similar to that of its binding partner, NudE(L) (Feng et al., 2000; Niethammer et al., 2000; Sasaki et al., 2000; Yan et al., 2003). Thus, these two proteins are likely intimately associated in a wide range of settings during development. Additionally, the subcellular distribution of cytLEK1 is revealed to be similar to that of other LIS1 pathway members (see Introduction), suggesting a common function in cells. The protein is detected in the cytoplasm with a perinuclear predominance, and it is found on both the spindle and spindle poles of mitotic cells.

In chapter III, these expression studies are placed in the context of the cytLEK1-NudE interaction discovered through a yeast two-hybrid screen. The association of these two proteins is determined to be dependent on the C domain within the spectrin repeat region of cytLEK1. Conversely, cytLEK1 binds to a region in NudE that overlaps with the putative dynein-binding domain, suggesting a possibly complex regulation of protein-protein interactions. Examination of the small myc-C protein reveals that it distributes to areas of high NudE concentration, especially at the centrosome. Studies of endogenous proteins confirm that cytLEK1 colocalizes with NudE in murine cells. Additional experiments reveal a similar result with cytLEK1 and the two known binding partners of NudE: dynein and LIS1. The codistribution is most evident around the nucleus, consistent with the cellular region where cytLEK1 is detergent resistant and likely associates with the cytoskeleton. The less apparent colocalization near the cell periphery suggests the existence of additional binding partners and functions for cytLEK1 at this subcellular location.

In chapter IV, experiments are conducted to test the function of cytLEK1 with regard to its association with the LIS1 pathway. Several approaches are utilized, including dominant negative protein expression, LEK1 knockdown, and cytLEK1 overexpression. These data reveal that cytLEK1 is essential for proper regulation of microtubule organization and function through the LIS1 pathway. These effects extend to repolymerization of microtubule networks after nocodazole challenge and, thus, suggest a broad role for cytLEK1 in cytoskeletal processes. Knockdown studies confirm the importance of LEK1 for microtubule networks and the requirement of proper LEK1 levels for cell viability. Experiments were initiated to examine the role of cytLEK1 within additional processes controlled by the LIS1 pathway. Organelle movement appears to be regulated by cytLEK1, suggesting a wide function for the protein in the LIS1 pathway.

By incorporating the results and discussion presented in this document, it is possible to begin to form a broad model for cytLEK1 function in cells (Figure 42). Clearly, the details of this model are incomplete, as the exact roles of even the established LIS1 pathway members are currently unknown (see Introduction). Based on its expression pattern, cytLEK1 appears to function predominantly in processes occurring during murine embryonic development. It likely plays a fundamental role in a wide variety of tissues and cells, consistent with other LIS1 pathway members (Hirotsune et al., 1998; Feng et al., 2000; Niethammer et al., 2000; Sasaki et al., 2000; Smith et al., 2000; Dujardin et al., 2003; Yan et al., 2003; Liang et al., 2004; Shu et al., 2004). However, the existence of some tissue-specific differences in expression pattern suggests that cytLEK1 is either more important in certain tissues and/or has additional functions in them. The importance of LIS1 pathway members during embryonic development is not surprising given the role of the pathway in controlling the processes of proliferation, migration, and differentiation (see Introduction). Such events occur at a very high rate in the developing organism with little room for error.

An interesting unanswered question remains, however, about the general developmental role of cytLEK1. Is cytLEK1 truly not expressed and thus not required in the adult mouse? If this is the case, then there are two possible explanations: Either the function of cytLEK1 is specific to cells in the embryo, or another protein takes over the role of cytLEK1 in the adult animal. Neither of these scenarios is especially convincing. CytLEK1 regulates basic cellular processes that occur, to some degree, in nearly all cells. Thus, it is difficult to imagine that its role is no

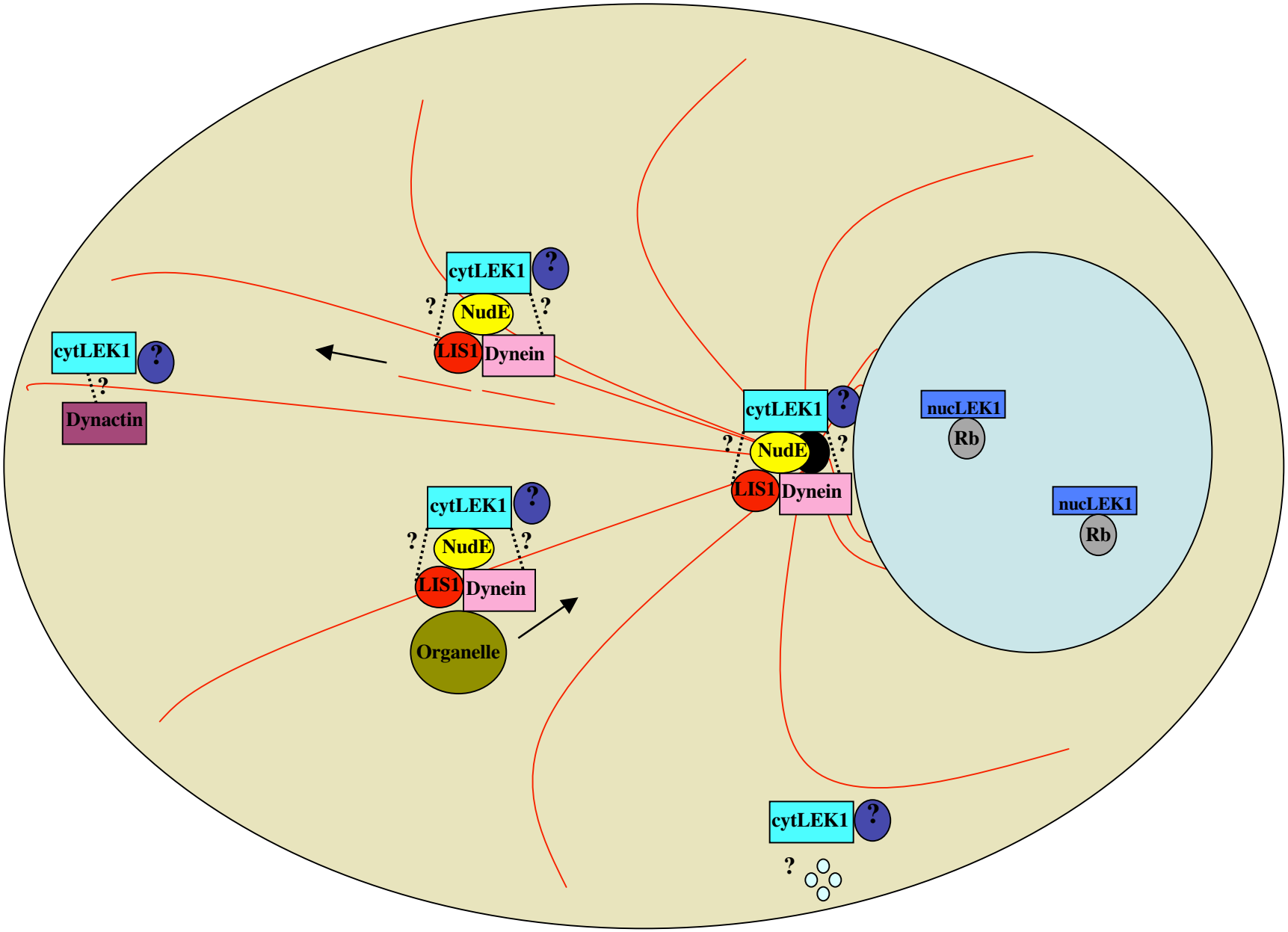

Figure 42. **Model of cytLEK1 function.** See text for details.

longer essential in adult cells. While no other Mitosin/CENP-F-like molecule has been detected in the mouse, the existence of such a protein would help explain this LEK1 expression issue. However, the severe effects caused by LEK1 depletion in cells suggest that other proteins are incapable of compensating for LEK1 knockdown, at least in a cell culture environment. Thus, a final possible explanation is that cytLEK1 is indeed present in adult tissues but at a low expression level, similar to NudE, that cannot be consistently detected (Feng et al., 2000). This scenario reinforces the proposal that cytLEK1 and other similar proteins are especially critical during development due to the unprecedented amount of proliferation, migration, and differentiation occurring at this time. In fact, immunofluorescence studies of adult tissues reveal that while cytLEK1 and nucLEK1 levels appear to be substantially reduced compared to embryonic stages, the proteins are not completely absent in adult organisms. Determination of whether cytLEK1 is then present in unique environments with embryonic characteristics, such as stem cell niches and tumors, is an intriguing avenue of future study. Notably, examination of stem cell microchip arrays reveals that LEK1 expression is upregulated in all tested cell lines (Abeyta et al., 2004).

Regarding the cellular function of cytLEK1 within our model, there are several important results to consider. Depletion of LEK1 has previously been shown to affect proliferation and differentiation of cells (Ashe et al., 2004), although the exact role of cytLEK1 versus nucLEK1 is unclear. It is likely that the interaction of nucLEK1 with Rb family members (Ashe et al., 2004) is important for control of cell division. However, cytLEK1 specifically has a greater potential for regulation of key cellular processes through its widespread cytoplasmic distribution and association with LIS1 family members. Our data here suggest that the cytLEK1-NudE interaction is most critical around the nucleus, including at the centrosome. As discussed in chapter IV, cytLEK1 likely forms a complex with NudE and other LIS1 pathway-related proteins at these locations. CytLEK1 may, in fact, function as a key scaffolding element of the centrosomal structure, such that disruption of cytLEK1 activity results in the inability to properly attach and reform microtubule networks from this organizing center and couple it to the nucleus. The effects of cytLEK1 dysfunction on the existing microtubule network may be partly related to this centrosomal role, as well as association of cytLEK1 with LIS1-containing complexes that transport microtubules to the periphery through the action of dynein motors. Based on this function of cytLEK1 and the presence of endogenous protein on the spindle, it is likely that

cytLEK1 is similarly required for proper mitotic progression, a process highly dependent on the LIS1 pathway.

The design of our dominant negative protein reveals that dissociating the NudE-binding domain from other regions of cytLEK1 disrupts functions of the LIS1 pathway. Any roles of additional domains of cytLEK1, however, are currently unknown. Interestingly, the overlap between the cytLEK1- and putative dynein-binding domain of NudE reveals that cytLEK1 may in fact control the dynein-NudE interaction, perhaps even through cytLEK1-dynein binding. Such regulation of protein associations may extend to additional LIS1 pathway members through other cytLEK1 regions. Our data here clearly reveal that the role of cytLEK1 is not simply to bind NudE, as the myc-C protein is able to perform this function and yet causes extensive disruption of cellular processes. Thus, cytLEK1, which is much larger in size than LIS1 or NudE(L), likely interacts with multiple LIS1 pathway members to bring them together into a functional complex at the correct subcellular location. LIS1 alone associates with NudE(L), dynactin, dynein, and microtubules, while NudE(L) binds to LIS1, cytLEK1, and dynein (see Introduction and chapter III). Thus, even the smaller protein members of this pathway exhibit multiple associations suggestive of a complex set of interactions. Our results imply that each cytLEK1 molecule, through a currently unknown mechanism, likely associates with only a subset of all potential interacting partners. This selectivity is based on the cellular position and function at hand, and it is consistent with published data on the incomplete colocalization of all LIS1 pathway members (see Introduction and chapter III).

Based on the speed with which expression of the myc-C protein results in cellular changes, cytLEK1 likely exists as a protein population that is constantly in flux with continuous formation/disruption of such interactions. Considering the dynamic nature of processes such as microtubule movement to the periphery, it is not surprising that cytLEK1 would first be recruited to a certain cellular location and then later be needed in a different position. It remains unclear whether cytLEK1 at the centrosome has a more permanent role. At the present time, the association with NudE, which itself binds to dynein and LIS1, is currently the only known piece of this potentially intricate regulation of cytLEK1-containing complexes. Future direct binding assays will elaborate on the dysbindin results and also likely reveal an interaction between cytLEK1 and Nudel. Importantly, recent studies in our laboratory suggest that other regions of cytLEK1 may associate with additional proteins related to the LIS1 pathway (Pooley et al.

unpublished data). These putative interactions with dynactin and certain vesicular trafficking proteins may represent the other molecules cytLEK1 brings together and may help better explain the role of cytLEK1 at the periphery of cells.

In summary, this model envisions cytLEK1 as a positive regulator of the LIS1 pathway during development (Figure 42). A certain subset of cytLEK1 protein near the nucleus interacts with NudE and other pathway members. By bringing together a specific set of proteins at the centrosome and other perinuclear regions, cytLEK1 enables components to be in place for LIS1-related processes utilizing dynein motors. Such events, which are especially key during embryonic development, include microtubule transport, cytoskeletal organization, cell morphology, migration, and organelle movement. This same population of cytoskeletal cytLEK1 also functions similarly at the spindle poles and spindle of mitotic cells, although future experiments are required to confirm this. CytLEK1 present at the periphery of cells likely plays a different role, which may be less related to LIS1 pathway functions. Preliminary data suggest it possibly acts in leading edge processes and vesicular trafficking, consistent with its peripheral localization. Future elaboration on this model is especially dependent on the discovery and confirmation of additional cytLEK1 binding partners. However, it is apparent from the studies in this document that cytLEK1 is a key regulator of the LIS1 pathway.

Future Directions

Additional examination of LEK1 expression and distribution pattern

Our data here present, for the first time, the expression pattern of cytLEK1 in tissues and cells. Additional studies examining the distribution of cytLEK1, however, are required. While current *in vivo* work has focused primarily on the heart, the association of cytLEK1 with LIS1 pathway members necessitates experiments in the developing brain. Although we show that cytLEK1 is expressed in this organ, detailed localization studies with tissue sections are needed to determine the exact distribution of cytLEK1. It will be interesting to reveal whether cytLEK1 is present only in a certain cell type, such as neurons, or in many different cells. Additionally, the presence of cytLEK1 in brain structures where neuroblast proliferation occurs would suggest a key role in mitotic processes during brain development, similar to other LIS1 pathway members (Hirotsune et al., 1998; Feng and Walsh, 2004; Shu et al., 2004). A comprehensive analysis of

protein expression via Western blot in this tissue will assist in determining the exact period of cytLEK1 expression and also whether oligomerization is truly occurring (chapter II). In addition to the brain, localization of cytLEK1 in the postnatal heart should be examined to discern the precise nature of the change in subcellular distribution that occurs at this stage (chapter II). Distinguishing between perinuclear and true nuclear localization of cytLEK1 is important for revealing the role of the protein in this tissue. In cell culture, additional studies utilizing confocal deconvolution analysis are required to examine cytLEK1 localization in mitotic cells. Conducting parallel experiments for nucLEK1 in all these cells and tissues will assist in delineating the individual functions of the LEK1 peptide products. Finally, a careful analysis of adult tissues using quantitative RT-PCR and multiple LEK1 antibodies is required in order to conclusively confirm that LEK1 is absent in the adult mouse.

The creation of additional LEK1 antibodies will assist these expression studies. Monoclonal antibodies specific for both cytLEK1 and nucLEK1 using the Spec1 and 863 epitopes are currently under development. In addition to confirming our existing data, these antibodies will allow, for the first time, colocalization studies between cytLEK1 and nucLEK1. Thus, it will be possible to determine, for example, whether the apparent nuclear distribution of cytLEK1 in the postnatal heart is instead uncleaved LEK1. The monoclonal antibodies may also have different reactivity with fixation/extraction conditions as compared to our current polyclonal reagents, thus enabling studies that have been difficult. Detailed examination of a codistribution of endogenous cytLEK1 and microtubules may then be possible.

Future experiments will not be limited to normal tissues and cells in culture. The increased expression of Mitosin/CENP-F in tumors (de la Guardia et al., 2001; Esguerra et al., 2004) and the putative role of LEK1 in proliferation processes make worthwhile the examination of LEK1 expression in murine cancers. Studies should investigate both cytLEK1 and nucLEK1 in various tumor tissues to see if there is upregulation of these proteins, consistent with a positive role in regulating proliferation. Additionally, adult stem cells are emerging as an exciting field of research in various organs (Sadiq and Gerber, 2004). As these cells may share characteristics with embryonic cells, they may also express cytLEK1 and nucLEK1. Existing microchip array data already reveal that LEK1 is expressed in certain stem cell lines (Abeyta et al., 2004). However, additional colocalization studies of cytLEK1 and stem cell markers in tissues are needed. Immunofluorescence cytLEK1 experiments on available stem cell lines may also yield

interesting data. It would not be surprising for cytLEK1 and other LIS1 pathway members to play a role in the recrutiment of stem cells, as processes such as proliferation, migration, and differentiation are involved.

For further examination of cytLEK1 localization and regulation, the *LIS1* +/- and *NudE* -/- mice generated by other laboratories (Hirotsune et al., 1998; Cahana et al., 2001; Feng and Walsh, 2004) can serve as useful reagents. Investigating the distribution of cytLEK1 in primary cells derived from these mice will reveal the function of LIS1 pathway members in directing cytLEK1 to its proper subcellular location. Our current model focuses on the role of cytLEK1 in bringing together proteins at critical cellular areas. However, it is also possible that cytLEK1 localization itself is dependent on LIS1 pathway members. If, for example, cytLEK1 distribution is altered in *NudE* -/- cells, then this would imply that cytLEK1 position is dictated by the NudE protein, likely through an interaction with the C domain. Such experiments are also feasible with an RNAi approach, although the often inconsistent efficacy of RNAi-induced knockdown would then be a complicating factor during analysis.

Finally, the lack of precise data on the cleavage event of LEK1 complicates LEK1 studies. Experiments utilizing protein sequencing and mass spectrometry techniques have been wholly unsuccessful at determining the exact cleavage site (Price et al. unpublished data). Generation of a full-length LEK1 mammalian expression construct may alleviate certain technical issues and allow examination of the cleavage event. However, our efforts to combine the available cytLEK1 and nucLEK1 constructs into a full-length product have been unsuccessful. The necessary triple ligation event appears to occur at a very low rate and is complicated by the incorporation of bacterial DNA into the vector product, perhaps due to a similarity of LEK1 sequence with part of the bacterial genome. As these experiments have been repeated multiple times with no success, this strategy does not appear to be feasible. A long-range RT-PCR approach may be possible, although a 10 kb product is extremely difficult to amplify and will likely contain multiple polymerase errors. Generation of full-length LEK1 is important not only for examining the cleavage event but also for conducting true overexpression and rescue studies. The current cytLEK1 and nucLEK1 constructs have serious detrimental effects on transfected cells, and it is unclear whether this is simply an artifact of incorrect protein size and resultant misfolding. The ability to overexpress full-length LEK1 in cells will help reveal the function of this protein and its cleavage. Experiments to rescue cells treated with

LEK1 morpholino will also be possible, thus serving as an additional control of knockdown specificity. In summary, the studies proposed in this section will reveal the distribution of cytLEK1 in key tissues and cells that have not previously been examined in detail.

Discovery of novel cytLEK1 binding partners

The function of cytLEK1 likely involves multiple associations with important cellular proteins, including members of the LIS1 pathway (see Conclusions). Discovering additional binding partners of cytLEK1 is thus key to better understanding its role in cells. For this reason, additional yeast two-hybrid screens utilizing unexamined parts of the protein as bait are of great importance. Already, such a screen has been performed with an N-terminal region of cytLEK1 and has yielded intriguing results related to dynactin and vesicle trafficking (Pooley et al. unpublished data). Confirmation of these interactions through co-IP and colocalization studies is the necessary next step. Remaining unexamined regions of cytLEK1 will require further yeast two-hybrid screens. Additionally, the putative interaction of the SRR with dysbindin must be confirmed, as discussed in chapter III. Direct yeast two-hybrid matings will examine whether cytLEK1, as predicted, is able to bind to Nudel. Mapping multiple binding partners of cytLEK1 to distinct domains enables discovery of its potential functions, especially with regard to forming protein complexes. Thus, revealing any interactions of cytLEK1 with additional LIS1 pathway members, such as LIS and dynein, is of great importance.

Once these binding partners of cytLEK1 are known, it will be interesting to examine how these proteins associate using a biochemical approach. Such studies will answer the question of whether cytLEK1 is essential for bringing together LIS1 pathway members into a functional complex. For example, it has been reported that RNAi-mediated knockdown of Nudel results in a decreased association of dynein and LIS1, suggesting that Nudel plays a key role in directing this interaction through its binding to both proteins (Shu et al., 2004). Similar experiments need to be conducted for cytLEK1. Morpholinos may be used for LEK1 knockdown in murine cells, and co-IPs can then be performed between various LIS1 pathway members from these lysates, as allowed by available reagents. For example, if cytLEK1 does indeed play a role in regulating the interaction of dynein with NudE, the morpholino-treated samples may have an altered amount of dynein that co-immunoprecipitates with NudE. If cytLEK1 enhances this association, then there may be a lower level of co-immunoprecipitated protein in the knockdown cells. A complicating

factor for these experiments is the cell death resulting from LEK1 knockdown. Thus, examination of such interactions in primary cells derived from a *LEK1* +/- mouse may be a more feasible alternative approach. Inducible expression of a dominant negative protein in cells may also provide a uniform population for conducting these studies. For example, expression of myc-C may disrupt the co-immunoprecipitation of two LIS1 pathway members, thus specifying the nature of the dominant negative effect. As additional binding partners of cytLEK1 are discovered, new dominant negative deletion constructs can be created to examine further protein interactions. Colocalization studies will also be conducted in parallel to examine changes in the distribution of the examined proteins. In summary, these experiments studying the interactions of cytLEK1 and LIS1 pathway members will provide critical biochemical information on the role of cytLEK1 in cells.

Characterization of additional functions of cytLEK1 in the LIS1 pathway

Multiple experiments have already been presented in chapter IV that examine the function of cytLEK1 in the LIS1 pathway. However, additional roles of this pathway remain that have not yet been studied in relation to cytLEK1. One such process is cell migration, which is regulated by the LIS1 pathway and is important during many stages of development (Hirotsune et al., 1998; Dujardin et al., 2003; Shu et al., 2004). Our data on the role of cytLEK1 in microtubule regulation suggest that cytLEK1 dysfunction likely also affects migration. However, direct experiments testing this hypothesis have not been conducted. We are thus in the process of examining the movement of cells expressing myc-C using a real-time light microscopy system. Additional actions of the LIS1 pathway suggest conducting a detailed analysis of organelle positioning in cells where cytLEK1 function is enhanced or disrupted. Our initial results with the Golgi apparatus in chapter IV require further quantification and confirmation. Additionally, it is possible to observe the movement of structures, such as lysosomes, using a real-time fluorescence microscopy system to examine the distinct motions that are regulated by cytLEK1, as has been previously done for Nudel (Liang et al., 2004). The role of both the LIS1 pathway and dysbindin in such lysosome-related processes (Li et al., 2003; Liang et al., 2004) makes the potential existence of a cytLEK1/NudE/dysbindin complex especially intriguing.

Examination of the function of cytLEK1 during mitosis is an important avenue of future research. Localization of the protein to key mitotic structures (chapter II) suggests that it may

play a role in regulation of cell division by the LIS1 pathway (Faulkner et al., 2000; Tai et al., 2002; Yan et al., 2003; Feng and Walsh, 2004). Although there have been some technical difficulties, synchronizing cells with disruptions in cytLEK1 function and examining their progression through the cell cycle is important. Attention should be paid to the formation of the spindle apparatus, as this process is regulated by NudE (Feng and Walsh, 2004), and also to the dynein-directed movement of chromosomes towards the spindle poles. Flow cytometry analysis can help reveal the exact disruptions in cell cycle progression due to cytLEK1 dysfunction. Notably, LEK1 knockdown has previously been shown to cause cell cycle arrest at multiple stages (Ashe et al., 2004). Finally, any ability of cytLEK1 to compensate for deficiencies of LIS1 pathway members is currently unknown. It would be interesting to overexpress cytLEK1, or full-length LEK1 when available, in cells heterozygous or homozygous null for a distinct LIS1 pathway member and then examine if cytLEK1 is able to rescue any of the known defects. The resulting phenotype will thus reveal the specific processes affected by cytLEK1. Conversely, a dominant negative protein may instead be expressed in these cells in order to determine whether cytLEK1 dysfunction has any additional effect in a cell already deficient for NudE, for example.

All these experiments examining the function of cytLEK1 on LIS1 pathway processes may be conducted with several reagents. The dominant negative myc-C protein remains the most appealing tool due to its specific examination of the cytLEK1-NudE interaction. However, morpholino knockdown of LEK1 has also been used successfully for several of our studies. Overexpression of full-length cytLEK1 is an option as well. The availability of *LEK1* +/- or -/- mice in the near future will create important primary cell reagents. Finally, the discovery of additional binding partners of cytLEK1 and characterization of the relevant binding domains will allow the generation of new dominant negative constructs examining the specific roles of different regions of cytLEK1. In addition to the C2C12 and 3T3 cell lines we primarily use, cardiomyocyte and neuronal cells may be utilized to examine the effects of cytLEK1 in specific tissues where it is believed to play an important role. The use of cardiomyocytes, especially, will enable examination of the function of the LIS1 pathway in the heart for the first time. In summary, these studies will reveal important additional roles of cytLEK1 in multiple cellular processes of the LIS1 pathway.

Examination of LEK1 function *in vivo*

For the functional studies that we present here, cultured cells are exclusively utilized. This approach was chosen due to the feasibility of such experiments and the extensive literature on LIS1 pathway members *in vitro* (see Introduction). As cytLEK1 function has now been shown to be important in regulating several key processes of the LIS1 pathway, *in vivo* experiments can be conducted in parallel with the proposed *in vitro* experiments described above. This approach will allow us to examine the role of cytLEK1 within the LIS1 pathway during murine development. Currently, a *LEK1* -/- conditional allele is being generated to examine LEK1 function in the heart (Pooley et al. unpublished data). It will be of interest to also study such an ablated allele in the developing brain, as it is an important site of LEK1 expression and LIS1 pathway function (see Introduction). The brain is ideally suited for examination of cell movement, and the heart is a useful model organ for proliferation studies due to the relatively abrupt termination of cell division at postnatal stages. If examination of the cytLEK1-NudE interaction specifically during embryogenesis is desired, then we can generate a transgenic mouse that expresses the myc-C protein in different tissues during key developmental periods.

Based on the *in vitro* data on cytLEK1 function, disruption of cytLEK1 during murine development is hypothesized to affect the LIS1 pathway processes of proliferation, migration, and differentiation. BrdU and immunofluorescence analyses will reveal any defects in proliferation and spindle function. Migration of cells may be significantly inhibited in the mice, and it will be interesting to examine whether the important nucleus-centrosome distance is different, as observed with Nudel (Shu et al., 2004). Experiments will also examine any altered localization of LIS1 pathway members in tissues. Many additional experiments can be conducted with both tissues and primary cells from these mice, and it is impractical to list all potential studies here. However, the overall focus will be on initially examining processes previously shown in our *in vitro* studies to be regulated by cytLEK1 and then performing further experiments related to the published functions of known cytLEK1 binding partners, including NudE. The generation of these mice disrupted in LEK1 activity will reveal whether the function of cytLEK1, like that of LIS1, is required for correct regulation of the LIS1 pathway during embryonic development.

REFERENCES

Abeyta, M.J., A.T. Clark, R.T. Rodriguez, M.S. Bodnar, R.A. Pera, and M.T. Firpo. 2004. Unique gene expression signatures of independently-derived human embryonic stem cell lines. *Hum Mol Genet*. 13:601-8.

Ahmad, F.J., C.J. Echeverri, R.B. Vallee, and P.W. Baas. 1998. Cytoplasmic dynein and dynactin are required for the transport of microtubules into the axon. *J Cell Biol*. 140:391-401.

Alam, M.R., R.C. Johnson, D.N. Darlington, T.A. Hand, R.E. Mains, and B.A. Eipper. 1997. Kalirin, a cytosolic protein with spectrin-like and GDP/GTP exchange factor-like domains that interacts with peptidylglycine alpha-amidating monooxygenase, an integral membrane peptide-processing enzyme. *J Biol Chem*. 272:12667-75.

Allan, V.J., and R.D. Vale. 1991. Cell cycle control of microtubule-based membrane transport and tubule formation in vitro. *J Cell Biol*. 113:347-59.

Altschul, S.F., W. Gish, W. Miller, E.W. Myers, and D.J. Lipman. 1990. Basic local alignment search tool. *J Mol Biol*. 215:403-10.

Ashe, M., L. Pabon-Pena, E. Dees, K.L. Price, and D. Bader. 2004. LEK1 is a potential inhibitor of pocket protein-mediated cellular processes. *J Biol Chem*. 279:664-76.

Backstrom, J.R., and E. Sanders-Bush. 1997. Generation of anti-peptide antibodies against serotonin 5-HT2A and 5-HT2C receptors. *J Neurosci Methods*. 77:109-17.

Banks, J.D., and R. Heald. 2001. Chromosome movement: dynein-out at the kinetochore. *Curr Biol*. 11:R128-31.

Beckwith, S.M., C.H. Roghi, B. Liu, and N. Ronald Morris. 1998. The "8-kD" cytoplasmic dynein light chain is required for nuclear migration and for dynein heavy chain localization in Aspergillus nidulans. *J Cell Biol*. 143:1239-47.

Bennin, D.A., A.S. Don, T. Brake, J.L. McKenzie, H. Rosenbaum, L. Ortiz, A.A. DePaoli-Roach, and M.C. Horne. 2002. Cyclin G2 associates with protein phosphatase 2A catalytic and regulatory B' subunits in active complexes and induces nuclear aberrations and a G1/S phase cell cycle arrest. *J Biol Chem*. 277:27449-67.

Benson, M.A., S.E. Newey, E. Martin-Rendon, R. Hawkes, and D.J. Blake. 2001. Dysbindin, a novel coiled-coil-containing protein that interacts with the dystrobrevins in muscle and brain. *J Biol Chem*. 276:24232-41.

Buckingham, M. 2001. Skeletal muscle formation in vertebrates. *Curr Opin Genet Dev*. 11:440-8.

Cahana, A., T. Escamez, R.S. Nowakowski, N.L. Hayes, M. Giacobini, A. von Holst, O. Shmueli, T. Sapir, S.K. McConnell, W. Wurst, S. Martinez, and O. Reiner. 2001. Targeted mutagenesis of Lis1 disrupts cortical development and LIS1 homodimerization. *Proc Natl Acad Sci U S A*. 98:6429-34.

Chong, S.S., S.D. Pack, A.V. Roschke, A. Tanigami, R. Carrozzo, A.C. Smith, W.B. Dobyns, and D.H. Ledbetter. 1997. A revision of the lissencephaly and Miller-Dieker syndrome critical regions in chromosome 17p13.3. *Hum Mol Genet*. 6:147-55.

Coquelle, F.M., M. Caspi, F.P. Cordelieres, J.P. Dompierre, D.L. Dujardin, C. Koifman, P. Martin, C.C. Hoogenraad, A. Akhmanova, N. Galjart, J.R. De Mey, and O. Reiner. 2002. LIS1, CLIP-170's key to the dynein/dynactin pathway. *Mol Cell Biol*. 22:3089-102.

Corthesy-Theulaz, I., A. Pauloin, and S.R. Rfeffer. 1992. Cytoplasmic dynein participates in the centrosomal localization of the Golgi complex. *J Cell Biol*. 118:1333-45.

Cotran, R.S., V. Kumar, and T. Collins. 1999. Robbins Pathologic Basis of Disease. W. B. Saunders, Philadelphia.

de la Guardia, C., C.A. Casiano, J. Trinidad-Pinedo, and A. Baez. 2001. CENP-F gene amplification and overexpression in head and neck squamous cell carcinomas. *Head Neck*. 23:104-12.

Dees, E., L.M. Pabon-Pena, R.L. Goodwin, and D. Bader. 2000. Characterization of CMF1 in avian skeletal muscle. *Dev Dyn*. 219:169-81.

Djinovic-Carugo, K., M. Gautel, J. Ylanne, and P. Young. 2002. The spectrin repeat: a structural platform for cytoskeletal protein assemblies. *FEBS Lett*. 513:119-23.

Dujardin, D.L., L.E. Barnhart, S.A. Stehman, E.R. Gomes, G.G. Gundersen, and R.B. Vallee. 2003. A role for cytoplasmic dynein and LIS1 in directed cell movement. *J Cell Biol*. 163:1205-11.

Echeverri, C.J., B.M. Paschal, K.T. Vaughan, and R.B. Vallee. 1996. Molecular characterization of the 50-kD subunit of dynactin reveals function for the complex in chromosome alignment and spindle organization during mitosis. *J Cell Biol*. 132:617-33.

Efimov, V.P., and N.R. Morris. 2000. The LIS1-related NUDF protein of Aspergillus nidulans interacts with the coiled-coil domain of the NUDE/RO11 protein. *J Cell Biol*. 150:681-8.

Esguerra, R.L., L. Jia, T. Kaneko, K. Sakamoto, N. Okada, and M. Takagi. 2004. Immunohistochemical analysis of centromere protein F expression in buccal and gingival squamous cell carcinoma. *Pathol Int*. 54:82-9.

Estrach, S., S. Schmidt, S. Diriong, A. Penna, A. Blangy, P. Fort, and A. Debant. 2002. The Human Rho-GEF Trio and Its Target GTPase RhoG Are Involved in the NGF Pathway, Leading to Neurite Outgrowth. *Curr Biol*. 12:307-12.

Faulkner, N.E., D.L. Dujardin, C.Y. Tai, K.T. Vaughan, C.B. O'Connell, Y. Wang, and R.B. Vallee. 2000. A role for the lissencephaly gene LIS1 in mitosis and cytoplasmic dynein function. *Nat Cell Biol*. 2:784-91.

Feng, Y., E.C. Olson, P.T. Stukenberg, L.A. Flanagan, M.W. Kirschner, and C.A. Walsh. 2000. LIS1 regulates CNS lamination by interacting with mNudE, a central component of the centrosome. *Neuron*. 28:665-79.

Feng, Y., and C.A. Walsh. 2004. Mitotic spindle regulation by Nde1 controls cerebral cortical size. *Neuron*. 44:279-93.

Geiser, J.R., E.J. Schott, T.J. Kingsbury, N.B. Cole, L.J. Totis, G. Bhattacharyya, L. He, and M.A. Hoyt. 1997. Saccharomyces cerevisiae genes required in the absence of the CIN8-encoded spindle motor act in functionally diverse mitotic pathways. *Mol Biol Cell*. 8:1035-50.

Gibbons, I.R. 1996. The role of dynein in microtubule-based motility. *Cell Struct Funct*. 21:331-42.

Giodini, A., M.J. Kallio, N.R. Wall, G.J. Gorbsky, S. Tognin, P.C. Marchisio, M. Symons, and D.C. Altieri. 2002. Regulation of microtubule stability and mitotic progression by survivin. *Cancer Res*. 62:2462-7.

Goodwin, R.L., L.M. Pabon-Pena, G.C. Foster, and D. Bader. 1999. The cloning and analysis of LEK1 identifies variations in the LEK/centromere protein F/mitosin gene family. *J Biol Chem*. 274:18597-604.

Hattori, M., H. Adachi, M. Tsujimoto, H. Arai, and K. Inoue. 1994. Miller-Dieker lissencephaly gene encodes a subunit of brain platelet-activating factor acetylhydrolase [corrected]. *Nature*. 370:216-8.

Hirokawa, N. 1998. Kinesin and dynein superfamily proteins and the mechanism of organelle transport. *Science*. 279:519-26.

Hirotsune, S., M.W. Fleck, M.J. Gambello, G.J. Bix, A. Chen, G.D. Clark, D.H. Ledbetter, C.J. McBain, and A. Wynshaw-Boris. 1998. Graded reduction of Pafah1b1 (Lis1) activity results in neuronal migration defects and early embryonic lethality. *Nat Genet*. 19:333-9.

Hussein, D., and S.S. Taylor. 2002. Farnesylation of Cenp-F is required for G2/M progression and degradation after mitosis. *J Cell Sci*. 115:3403-14.

Kennedy, S.P., S.L. Warren, B.G. Forget, and J.S. Morrow. 1991. Ankyrin binds to the 15th repetitive unit of erythroid and nonerythroid beta-spectrin. *J Cell Biol.* 115:267-77.

Lansbergen, G., Y. Komarova, M. Modesti, C. Wyman, C.C. Hoogenraad, H.V. Goodson, R.P. Lemaitre, D.N. Drechsel, E. van Munster, T.W. Gadella, Jr., F. Grosveld, N. Galjart, G.G. Borisy, and A. Akhmanova. 2004. Conformational changes in CLIP-170 regulate its binding to microtubules and dynactin localization. *J Cell Biol.* 166:1003-14.

Lee, W.L., J.R. Oberle, and J.A. Cooper. 2003. The role of the lissencephaly protein Pac1 during nuclear migration in budding yeast. *J Cell Biol.* 160:355-64.

Lei, Y., and R. Warrior. 2000. The Drosophila Lissencephaly1 (DLis1) gene is required for nuclear migration. *Dev Biol.* 226:57-72.

Li, W., Q. Zhang, N. Oiso, E.K. Novak, R. Gautam, E.P. O'Brien, C.L. Tinsley, D.J. Blake, R.A. Spritz, N.G. Copeland, N.A. Jenkins, D. Amato, B.A. Roe, M. Starcevic, E.C. Dell'Angelica, R.W. Elliott, V. Mishra, S.F. Kingsmore, R.E. Paylor, and R.T. Swank. 2003. Hermansky-Pudlak syndrome type 7 (HPS-7) results from mutant dysbindin, a member of the biogenesis of lysosome-related organelles complex 1 (BLOC-1). *Nat Genet.* 35:84-9.

Liang, Y., W. Yu, Y. Li, Z. Yang, X. Yan, Q. Huang, and X. Zhu. 2004. Nudel functions in membrane traffic mainly through association with Lis1 and cytoplasmic dynein. *J Cell Biol.* 164:557-66.

Liao, H., R.J. Winkfein, G. Mack, J.B. Rattner, and T.J. Yen. 1995. CENP-F is a protein of the nuclear matrix that assembles onto kinetochores at late G2 and is rapidly degraded after mitosis. *J Cell Biol.* 130:507-18.

Liu, Z., R. Steward, and L. Luo. 2000. Drosophila Lis1 is required for neuroblast proliferation, dendritic elaboration and axonal transport. *Nat Cell Biol.* 2:776-83.

Liu, Z., T. Xie, and R. Steward. 1999. Lis1, the Drosophila homolog of a human lissencephaly disease gene, is required for germline cell division and oocyte differentiation. *Development.* 126:4477-88.

Lo Nigro, C., C.S. Chong, A.C. Smith, W.B. Dobyns, R. Carrozzo, and D.H. Ledbetter. 1997. Point mutations and an intragenic deletion in LIS1, the lissencephaly causative gene in isolated lissencephaly sequence and Miller-Dieker syndrome. *Hum Mol Genet.* 6:157-64.

Lodish, H.F. 2004. Molecular cell biology. W.H. Freeman and Company, New York. 1 v. (various pagings) pp.

Mathur, A., and J.F. Martin. 2004. Stem cells and repair of the heart. *Lancet.* 364:183-92.

McGill, C.J., and G. Brooks. 1995. Cell cycle control mechanisms and their role in cardiac growth. *Cardiovasc Res*. 30:557-69.

Mikawa, T., L. Cohen-Gould, and D.A. Fischman. 1992. Clonal analysis of cardiac morphogenesis in the chicken embryo using a replication-defective retrovirus. III: Polyclonal origin of adjacent ventricular myocytes. *Dev Dyn*. 195:133-41.

Mukai, H., M. Toshimori, H. Shibata, H. Takanaga, M. Kitagawa, M. Miyahara, M. Shimakawa, and Y. Ono. 1997. Interaction of PKN with alpha-actinin. *J Biol Chem*. 272:4740-6.

Naya, F.S., and E. Olson. 1999. MEF2: a transcriptional target for signaling pathways controlling skeletal muscle growth and differentiation. *Curr Opin Cell Biol*. 11:683-8.

Nguyen, M.D., T. Shu, K. Sanada, R.C. Lariviere, H.C. Tseng, S.K. Park, J.P. Julien, and L.H. Tsai. 2004. A NUDEL-dependent mechanism of neurofilament assembly regulates the integrity of CNS neurons. *Nat Cell Biol*. 6:595-608.

Niethammer, M., D.S. Smith, R. Ayala, J. Peng, J. Ko, M.S. Lee, M. Morabito, and L.H. Tsai. 2000. NUDEL is a novel Cdk5 substrate that associates with LIS1 and cytoplasmic dynein. *Neuron*. 28:697-711.

Numakawa, T., Y. Yagasaki, T. Ishimoto, T. Okada, T. Suzuki, N. Iwata, N. Ozaki, T. Taguchi, M. Tatsumi, K. Kamijima, R.E. Straub, D.R. Weinberger, H. Kunugi, and R. Hashimoto. 2004. Evidence of novel neuronal functions of dysbindin, a susceptibility gene for schizophrenia. *Hum Mol Genet*. 13:2699-708.

O'Shea, E.K., R. Rutkowski, W.F. Stafford, 3rd, and P.S. Kim. 1989. Preferential heterodimer formation by isolated leucine zippers from fos and jun. *Science*. 245:646-8.

Otey, C.A., F.M. Pavalko, and K. Burridge. 1990. An interaction between alpha-actinin and the beta 1 integrin subunit in vitro. *J Cell Biol*. 111:721-9.

Pabon-Pena, L.M., R.L. Goodwin, L.J. Cise, and D. Bader. 2000. Analysis of CMF1 reveals a bone morphogenetic protein-independent component of the cardiomyogenic pathway. *J Biol Chem*. 275:21453-9.

Pasumarthi, K.B., and L.J. Field. 2002. Cardiomyocyte cell cycle regulation. *Circ Res*. 90:1044-54.

Pilz, D.T., N. Matsumoto, S. Minnerath, P. Mills, J.G. Gleeson, K.M. Allen, C.A. Walsh, A.J. Barkovich, W.B. Dobyns, D.H. Ledbetter, and M.E. Ross. 1998. LIS1 and XLIS (DCX) mutations cause most classical lissencephaly, but different patterns of malformation. *Hum Mol Genet*. 7:2029-37.

Redkar, A., J.K. deRiel, Y.S. Xu, M. Montgomery, V. Patwardhan, and J. Litvin. 2002. Characterization of cardiac muscle factor 1 sequence motifs: retinoblastoma protein binding and nuclear localization. *Gene*. 282:53-64.

Reiner, O., R. Carrozzo, Y. Shen, M. Wehnert, F. Faustinella, W.B. Dobyns, C.T. Caskey, and D.H. Ledbetter. 1993. Isolation of a Miller-Dieker lissencephaly gene containing G protein beta-subunit-like repeats. *Nature*. 364:717-21.

Ross, M.H., L.J. Romrell, and G.I. Kaye. 1995. Histology: A Text and Atlas. Williams & Wilkins, Baltimore.

Russo, P., M. Loprevite, A. Cesario, and A. Ardizzoni. 2004. Farnesylated proteins as anticancer drug targets: from laboratory to the clinic. *Curr Med Chem Anti-Canc Agents*. 4:123-38.

Rybakova, I.N., K.J. Amann, and J.M. Ervasti. 1996. A new model for the interaction of dystrophin with F-actin. *J Cell Biol*. 135:661-72.

Sadiq, T.S., and D.A. Gerber. 2004. Stem cells in modern medicine: reality or myth? *J Surg Res*. 122:280-91.

Sapir, T., M. Elbaum, and O. Reiner. 1997. Reduction of microtubule catastrophe events by LIS1, platelet-activating factor acetylhydrolase subunit. *Embo J*. 16:6977-84.

Sasaki, S., A. Shionoya, M. Ishida, M.J. Gambello, J. Yingling, A. Wynshaw-Boris, and S. Hirotsune. 2000. A LIS1/NUDEL/cytoplasmic dynein heavy chain complex in the developing and adult nervous system. *Neuron*. 28:681-96.

Shu, T., R. Ayala, M.D. Nguyen, Z. Xie, J.G. Gleeson, and L.H. Tsai. 2004. Ndel1 Operates in a Common Pathway with LIS1 and Cytoplasmic Dynein to Regulate Cortical Neuronal Positioning. *Neuron*. 44:263-77.

Sinensky, M. 2000. Recent advances in the study of prenylated proteins. *Biochim Biophys Acta*. 1484:93-106.

Smith, D.S., M. Niethammer, R. Ayala, Y. Zhou, M.J. Gambello, A. Wynshaw-Boris, and L.H. Tsai. 2000. Regulation of cytoplasmic dynein behaviour and microtubule organization by mammalian Lis1. *Nat Cell Biol*. 2:767-75.

Smith, P.K., R.I. Krohn, G.T. Hermanson, A.K. Mallia, F.H. Gartner, M.D. Provenzano, E.K. Fujimoto, N.M. Goeke, B.J. Olson, and D.C. Klenk. 1985. Measurement of protein using bicinchoninic acid. *Anal Biochem*. 150:76-85.

Smits, V.A., and R.H. Medema. 2001. Checking out the G(2)/M transition. *Biochim Biophys Acta*. 1519:1-12.

Soonpaa, M.H., and L.J. Field. 1998. Survey of studies examining mammalian cardiomyocyte DNA synthesis. *Circ Res*. 83:15-26.

Soonpaa, M.H., K.K. Kim, L. Pajak, M. Franklin, and L.J. Field. 1996. Cardiomyocyte DNA synthesis and binucleation during murine development. *Am J Physiol*. 271:H2183-9.

Sucov, H.M. 1998. Molecular insights into cardiac development. *Annu Rev Physiol.* 60:287-308.

Swan, A., T. Nguyen, and B. Suter. 1999. Drosophila Lissencephaly-1 functions with Bic-D and dynein in oocyte determination and nuclear positioning. *Nat Cell Biol.* 1:444-9.

Tai, C.Y., D.L. Dujardin, N.E. Faulkner, and R.B. Vallee. 2002. Role of dynein, dynactin, and CLIP-170 interactions in LIS1 kinetochore function. *J Cell Biol*. 156:959-68.

Tam, S.K., W. Gu, V. Mahdavi, and B. Nadal-Ginard. 1995. Cardiac myocyte terminal differentiation. Potential for cardiac regeneration. *Ann N Y Acad Sci*. 752:72-9.

Tanaka, T., F.F. Serneo, C. Higgins, M.J. Gambello, A. Wynshaw-Boris, and J.G. Gleeson. 2004. Lis1 and doublecortin function with dynein to mediate coupling of the nucleus to the centrosome in neuronal migration. *J Cell Biol*. 165:709-21.

Toomre, D., P. Keller, J. White, J.C. Olivo, and K. Simons. 1999. Dual-color visualization of trans-Golgi network to plasma membrane traffic along microtubules in living cells. *J Cell Sci*. 112 (Pt 1):21-33.

Toyo-oka, K., A. Shionoya, M.J. Gambello, C. Cardoso, R. Leventer, H.L. Ward, R. Ayala, L.H. Tsai, W. Dobyns, D. Ledbetter, S. Hirotsune, and A. Wynshaw-Boris. 2003. 14-3-3epsilon is important for neuronal migration by binding to NUDEL: a molecular explanation for Miller-Dieker syndrome. *Nat Genet*. 34:274-85.

Vallee, R.B., C. Tai, and N.E. Faulkner. 2001. LIS1: cellular function of a disease-causing gene. *Trends Cell Biol.* 11:155-60.

Wei, Y., D. Bader, and J. Litvin. 1996. Identification of a novel cardiac-specific transcript critical for cardiac myocyte differentiation. *Development*. 122:2779-89.

Willins, D.A., B. Liu, X. Xiang, and N.R. Morris. 1997. Mutations in the heavy chain of cytoplasmic dynein suppress the nudF nuclear migration mutation of Aspergillus nidulans. *Mol Gen Genet*. 255:194-200.

Wynshaw-Boris, A., and M.J. Gambello. 2001. LIS1 and dynein motor function in neuronal migration and development. *Genes Dev*. 15:639-51.

Xia, H., S.T. Winokur, W.L. Kuo, M.R. Altherr, and D.S. Bredt. 1997. Actinin-associated LIM protein: identification of a domain interaction between PDZ and spectrin-like repeat motifs. *J Cell Biol*. 139:507-15.

Xiang, X., A.H. Osmani, S.A. Osmani, M. Xin, and N.R. Morris. 1995. NudF, a nuclear migration gene in Aspergillus nidulans, is similar to the human LIS-1 gene required for neuronal migration. *Mol Biol Cell*. 6:297-310.

Yan, X., F. Li, Y. Liang, Y. Shen, X. Zhao, Q. Huang, and X. Zhu. 2003. Human Nudel and NudE as regulators of cytoplasmic dynein in poleward protein transport along the mitotic spindle. *Mol Cell Biol*. 23:1239-50.

Yee, A.S., H.H. Shih, and S.G. Tevosian. 1998. New perspectives on retinoblastoma family functions in differentiation. *Front Biosci*. 3:D532-47.

Young, P., C. Ferguson, S. Banuelos, and M. Gautel. 1998. Molecular structure of the sarcomeric Z-disk: two types of titin interactions lead to an asymmetrical sorting of alpha-actinin. *Embo J*. 17:1614-24.

Zhu, X. 1999. Structural requirements and dynamics of mitosin-kinetochore interaction in M phase. *Mol Cell Biol*. 19:1016-24.

Zhu, X., K.H. Chang, D. He, M.A. Mancini, W.R. Brinkley, and W.H. Lee. 1995a. The C terminus of mitosin is essential for its nuclear localization, centromere/kinetochore targeting, and dimerization. *J Biol Chem*. 270:19545-50.

Zhu, X., M.A. Mancini, K.H. Chang, C.Y. Liu, C.F. Chen, B. Shan, D. Jones, T.L. Yang-Feng, and W.H. Lee. 1995b. Characterization of a novel 350-kilodalton nuclear phosphoprotein that is specifically involved in mitotic-phase progression. *Mol Cell Biol*. 15:5017-29.